

UNIVERSITY OF ALBERTA

**Applications of Ensemble Kalman Filter for Characterization and History
Matching of SAGD Reservoirs**

by

ALI GUL

A thesis submitted to the Faculty of Graduate Studies and Research
in partial fulfillment of the requirements for the degree of

Master of Science

in

Petroleum Engineering

Department of Civil and Environmental Engineering

©Ali Gul

Fall 2011

Edmonton, Alberta

Permission is hereby granted to the University of Alberta Libraries to reproduce single copies of this thesis and to lend or sell such copies for private, scholarly or scientific research purposes only. Where the thesis is converted to, or otherwise made available in digital form, the University of Alberta will advise potential users of the thesis of these terms.

The author reserves all other publication and other rights in association with the copyright in the thesis and, except as herein before provided, neither the thesis nor any substantial portion thereof may be printed or otherwise reproduced in any material form whatsoever without the author's prior written permission.

Examining Committee

Dr. Japan Trivedi, Civil and Environmental Engineering (Supervisor)

Dr. Ergun Kuru, Civil and Environmental Engineering (Internal Examiner)

Dr. Rajendar Gupta, Chemical and Materials Engineering (External Examiner)

Dedication

To my Parents, Brothers, Sisters, and their Sweet Kids

For their Love, Motivation and Prays for my Success

Also to my Teachers and Friends

For their unconditional support

Abstract

Steam-assisted gravity drainage (SAGD) is the most robust thermal recovery process that has unlocked western Canadian heavy oil and bitumen reserves into economical recovery. The prime challenges in SAGD heavy oil developments and well planning in the Northern Alberta formations are: characterizing the reservoir heterogeneity and identifying the potential steam barriers that may interfere with the recovery process. If characterized earlier, the field development plans could be efficient and effective. In SAGD projects, temperature sensors at several depths within observation wells are available for monitoring steam chamber growth. Characterization using data available from these real-time sensors and dynamic production data integrated in a closed-loop could be a probable solution.

Ensemble Kalman filter (EnKF), a state and parameter estimation technique, has shown good promise for reservoir characterization using dynamic production data in conventional reservoirs. For the above discussed problem, constrained based adaptive EnKF approach was implemented.

We have shown that using real-time temperature and early production data assimilation of single well steam assisted gravity drainage (SW-SAGD), twin-well SAGD, and multilateral well SAGD models, early characterization of heterogeneity is possible. For a McMurray type formation, integration of online temperature into closed-loop history matching was successfully done. The implemented approach resulted in a better reservoir model configuration, significant reduction of uncertainty in steam chamber propagation and production forecast. The best-ranked characterized geological model generated could then be used for planning and decision-making of other field development strategies such as infill drilling, various SAGD well configurations, or implementing ESSAGD, CSS, or SAGP.

Acknowledgement

This thesis owes more than I can say to Dr. Japan J. Trivedi. He provided me an opportunity to work under his supervision, and allowed me to explore ideas that I was interested most. Therefore, I would like to express my sincere gratitude to my supervisor Assistant Prof. Japan Trivedi, who is the best advisor and mentor one could ever have. He offered me a lot of brilliant ideas and helped me to dig deep insights in research and invaluable guidance. I also appreciate his patience and encouragement during my difficult moments. I am also thankful to Dr. Ergun Kuru and Dr. Rajendar Gupta for serving as members on the examination committee.

During the period of my research work, I have had close interactions with Dr. Srish L. Shah and his group, especially his Ph.D student Saneej B. Chitralkha. Saneej and I presented poster in Graduate Research Symposium arranged by Faculty of Engineering UofA and we won Best Poster Award. I really enjoyed the company of Saneej and learned a lot about Ensemble Kalman Filter and MATLAB coding from him. I would like to thank my group fellows Siavash Nijadi, Amit Panwar, Mudit Chordia, and Santhosh Kumar, along whom I shared office and exchange ideas and concepts.

The Natural Sciences and Engineering Research Council of Canada (NSERC) Discovery Grant and the University of Alberta supported this research work. CMG-STARS thermal reservoir simulator was provided by Computer Modeling Group Ltd. MATLAB and S-GeMS softwares were used to run Sequential Gaussian Simulation for the present study. I am thankful for scholarship from FGSR and GSA to present research paper at World Heavy Oil Congress 2011, Edmonton AB, Canada. The author would like to extend his heartiest gratitude to Statoil Canada Ltd. for recognizing my research project and providing me opportunity to work as Reservoir Engineer to carry out research on this topic during my professional career.

Finally yet importantly, I owe a lot of love and care to my family and siblings in Pakistan, as well as all my friends in Edmonton. Without their moral support and encouragement, this work could not be completed. The number of friends in Edmonton seems countless for me to enlist the names of all of them here but if I mention them in one group that would be PSA at U of A.

Table of Contents

Abstract.....	iv
Acknowledgement	v
List of Table.....	x
List of Figures.....	xi
Chapter 1	1
Introduction	1
1.1 Objective.....	2
1.2 Thesis Overview	2
1.3 Unconventional Oil Reservoirs.....	3
1.4 EOR Recovery Techniques.....	3
1.5 Review of SAGD Process.....	5
1.6 Major Challenges.....	7
1.7 History Matching Process in Reservoir Simulation.....	10
Chapter 2	12
Theoretical Framework of EnKF	12
2.1 Statistics Fundamentals	12
2.2 Kalman Filter (KF)	18
2.3 Extended Kalman Filter (EKF).....	20

2.4	Ensemble Kalman Filter (EnKF)	21
Chapter 3		28
	EnKF for Continuous Reservoir Model Updating	28
3.1	EnKF Workflow for History Matching Problems	28
3.2	Constrained EnKF	30
Chapter 4		35
	Constrained EnKF for Continuous SAGD Reservoir Model Updating - Twin Well SAGD Model.....	35
4.1	Unconventional Oil Reservoir Fluid and Rock Properties	36
4.2	CASE STUDY - 1: Twin Well SAGD Model and the EnKF Scheme	39
4.3	Twin Well SAGD Model Results	41
4.4	CASE STUDY - 2: Multi Pair SAGD Model.....	51
4.5	Multi Pair SAGD Model Results	55
Chapter 5		62
	Constrained EnKF for Continuous SAGD Reservoir Model Updating - Single Well SAGD Model.....	62
5.1	Single Well SAGD Reservoir Model with Hybrid Grids	63
5.2	Case - 1: Single Well SAGD Model Results	67
5.3	Case - 2: Single Well SAGD Model Results	73
Chapter 6		78

Constrained EnKF for Continuous SAGD Reservoir Model Updating - Multilateral Wells SAGD Model	78
6.1 Twin Multilateral Wells SAGD Model With Parallel Branches	79
6.2 Multilateral Wells SAGD Model Results	83
6.3 Single Multilateral Well SAGD Model	88
6.4 Single Multilateral Well SAGD Model Results	92
Chapter 7	98
Discussion and Conclusions	98
7.1 Discussion	98
7.2 Conclusions	100
Nomenclature	102
Bibliography	104

List of Table

Table 4. 1 TWSAGD Model Reservoir Properties 40

Table 4. 2 MPSAGD Model Reservoir Properties..... 52

Table 5. 1 SWSAGD Model Reservoir Properties 64

Table 6. 1 Twin MLW-SAGD Model Reservoir Properties..... 80

Table 6. 2 Single MLW-SAGD Model Reservoir Properties 90

List of Figures

Figure 1.1: EOR Processes Classification, (Farouk and Thomas, 1996).....	4
Figure 1.2: SAGD Process layout, (Norwest Corporation website)	6
Figure 2.1: Cumulative Distribution Function.....	14
Figure 2.2: Probability Density Function.....	15
Figure 3.1: EnKF Workflow for History Match Problems, (Seiler et. al. 2009) ..	30
Figure 4.1: Bitumen Viscosity vs Temperature	36
Figure 4.2: Relative Permeability of Oil and Water vs S_w	38
Figure 4.3: Relative Permeability of Gas and Liquid vs S_L	38
Figure 4.4: 3D view of Twin Well SAGD Model in CMG STARS Simulator	39
Figure 4.5: TWSAGD model X-Z cross sections, True Perm Case (left col.), and Initial Mean Perm Case (right col.).....	42
Figure 4.6: TWSAGD model X-Z cross sections, True Perm Case (left col.), Initial Mean Perm Case (mid col.) and Updated mean Perm Case (right col.)	43
Figure 4.7: Field Oil Production Rate, m ³ /d, TWSAGD Model	44
Figure 4.8: Cumulative Steam Oil Ratio, TWSAGD Model	45

Figure 4.9: Reservoir Temperature at grid location 9, 3, 21, TWSAGD Model ..	46
Figure 4.10: Reservoir Temperature at grid location 21, 3, 17, TWSAGD.....	46
Figure 4.11: 3D model cross sections, Steam Chamber Growth in True Case (top), Steam Chamber Growth in Initial Ensemble Case (mid) and Steam Chamber Growth in Updated Ensemble Case (bottom).....	48
Figure 4.12: Weighted Mean Square Error (WMSE), TWSAGD Model.....	50
Figure 4.13: Weighted R Square (WR ²) Graph, TWSAGD Model	51
Figure 4.14: A cross section 3D view of MPSAGD Model showing the location of wells	52
Figure 4.15: Reference Permeability Field (md) for MPSAGD Model.....	54
Figure 4.16: Corehole Locations where hard data is available for MPSAGD Model	54
Figure 4.17: Initial Mean Permeability (md) for MPSAGD Model	55
Figure 4.18: Updated Mean Permeability Field of MPSAGD Model	56
Figure 4.19: MPSAGD Model Field Oil Production Rate (BPD)	57
Figure 4.20: MPSAGD Model Cumulative Steam Oil Ratio (CSOR)	58
Figure 4.21: Reservoir Temperature (°F) at sensor location 30, 5, 1	58
Figure 4.22: Reservoir Temperature (°F) at sensor location 30, 2, 3.....	59
Figure 4.23: Weighted Mean Square Error (WMSE), MPSAGD Model	60
Figure 4.24: Weighted R Square (WR ²) Graph, MPSAGD Model	60

Figure 5.1: 3D view of Single Well SAGD Model in CMG STARS Simulator ..	63
Figure 5.2: Reference Permeability Field (md), SWSAGD Model	65
Figure 5.3: Corehole Locations where hard data is available SWSAGD Model..	65
Figure 5.4: Initial Mean Permeability Field (md), SWSAGD Model.....	66
Figure 5.5: Updated Mean Permeability of 30 realizations, SW-SAGD Model...	67
Figure 5.6: Permeability field update at different time steps, SWSAGD Model..	68
Figure 5.7: Field Oil Production Rate (m ³ /d) , SWSAGD Model.....	69
Figure 5.8: Cumulative Steam Oil Ratio, SW-SAGD Model.....	70
Figure 5.9: Reservoir Temperature (C) at grid location 12, 11, 6, SW-SAGD Model	70
Figure 5.10: Reservoir Temperature (C) at grid location 12, 16, 4, SW-SAGD Model	71
Figure 5.11: Weighted mean square error (WMSE), SW-SAGD Model	72
Figure 5.12: Weighted R Square (WR ²), SW-SAGD Model.....	72
Figure 5.13: Updated mean permeability (md) without temp observations in history matching process, SW-SAGD Model.....	73
Figure 5.14: Comparison between Permeability Update of two cases, SWSAGD Model	74
Figure 5.15: Field Oil Production Rate (m ³ /d), SW-SAGD Model	75
Figure 5.16: Cumulative Steam Oil Ratio, SWSAGD Model	75
Figure 5.17: Weighted mean square error (WMSE), SWSAGD Model.....	76

Figure 5.18: Weighted R Square (WR^2), SWSAGD Model	77
Figure 6.1: Various types of advanced wells, (Gadelle and Renard, 1999).....	79
Figure 6.2: Various types of advanced wells, (Gadelle and Renard, 1999).....	80
Figure 6.3: Reference Permeability Field of MLW-SAGD Model	82
Figure 6.4: Initial Mean Permeability Field of 30 Realizations.....	82
Figure 6.5: Updated mean permeability field, MLWSAGD model.....	84
Figure 6.6: Field Oil Production Rate, m^3/d , MLWSAGD Model	85
Figure 6.7: Cumulative Steam Oil Ratio, MLWSAGD Model	85
Figure 6.8: Reservoir Temperature ($^{\circ}C$) at grid location 20, 7, 6, Twin MLW-SAGD Model	86
Figure 6.9: Reservoir Temperature ($^{\circ}C$) at grid location 5, 2, 2, Twin MLW-SAGD Model	86
Figure 6.10: Weighted Mean Square Error (WMSE), MLWSAGD	87
Figure 6.11: Weighted Root Square (WR^2), MLWSAGD Model	88
Figure 6.12: 3D view of single MLW-SAGD model with four branches	89
Figure 6.13: Reference permeability field of single MLW-SAGD model	91
Figure 6.14: Initial mean permeability field of single MLW-SAGD model	91
Figure 6.15: Updated Mean Permeability Field of Single MLW-SAGD Model..	93
Figure 6.16: Field Oil Production Rate, m^3/d , Single MLW-SAGD Model	94
Figure 6.17: Cumulative Steam Oil Ratio (SOR), Single MLW-SAGD Model ..	94

Figure 6.18: Reservoir Temperature at grid location 3, 10, 7, Single MLW-SAGD Model	95
Figure 6.19: Reservoir Temperature at grid location 19, 10, 6, Single MLW-SAGD Model	95
Figure 6.20: Weighted Mean Square Error (WMSE), Single MLW-SAGD Model	96
Figure 6.21: Weighted R Square (WR2), Single MLW-SAGD Model	97

Chapter 1

Introduction

A huge quantity of heavy oil and bitumen reserves are present worldwide. These reserves have been estimated to be as much as double that of the total discovered conventional crude oil in place. Around 90% of the world's heavy oil and bitumen reserves are deposited in Venezuela and Canada, over 1.8 trillion barrels of original heavy oil in place is present in Venezuela and 1.7 trillion barrels of original heavy oil in place is present in Canada, Burton et. al. (2005). As the available resources of conventional crude oil continue to decline throughout the world, further development of unconventional oil recovery technologies is critical in meeting world's present and future energy requirements. Unconventional oil reserves like in Athabasca Oil Sands deposit has viscosity greater than 1 million cp at reservoir conditions; oil flow rate is negligible through the porous media at such high viscosity values. Thus, the recovery of oil sand deposits requires efficient in situ viscosity reduction techniques. Recent thermal recovery technology developments have focused on SAGD process, which is found to be the most promising EOR method for heavy oil and bitumen reservoirs.

The closed-loop reservoir management in petroleum industry is currently receiving significant attention and it allows real time decisions to be made that maximize recovery factor from a reservoir. Important elements of closed loop reservoir management are model based optimisation and data assimilation technique, which is known as automatic history matching. Ensemble Kalman Filter is a new technique of automatic history matching, introduced by Evensen G. (1994) for use on large non-linear oceanic models. Naevdel et. al. (2002) applied this technique first time to perform history matching of reservoir simulation models. Since the last decade, this technique has emerged as an effective tool for performing continuous updating of reservoir models and shown promising results on several history matching cases.

1.1 Objective

The objective of this work is to study the applications of closed loop data assimilation technique (i.e. Ensemble Kalman Filter) to perform automated history matching of unconventional oil reservoirs. Moreover, EnKF also provides valuable information about reservoir state after data assimilation process, therefore, Ensemble Kalman Filter is used to carry out reservoir characterization and production management. In this work, main focus was to study the Alberta oil sands deposit where SAGD process can be applicable. Different SAGD well patterns are also studied in this work including Twin well SAGD pattern, widely used in current scenario of oil and gas industry, Single well SAGD pattern and Multilateral well SAGD pattern. Each pattern provided better results in terms of data assimilation and model parameters update after applying EnKF based history matching technique.

1.2 Thesis Overview

This dissertation consists of six chapters. Chapter 1 presents an introduction of research and general information about unconventional oil reservoirs, SAGD process and history matching technique in reservoir simulation models. This short introduction is followed by Chapter 2 in which statistical background can be refreshed, and theory behind the Constrained Ensemble Kalman Filter is explained in detail. EnKF methodology practically studied and applied to two twin wells SAGD models by integrating production measurements, temperature observations and prior geological model information for continuous reservoir model updating, is explained in Chapter 3. Chapter 4 gives the comparative study, performed on single well SAGD model, to evaluate the effect of temperature observations on model parameters update during EnKF based history matching method. Implementation of SAGD process in advanced well technology, where multibranch well drilled through vertical hole in different directions, is discussed in Chapter 5. Later on in this chapter, EnKF based history matching method is

applied to two multilateral well SAGD models. Finally, Chapter 6 contains the summary and future work of applying EnKF method to SAGD models.

1.3 Unconventional Oil Reservoirs

The term "unconventional reserves" is commonly used for energy resources like oil sands, coal beds, tight shale gas reserves, and low permeability sandstones. While unconventional hydrocarbon reserves are very large as compared to conventional reserves, economically recoverable reserves are much smaller because of the greater cost and advanced technology needed for production. In past, lower price of crude oil in international market, made these reserves almost uneconomical. Over the last two decades, due to increase in demand for crude oil and depletion of conventional reserves, increased the prices of crude oil in international market which converted the unconventional reserves from uneconomical to economical phase. Specialized techniques have also been developed which increased the recovery of unconventional resources.

Rest of this work will refer unconventional reserves as oil sands deposit or bitumen reserves. We focused on the Western Canadian oil sands deposit in our study, where more than 1.7 trillion barrels of bitumen reserves are present. Only Athabasca oil sands deposit contains more than one trillion barrels of bitumen reserves which is one of the largest heavy oil reservoir in the world, Burton et. al. (2005). At reservoir conditions, crude oil has more than a million (10^6) cp viscosity which makes it immobile inside the porous media. Therefore; the recovery of bitumen reservoirs require in-situ viscosity reduction techniques.

1.4 EOR Recovery Techniques

Enhanced Oil Recovery (EOR) refers to all processes in which heat, solvents, chemicals and bacterial are supplied to reservoir as additional energy to establish pressure / temperature gradients, change interfacial tensions and wettability and modify reservoir fluid properties in such a way that oil flows towards producing well. There are several classifications of EOR methods depending on reservoir

and fluid properties. According to Farouk and Thomas (1996), EOR processes can be classified broadly into thermal and non-thermal. Thermal methods applied to extra heavy oil or bitumen reservoirs, whereas non-thermal methods applied to heavy or medium oil reservoirs. A complete classification of EOR processes is given in figure 1.1.

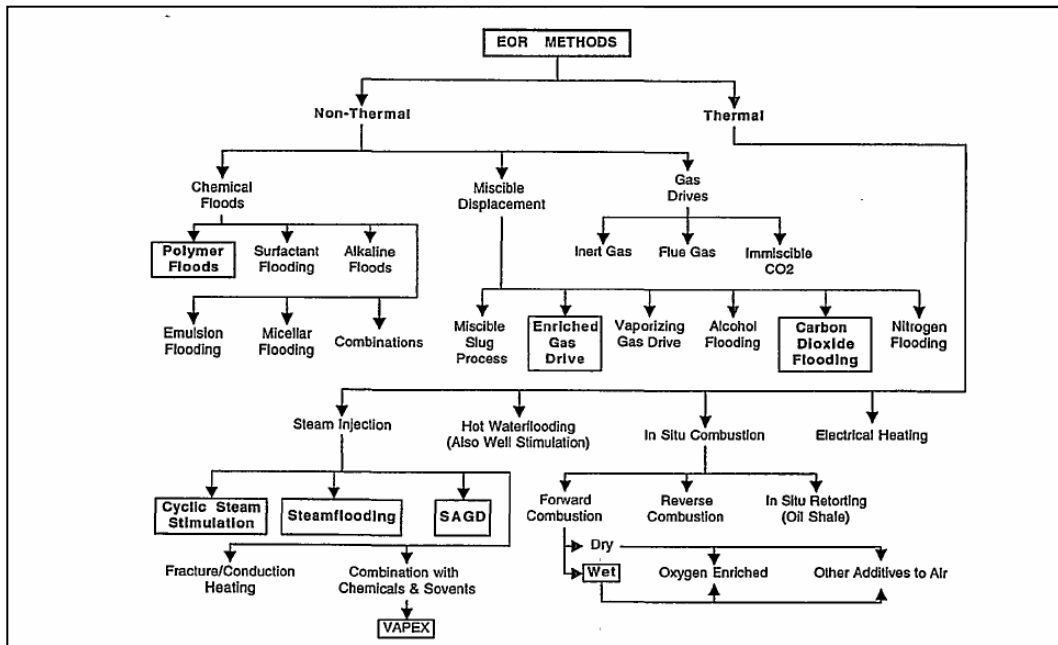


Figure 1.1: EOR Processes Classification, (Farouk and Thomas, 1996)

1.4.1 Non Thermal EOR Processes

Chemical flooding, miscible solvent injection and immiscible gas drives are commonly considered as non-thermal EOR process. Chemical flooding methods are applied to recover residual oil left in the reservoir after primary and / or secondary recovery techniques. Polymer flooding, surfactant flooding, alkaline flooding and alkaline-surfactant-polymer flooding are sub-categories of chemical flooding. In solvent injection EOR process, the displacing fluid is soluble in crude oil, therefore; there will be zero interfacial tension between reservoir fluid and injected solvent. In miscible displacement, the theoretical residual oil saturation will be zero. The sub-categories of solvent injection EOR process are; miscible slug flooding, vaporizing gas drive, condensing gas drive, CO₂ flooding. In

immiscible gas drive EOR process, Inert gases or flue gases are injected in the reservoir which pushes the oil towards the producing well and maintain the reservoir pressure.

1.4.2 Thermal EOR Processes

Thermal based recovery process refers to extra heavy oil recovery processes where heat plays the major role. Thermal energy is injected into the reservoir to reduce the heavy oil viscosity and to increase the mobilization efficiency, as oil can flow easily through the porous media towards the producing well. Thermal recovery techniques have been developed over the last two decades extensively for oil sands deposit production. Thermal based recovery processes are subdivided into the In-Situ Combustion, Steam Flooding, Cyclic Steam Stimulation (CSS) and recently developed technique Steam Assisted Gravity Drainage (SAGD). Almost all of these techniques have been applied to recover heavy oil resources worldwide, especially bitumen reserves of Canada and Venezuela.

1.5 Review of SAGD Process

The most promising and emerging thermal based recovery technique is the SAGD process. The concept of SAGD was initially proposed by Butler R. (1981). Butler's proposed SAGD process contains two parallel horizontal wells vertically separated by the distance of 5m to 10 m. Steam is continuously injected into the upper well (Injector) to heat up the bitumen and reduce its viscosity, causing the heated bitumen to convert to mobile oil which drain into the lower well (Producer), where it is pumped out as shown in figure 1.2.

Cold bitumen surrounding the steam chamber is heated mainly by thermal conduction. The rising steam condenses on the boundary of chamber, heating and entraining the oil to the production well. At the initial stages, steam chamber grows vertically and when it reaches the top of the formation, it grows laterally. Oil drainage inside the steam chamber can be classified into two types, namely;

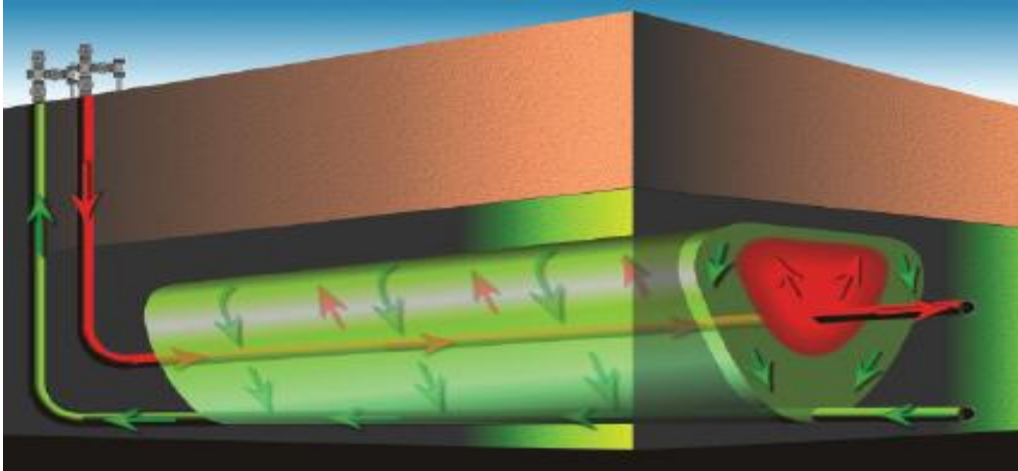


Figure 1.2: SAGD Process layout, (Norwest Corporation website)

Slope drainage and Ceiling drainage, which are differentiated by orientation of the steam front with respect to gravity. In slope drainage, heated oil flows parallel to the front of steam chamber and accumulates down the slope, while in ceiling drainage, newly heated oil is continuously pulled away from the front of steam by gravity and accumulate at the base of the steam chamber.

Since the reservoir fluid in oil sands deposit is immobile at initial reservoir conditions, it is necessary to preheat the reservoir before converting the well pair to full SAGD operation and establish an effective thermo hydraulic communication between the injector and producer wells. Vincent et. al. (2004) described three steps to initialize the SAGD operation at its full scale. In the first step, steam is circulated in both wells through tubing and annulus strings and heat transferred to vicinity of wellbore through conduction process. In the second step, a pressure differential is imposed between the injector and producer wells. In the third step, the well pair is shifted to full SAGD operations. Steam is injected through injector well continuously and grows within the reservoir to develop the steam chamber. The steam heats up the bitumen around the chamber. Heated oil and any condensed water moves down by gravity in the reservoir, where it is produced through producer well continuously. The oil production rate is controlled such that the bottom hole temperature of produced oil is a few degrees below the saturated steam temperature at the operating pressure. This temperature

differential is known as Subcool. The subcool level impacts the level of condensed fluid that builds above the horizontal producer. The steam chamber cones down below the injection well, but not into the producer well.

Numerical simulation of SAGD process has been widely studied by many researchers. For this purpose, a commercial simulator CMG STARS is mostly used to investigate the physical process and practical operation of SAGD. Chow and Butler (1996), Gittens et. al. (1992), Sui et. al. (1990), Edmunds et. al. (1988), investigated the different aspects of SAGD process using CMG STARS thermal simulator. Through numerical simulation study, Edmunds et. al. (1994) analyzed the steam trap control in SAGD operation, Ito and Suzuki (1999) predicted recovery performances of SAGD project in the Hangingstone oil sands deposit and investigated the subcooling temperature optimization, Tan et. al. (2002) investigated the importance of using discretized wellbore for SAGD model and found that a discretized wellbore simulation model is important for predicting temperature and saturation profiles accurately.

1.6 Major Challenges

The underground test facility (UTF) Phase A was constructed in 1985 at Fort McMurray, Alberta, Canada by the AOSTRA (Alberta Oil Sand Technology and Research Authority) to test the concept of SAGD proposed by Butler (1981). The SAGD process was tested from 1987 to 1990 with Phase-A involving three well pairs 50m long and 25m apart. This project was the first successful field demonstration of the SAGD process and it also provided the operational information, which was essential to its successful commercial applications. After the success of UTF Phase A project, AOSTRA carried out Phase B project at UTF to further investigate the commercial viability of SAGD process. This time they drilled five additional well pairs with 500m length and 70m apart. This pilot project was operated until 2004 and reported as successful with ultimate recovery of 65% and steam oil ratio (SOR) of 2.5, (Edmunds et. al. 1988; Gittens et. al. 1992; Mukherjee et. al. 1995).

SAGD technique successfully applied to UTF project and provided promising results, which encouraged many operators to apply SAGD technique commercially at oil sands deposit of Western Canada. In spite of successful results from some projects, field applications have shown many issues of considerable importance to the recovery performance of SAGD process. Jimenez (2008) reviewed a large database of SAGD projects in Canada and in his conclusion he emphasized the formation geology and steam trap control at wells for preventing live steam production. Farouq (1997) also indicated that formation geology has a great influence on steam chamber growth.

1.6.1 Reservoir Heterogeneity

Due to the complex depositional environment of geological formations, heterogeneity always exists in the form of shale lenses, silt layer, mixture of clay particles with sand make it dirty sand and irregular shape of formation particles itself change the reservoir permeability in horizontal and vertical directions. Sometimes within the same field, reservoir geology changes significantly from one well to another well. Reservoir heterogeneities have strong impact on SAGD performance as steam chamber growth is greatly influenced by reservoir heterogeneity. Many researchers investigated numerically and experimentally the role of reservoir heterogeneity in steam chamber growth. Albahlani and Babadagli (2008) presented detailed review about SAGD process since its generation and indicated the weaknesses and strengths of process. They discussed effects of different reservoir and fluid parameters on SAGD operations and concluded that permeability is one of the most important reservoir parameter that controls SAGD performance. Edmunds et. al. (1994) analysed reservoir heterogeneities in UTF project and discussed the influence of shale lenses on steam chamber growth. They investigated that continuous shale with few breaks will restrict steam and oil to pass counter-currently through the breaks, which will severely constrain drainage from top. Yang and Butler (1992) studied two different sorts of reservoirs, one with horizontal layers of different permeabilities and second with thin shale layers. They concluded that in the first case, higher recovery was

obtained with higher permeability in upward trend and vice versa and in second case, only a long shale barrier decreased the production whereas short horizontal shale barriers have no significant effect on SAGD performance. Begci (2004) investigated the effect of fractures on SAGD process and observed that vertical fractures improved SAGD performance. He also indicated that vertical fractures could also be used to increase the initial oil production rate.

1.6.2 Temperature Control

In SAGD process, steam chamber growth and movement can only be obtained through temperature sensors. Therefore, vertical observation wells are drilled along the horizontal well length of each pair to deploy down hole gauges permanently. Temperature data obtained from observation wells have great potential in providing better insight of steam chamber propagation. Data obtained from temperature sensors also provide essential information about vertical heterogeneity of reservoir. Gotawala and Gates (2008) summarized the rise rate data for SAGD steam chambers from field operations. These rise data were strongly dependent on bitumen viscosity which is strong function of the steam temperature. Li et al. (2010) provided a method that evaluates the reservoir characterization using down-hole temperature measurements. Gul et al. (2011) included temperature data along with dynamic production data for direct characterization of reservoir heterogeneity. Moreover, accurate measurement of reservoir temperature after steam injection helps in efficient steam trap control. A steam trap control is usually used as an operational control to minimize steam withdrawal from the steam chamber in the reservoir, Doan et. al. (1999). It is managed by adjusting the fluid production rate in such a way that the temperature of produced fluid remains below the steam saturation temperature by a preset subcooling temperature. Das (2005) observed a positive effect of subcool temperature of more than 20 °C. Edmunds (1998) analyzed steam trap control in SAGD process with thermodynamic approach and found that a steam trap of 20 - 30 °C is optimum for a specific case. He also suggested three techniques of steam trap controls in numerical simulation. First, set injection and production pressures

to the same value. Second, to use a gas rate as a production constraint to produce a small amount of steam. Third is a thermodynamic approach based on a downhole thermocouple to estimate the reservoir bottom hole temperature.

1.7 History Matching Process in Reservoir Simulation

One of the main reasons for performing a reservoir simulation is to predict the future performance of reservoir in relation to increase the oil or gas recovery and to reduce the capital investment through proper reservoir management. The procedure of adjusting the variables in reservoir simulation model to match field observations of fluid rates, fluid ratios, pressure, temperature, saturations and other variables is known as History Matching. This process starts with the building of an initial reservoir model on the basis of available geological and reservoir fluid properties data. Then adjust this simulation model until the model predicted data matches the historical data observed at field location. Finally, use this adjusted model to predict the future performance of reservoir. In many cases, general geological information also needs to be honoured, for example; porosity and permeability values at core hole location, variogram structure, near field geological analogy. History matching process requires the minimization of the square of the mismatch between all predictions and observations, (Gu and Oliver, 2005). It also needs numerous iterations or runs that make the process very costly and time consuming. History matching is not only difficult to solve but it is also non-unique inverse problem, which makes future predictions non-unique. An important application of history matching is to estimate the uncertainty in reservoir parameters which are least known such as reservoir temperature and pressure, fluid saturations, reservoir permeability and porosity from field measurements indirectly. The accuracy of a history matching method depends on the quality of the simulation model and the quality and quantity of observed data.

Traditional history match process is a trial-and-error method. The reservoir engineer investigates the difference between simulated and measured data and makes manual changes to the simulation model in order to minimize the

difference. The success of the manual history matching depends on the engineer's knowledge about the reservoir simulation and experience of field operations. Jansen et al. (2009) discussed three drawbacks of manual history match technique. First, it is usually performed on a campaign basis after years because it is time consuming approach. Second, the updated models often violate essential geological constraints. Third, manually history matched models may reproduce the production data perfectly but have no predictive capacity because they have been over fitted by adjusting a large number of unknown reservoir parameters using much smaller number of observations.

To overcome these limitations, lot of research has been carried out to develop new history matching methods called as automatic history matching. It is the same traditional history matching process, but assisted by a computer. This is achieved by calculating the mismatch between measured and simulated data in an objective function. Objective function is defined as the difference between simulated and measured data. The objective function can be minimized using gradient based or non gradient based optimization algorithm, to achieve the optimal results for the history matching parameters. Gradient based methods apply deterministic algorithms which use traditional optimization approaches to obtain a local minimum of the objective function. This is done by calculating the gradient of the objective function and then determining the direction of the optimization search, (Zhang and Reynolds, 2002). Commonly well-known gradient based optimization algorithms are, Steepest decent method, Levenberg-Marquardt algorithm, Gaussian-Newton method, Quasi-Newton method and Conjugate Gradient algorithm. Non gradient based methods are stochastic algorithms which take considerable computational time as compared to gradient based methods and theoretically reach the global optimum. They require a large number of simulation runs to converge and are usually used to quantify the uncertainty of performance predicted by equally probable models. Some well-known non-gradient based methods are; Simulating annealing, Evolutionary algorithms, Genetic algorithm and Kalman Filter.

Chapter 2

Theoretical Framework of EnKF*

This chapter will present a comprehensive review of important aspects to understand the Ensemble Kalman Filter (EnKF). Then it focuses on the algorithm formulation and the theoretical framework. There are several techniques to automatic history matching which differ in the way they use the parameter set that minimizes the objective function. One approach which is widely used to address the history matching problem is data assimilation. It combines a mathematical physical model with available observations in order to estimate the current state and predict future performance of reservoir.

2.1 Statistics Fundamentals

Statistics are properties of the sample variable and statistical models are to be used in predictive and stochastic mode, awaiting more data for deterministic knowledge. Statistical models create realizations of what could happen and process those realizations to assess the results. Here we briefly describe the basic terminology and principles that are necessary to understand the Ensemble Kalman Filter theory. The statistics terms given here are short overview of some of the fundamentals, providing a basis for understanding the filter theory.

2.1.1 Uncertainty

Numerical model would be found erroneous, if un-sampled formation is drilled and take some measurements of reservoir properties.

*Some sections of this chapter have been taken from the paper (WHOC11-568) presented at World Heavy Oil Congress Conference 2011, held at Edmonton AB, Canada, on March 15 - 17. (Gul et. al., 2011)

There will also be uncertainty in reservoir state variables (pressure, temperature and saturations) predictions related to the reservoir parameters (porosity and permeability). This uncertainty exists because of lack of knowledge about reservoir parameters which are responsible to predict the state of reservoir. Uncertainty can't be ignored but can be reduced by consideration of all relevant data and can be managed. In conceptualized numerical models, uncertainty should be quantified in each of inputs and transfer the input uncertainty through to output uncertainty. An optimal decision can be made in the presence of range of uncertainty in any predicted variable.

2.1.2 Random Variables (RVs)

Random occurrence is the probability that some event in a sample space will occur. A random variable is a series of outcomes, each with a certain probability or frequency of occurrence. There are two types of RVs, discrete and continuous variables. Discrete variables take one value from a set of discrete values and continuous variables take their values continuously between a range of possible values. Upper case letters X, Y, Z... denote a RVs that are not known precisely and their possible outcomes are denoted with the corresponding small letters $\{x_i, y_i, z_i, \text{ where } i = 1, 2, \dots, n\}$ for a discrete variables with n outcomes, or $\{x \in [x_{min}, x_{max}]\}$ for a continuous variable ranged in the interval bounded by a minimum and maximum value. A set of RVs $\{X_i, \text{ where } i = 1, 2, \dots, N\}$ is referred to as a random function, which could represent same variable at different times and locations or could represent different variables.

2.1.3 Cumulative Distribution Function (CDF)

A common function representing the probability of random variables is known as the cumulative distribution function. A real random variable is a real finite valued function and for every real number, the inequality $\{X(w) \leq x \dots\}$ defines a set of w whose probability is defined. The cumulative distribution function (CDF) is given as

$$F_x = \Pr[X(w) \leq x] \in [0,1] \quad (2.1)$$

A CDF provides the probability for the random variable not to exceed a given threshold value x as shown in figure 2.1.

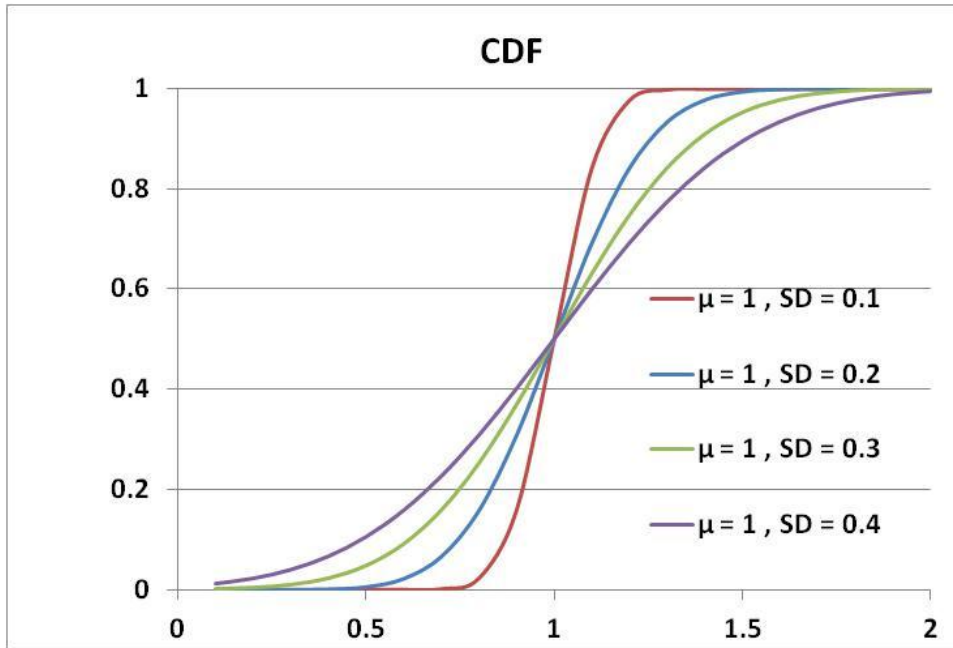


Figure 2.1: Cumulative Distribution Function

2.1.4 Probability Density Function (PDF)

A PDF is defined as the derivative of the CDF at x values of non-discontinuity. It describes the probability that a random variable X will take a particular value x . The PDF must satisfy some properties such as, slope of a non-decreasing function is non-negative, integral of the derivative is back to the function and integrates to 1 at plus infinity. There exist many distributions for random variables, the most common is the normal or Gaussian distribution. The normal distribution PDF is given by

$$f_X(x) = \frac{1}{\sqrt{2\pi}\sigma} \left[-\frac{1}{2\sigma^2} (x - E[X])^2 \right] \quad (2.2)$$

Figure 2.2 shows the PDF of above CDF graphs;

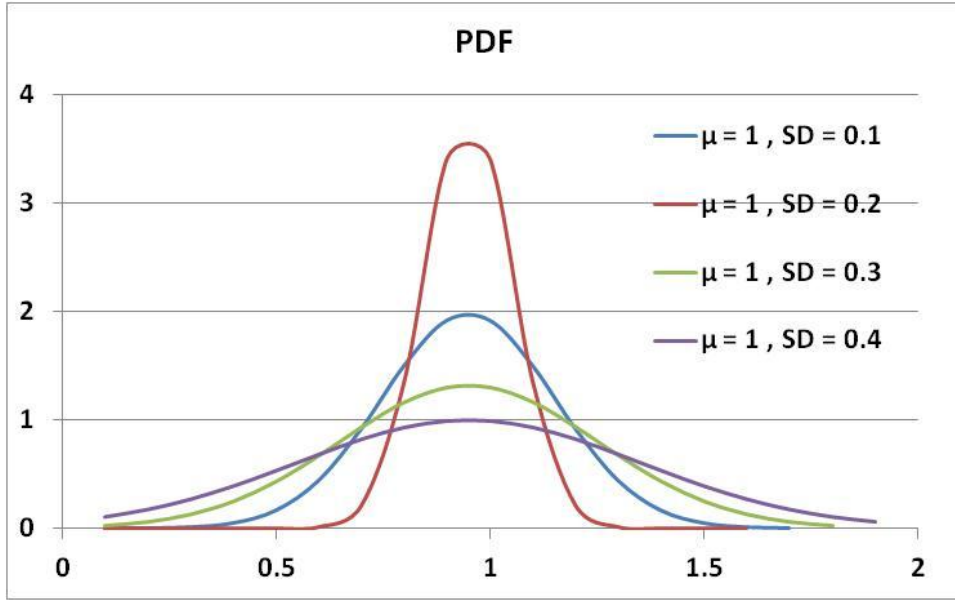


Figure 2.2: Probability Density Function

2.1.5 Expected Values and Mean

The expected value of a random variable is the integral of that random variable with respect to its probability measure.

$$E\{X\} = \int_{-\infty}^{\infty} x.f(x)dx \tag{2.2}$$

For some N samples of random variable X , the probability weighted average is known as mean of all samples.

$$m = \bar{X} = \frac{1}{N} \sum_{i=1}^N x_i \tag{2.3}$$

Often, mean is obtained by analytical equation for most parametric distributions but solved with numerically for discrete data. The expected value or mean of random variable is also known as the moment of order one and it can be interpreted as the center of mass of the PDF.

2.1.6 Variance and Standard Deviation

The variance of a random variable is a measure of statistical dispersion, averaging the squared distance of its possible values from the mean. The variance of X , denoted by $VAR(X)$ or σ^2 is

$$\sigma^2 = E[X - m]^2 = \frac{1}{N-1} \sum_{i=1}^N (x_i - m)^2 \quad (2.4)$$

Where, $N-1$ is used rather than N to provide an unbiased estimator for the variance. The square root of a variance is called as the Standard Deviation. It is also a useful statistical unit of measure because it has the same units as the original property. The standard deviation is denoted as σ .

2.1.7 Covariance and Correlation Coefficient

The covariance is the natural extension of variance and it measures how much two variables change together. The covariance of X and Y , denoted by $COV[X, Y]$ is

$$COV[X, Y] = E[(X - m_x)(Y - m_y)] = E[XY] - m_x m_y \quad (2.5)$$

The covariance between the same variable is its variance. Correlation coefficient is a standardized measure, a correlation of 1 implies that two variables are perfectly correlated and zero correlation between two variables means both are independent.

$$\rho_{XY} = \frac{COV[X, Y]}{\sigma_x \sigma_y} \quad (2.6)$$

2.1.8 Gaussian Probability Distribution

Random variables have a particular distribution given by their PDF. There exist many distributions for a random variables but the most common is the normal or Gaussian distribution. A Gaussian function is the probability function of the normal distribution in the form of

$$f_X(x) = \frac{1}{\sigma\sqrt{2\pi}} e^{-(x-m)^2/2\sigma^2} \quad (2.7)$$

where, $X \sim N(m, \sigma^2)$ is also expressing that a random variable X is normally distributed with a mean value m and standard deviation σ . If X is a vector of Gaussian distributed random variables with mean m and covariance matrix Q then this can be denoted as $X \sim N(m, Q)$. The diagonal elements of Q denotes the variance for each of the random variables in X and off-diagonal elements represent the covariance between the variables.

2.1.9 Variogram Model

The expected squared difference between two data values separated by a distance vector h is known as Variogram. Consider a random variable X with known mean m and variance σ^2 , independent of location. Often there are areal and vertical trends in the mean m , which are handled by a deterministic modeling of the mean. The variogram is defined as

$$2\gamma(h) = E\{[X(u) - X(u+h)]^2\} \quad (2.8)$$

The semi-variogram $\gamma(h)$ is one half of the variogram $2\gamma(h)$. In literature, to avoid excessive jargon, it is simply referred to as the variogram, except where mathematical difficulty requires a precise definition. The variogram is a measure of spatial variability, it increases as sample becomes more dissimilar. The covariance is statistical measure that is used to measure correlation, it is a measure of similarity. Expanding the square in equation leads to following relation between the variogram and covariance;

$$\gamma(h) = \sigma^2 - C(h) \quad (2.9)$$

This relation is the foundation for variogram interpretation. The sill of the variogram is the variance, which is the variogram value that corresponds to zero correlation. The correlation between $X(u)$ and $X(u+h)$ is positive when the variogram value is less than sill and vice versa. Geostatistical modeling generally

uses the variogram instead of covariance, the variogram is a measure of geological variability versus distance. The geological variability is quite different in different directions.

2.2 Kalman Filter (KF)

One of the most famous data assimilation techniques is the Kalman Filter method, introduced by Rudolph E. Kalman (1960). He described a recursive solution to the discrete data linear filtering problem. The Kalman Filter is a set of mathematical equations that provides an efficient computational means to estimate the state of a process, in a way that minimizes the mean of squared error. The filter is very powerful in several aspects, it supports estimations of past, present and future states and it can do so even when the precise nature of the modeled system is unknown. It estimates the state of a linear dynamic system from a series of noisy measurements, (Sorenson, 1970; Gelb, 1974; Maybeck, 1979; Lewis, 1986; Brown and Hwang, 1992; Grewal and Andrews, 1993; Jacobs, 1993; Stengel, 1994).

The basic equations for the discrete Kalman Filter for a simple linear system have been discussed below;

$$y_k^p = Ay_{k-1}^a \quad (2.10)$$

$$C_{y_k^p} = AC_{y_{k-1}^a}A^T + C_\varepsilon \quad (2.11)$$

Here y_k represents the system state at time t_k and y_{k-1} is the system state at previous time step t_{k-1} . A is the matrix describing the dynamics of the system; where C_y is covariance matrix of the state vector of the system and C_ε is covariance matrix representing the model noise. Superscripts p and a represent *predicted* and *analysed* states of system.

The update step is where the analysed estimates are computed. The analysed state updated using the following equation

$$y_k^a = y_k^p + K_k(d_{obs,k} - Hy_k^p) \quad (2.12)$$

Where K is the Kalman gain matrix; d_{obs} is the observed field history and H is the matrix provides the relationship between the measurements and states. The Kalman gain can be calculated as given below

$$K_k = C_{y_k^p} H^T (H C_{y_k^p} H^T + C_{D_k})^{-1} \quad (2.13)$$

Where C_D is the covariance matrix of the measurement error and analysed covariance matrices are updated as follows

$$C_{y_k^a} = (I - K_k H) C_{y_k^p} \quad (2.14)$$

The Kalman Filter can be summarized in Algorithm 1

```

Input:  $\bar{y}_0, \rightarrow C_{y,0}, \rightarrow C_{D,0}$            %System at Initial state
k = 1
While true do
  Forward Step
   $y_k^p = A y_{k-1}^a$                        %Prediction of state one step ahead
   $C_{y_k^p} = A C_{y_{k-1}^a} A^T + C_\varepsilon$      %Prediction of Covariance matrix ahead
  Update Step
   $K_k = C_{y_k^p} H^T (H C_{y_k^p} H^T + C_{D_k})^{-1}$  %Calculation of Kalman gain
   $y_k^a = y_k^p + K_k (d_{obs,k} - H y_k^p)$  %Analysed state calculation
   $C_{y_k^a} = (I - K_k H) C_{y_k^p}$          %Update the covariance matrix
  k  $\rightarrow$  k + 1                          %Next time step
end

```

Algorithm 2.1: Basic Linear Kalman Filter (KF)

The given equations describe that the Kalman Filter technique consists of two sequential steps. One is a forecast based on solution of the dynamical equations for flow and transport in the reservoir. The other is analysis step based on data assimilation to update the model by correcting the variables describing the state of the system to honour the observations. The model for Kalman filter is referred to as the state vector, which contains all the uncertain and dynamic variables that define the state of the system. The state vector at time k is defined as

$$y_k = \begin{Bmatrix} m_k \\ u_k \\ d_k \end{Bmatrix} \quad (2.15)$$

In the Kalman Filter theory, the state vector y is augmented to include the model parameters, as well as measurements. The joint model-observation state vector can include three types of parameters. For the reservoir case, these types are the static model parameters, m_k (e.g. porosity and permeability), dynamic state variables varying with time, u_k (e.g. pressure, temperature and phase saturations) and the production data, usually measured at wells, d_k (e.g. reservoir fluid production rates, fluid production ratios, bottom hole pressure and temperature observations). Also notice that the effect of the forward step over model parameters is null, nothing happens to m_k when moving from time k to time $k+1$. They are updated in analysis step when measurement $d_{obs,k}$ matrix is available.

2.3 Extended Kalman Filter (EKF)

The extended Kalman Filter was developed for updating parameter models that are related to measured responses through a non-linear transfer function. A friendly introduction of extended Kalman Filter (EKF) can be found in books, Jazwinski (1970) and Brown and Hwang (1992). Replacing equation (2.10) with;

$$y_{k+1}^p = F_k(y_k^a) \quad (2.16)$$

Where, F_k is a suitable differentiable function. In the estimation theory, the Extended Kalman Filter (EKF) is the nonlinear version of the Kalman Filter that linearizes about the current mean and covariance. The EKF provides an approximation of the optimal minimum mean-square estimate by linearization and at each step the non-linear dynamics are linearized around the last consecutive predicted and filtered state estimates. Based on the linearized dynamics the extended Kalman Filter applies the standard Kalman Filter to obtain estimates of first and second order moments of the posterior distribution. To find a valid solution, this linearization should be a good approximation of the non-linear state

space model in the entire uncertainty domain related to the model variable estimate.

There are some problems regarding the usage of Kalman Filter and EKF with high dimensional and nonlinear dynamics. Using a KF and EKF on large dimensional problems requires some demands of storage and computation time. Given a model with n unknowns in the state vector, then the error covariance matrix will have n^2 unknowns. The update of the error covariance matrix according to equation (2.14) needs the cost of $2n$ model integrations. Consequently, Kalman Filter and EKF are not very suitable for high dimensional systems. Another issue is the linearization done in EnKF, it leads to poor error covariance updates and in some cases unstable growth. To deal with this, higher order approximations may be used, but this leads to a higher storage requirement and more calculation time.

2.4 Ensemble Kalman Filter (EnKF)

EnKF has gained popularity for reservoir monitoring and continuous model updating because of its simple formulation, the ability to account for possible model noise and error, and the relative ease of implementation for any simulators. EnKF, was first introduced by Geir Evensen in 1994 for data assimilation of nonlinear ocean models. Since its introduction, the EnKF has been applied and examined in a number of studies. Diverse applications of EnKF can be found in atmospheric modeling (Hamill and Snyder, 2000; Houtekamer and Mitchell, 2005) oceanographic modeling (Anderson and Anderson, 1999; Snyder and Zhang, 2003) hydrological modeling (Reichle et al., 2002; Chen and Zhang, 2006; Wang et al., 2009). Recently, several investigations have also illustrated promising results of the EnKF technique for continuous updating of reservoir simulation models, as an alternative to traditional history matching. This was first introduced in petroleum industry by Lorentzen et al. (2001) for real time interpretation of drilling data. Application of the EnKF to petroleum reservoir engineering was introduced by Naevdal et al. (2002), and has been reviewed by Aanosen et al. (2009), other researchers who applied EnKF in petroleum reservoir

engineering are (Naevdel et al., 2005; Gu and Oliver, 2005; Evensen et al. 2007; Bianco et al., 2007; Oliver et al., 2008; Haugen et al., 2008; Chitralekha et al., 2010; and Nejadi et al., 2011). EnKF has a promising potential in reservoir characterization, since it has a simple conceptual formulation and can be implemented relatively easily for reservoir models. The method does not need integrations backward in time, and prohibits computation of the gradient operator or adjoint equations. An important advantage is that any reservoir simulator forward model can be used in the EnKF history matching process without additional amount of work.

EnKF is a Monte Carlo type sequential Bayesian inversion method firmly grounded on the theory of Kalman Filter. The basic idea behind the EnKF is to provide a filter used for large scale nonlinear systems. The EnKF runs multiple simulation models independently, assimilates the new measurements and updates the multiple models simultaneously. After each updating, it describes mean and variance, where mean represents the most probable model and variance represents the change range or uncertainty. The correlation between reservoir responses and reservoir parameters can be estimated from the ensemble. An estimate of uncertainty in future reservoir performance can also be obtained from the ensemble, (Gu and Oliver, 2005).

2.4.1 EnKF Formulation

The EnKF depends on initial ensemble of reservoir models conditioned to all previously available static data. The ensembles are generally generated using geostatistical interpolation techniques such as Sequential Gaussian Simulation, (Deutsche and Journal, 1998). It may be described as random samples from a multi-dimensional Gaussian prior probability distribution function (pdf) with a specified mean and variance that reflect uncertainty in these initial estimates. The process of data assimilation attempts to improve the initial estimates of these model variables that could include the spatial distribution of permeability, porosity, fluid saturation, etc. The updated models comprise samples from a

posterior pdf that are consistent with all previously acquired static data and observations.

The EnKF for continuous model updating propagates an ensemble of initial reservoir realizations along time to assimilate data. The ensemble of vectors is denoted by:

$$\Psi = \{y^1, y^2, \dots, y^{N_e}\} \quad (2.17)$$

where N_e is the total number of realizations and $y_j, j = 1, \dots, N_e$ are state vectors. Each state vector consists of model parameters (m), such as porosity and permeability, state variables (u), such as pressure and saturation, which are time dependent variables, and observations (d), such as reservoir fluid production rate, producing fluids ratio, pressure and temperature records. At a certain time step t_k for $k = 1 \dots N_t$, the state vector for reservoir simulation model is represented as;

$$y_k = \begin{Bmatrix} m_k \\ u_k \\ d_k \end{Bmatrix} \quad (2.18)$$

where, k denotes the time step in which data are assimilated.

The main idea of EnKF for data assimilation contains two sequential steps. One is the *forecast step*, in which the forecast model is applied to each ensemble separately using a reservoir simulator forward in time based on solution of the dynamical equations for flow and transportation of fluid in the porous media:

$$y_k^{p,j} = F(y_{k-1}^{a,j}) + \varepsilon^m, j = 1, \dots, N_e \quad (2.19)$$

where, $F(.)$ is the forecast operator representing the reservoir simulator and ε^m represents the model error. Subscript and superscript p and a denote the predicted and analyzed states, respectively. This step does not change the rock properties, but replace the pressure, saturation and simulated data in the predicted state vector. The initial ensemble for $k = 1$ refers to the collection of the initial state vectors, which are sampled from prior probability density function of the state

vector before any data assimilation. The forecast step is often the most computationally demanding step especially for large reservoir models and large ensemble sizes.

The other is the *analysis step*, in which model update is done by correcting the variables representing the state of the system to honour the observations. The update to each ensemble member is made by using the Kalman update formula:

$$y_k^{a,j} = y_k^{p,j} + K_e (d_k^j - H y_k^{p,j}) \quad (2.20)$$

Where, K_e is the Kalman Gain and H is the observation operator, which extracts the simulated data from the state vector y^p :

$$H = [0 \mid I] \quad (2.21)$$

Where, 0 is an $N_d \times (N_m + N_u)$ matrix with all 0 's as its entries and I is an $N_d \times N_d$ identity matrix. And d_k^j is the perturbed observation data at the k^{th} time step that has the same distribution with the observation error. An ensemble of perturbed observations is generated as:

$$d_k^j = d_{obs,k} + \varepsilon_k^{j,d} \quad (2.22)$$

Where, d_{obs} is field observed data and $\varepsilon_k^{j,d}$ is a Gaussian zero mean perturbation with covariance C_D . Since the noises in the observations are often uncorrelated, C_D is a diagonal matrix. The ensemble Kalman gain K_e is defined as:

$$K_e = C_{y_k^p} H^T (H C_{y_k^p} H^T + C_{D_k})^{-1} \quad (2.23)$$

Where, $C_{y_k^p}$ is the state cross covariance matrix, and C_{D_k} is the error covariance matrix. The cross covariance matrix is calculated as:

$$C_{y_k^p} = \frac{1}{N_e - 1} \sum_{j=1}^{N_e} \left\{ \left(y_j^p - \overline{y^p} \right) \left(y_j^p - \overline{y^p} \right)^T \right\} \quad (2.24)$$

Where, $\overline{y^p}$ is the mean of the N_e ensemble members at the current data assimilation step. Since only partial entries of the cross covariance are required in equation (2.24), there is no need to calculate entire matrix. Equation (2.23) can be simply reduced to:

$$K_e = C_{yd} (C_{dd} + C_D)^{-1} \quad (2.25)$$

Where, C_{yd} represents the cross covariance matrix between model parameters and simulated data, C_{dd} is the covariance matrix of simulated data and C_D is the observation error covariance matrix.

The Ensemble Kalman Filter is summarized in algorithm 2.2.

2.4.2 EnKF Advantages

The EnKF is a new technique and computationally efficient as compared to the traditional gradient based methods. They have been around for a long time and several modifications have been done since the description of these methods, Dougherty (1972). EnKF is derivative free, it does not rely on the specific reservoir simulator, and it only requires output from simulator. Coding for the EnKF algorithm can be adjusted to any reservoir simulator on a plug-in basis, (Gu and Oliver, 2005). EnKF method also reduces a nonlinear minimization problem in a large parameter space involving the minimization of an objective function with multiple local minima to a statistical minimization problem in the ensemble space.

Thus, by searching for the mean rather than many modes of the posterior pdf, the technique prevents getting trapped in local minima, (Evensen et. al., 2007). Finally, EnKF technique takes one simulation run per realization and each one is independent with the others. There are far fewer runs than other methods, such as RML and it samples more efficiently than most MCMC methods do, (Gao et. al., 2006).

```

Input: Q, R, dobs
Ψ → Generate Initial Ensemble of model parameters
y0j → The number of initial states of system, as per number of realizations
For k = 1 : tk
While true do
    Forward Step
    εm → Calculate model noise as N(0, Q)
    ykp,j = F(yk-1a,j) + εm %Forward Step
    Cykp =  $\frac{1}{N_e - 1} \sum_{j=1}^{N_e} \left\{ \left( y_j^p - \overline{y^p} \right) \left( y_j^p - \overline{y^p} \right)^T \right\}$  %Covariance calculation
    Update Step
    εkj,d → Calculate measurement noise as N(0, R)
    dkj = dobs,k + εkj,d %Perturbed measurements
    Ke = Cykp HT (H Cykp HT + CDk)-1 %Kalman gain calculation
    yka,j = ykp,j + Ke (dkj - H ykp,j) %update model parameters
    k → k + 1 %next time step
end

```

Algorithm 2.2: Ensemble Kalman Filter (EnKF)

The main advantage of the Ensemble Kalman Filter is that it is a Bayesian Approach. EnKF is initialized by generating permeability and /or porosity fields using prior geostatistical assumptions. The production data are assimilated sequentially with time, and the porosity and permeability fields are updated as new production data are introduced. Along with the model parameters (porosity and permeability), the state variables (fluid saturation and pressure) also get updated which is suitable for online updating of the model. The estimated fields depend on the initial ensemble that is generated stochastically. The EnKF works very well when the prior probability distributions are Gaussian and when the

relationships between the model parameters, state variables and measurement data are linear.

2.4.3 EnKF Disadvantages

Generally, there are two approximations made in the EnKF;

- The update is based on covariance matrices only
- These covariance matrices are calculated from a finite ensemble size.

In first approximation, third and higher order moments of the joint pdf of the model variables (including parameters and predicted observations) are neglected, which makes it difficult to maintain a priori imposed non-Gaussian distributions. Therefore, EnKF update step neglects any non-Gaussian contributions in the predicted pdf, when the update increments are computed. But the updated ensemble will inherit the non-Gaussian contributions already present in the forecast ensemble. The use of truncated pluri-Gaussian method (Agbalaka and Oliver, 2008) and Gaussian mixture models (Dovera and Rossa, 2007) can be referred to as possible ways to handle non-Gaussian prior models in EnKF.

In the second approximation, the use of limited number of model realization, introduces errors in the covariance estimation, leading to incorrect updates. Such errors tend to lead to systematic under-estimation of model error variances and eventually to filter divergence, (Hamil and Whitaker, 2001). Aanonsen et. al. (2009) provided many practical experiences from previous work which show that similar problems can be encountered when large number of relatively accurate data are assimilated. By applying local analysis and covariance localization, one can handle this issue of large number of measurements.

Chapter 3

EnKF for Continuous Reservoir Model

Updating*

3.1 EnKF Workflow for History Matching Problems

The EnKF offers an ideal setting for real time updating and prediction in reservoir simulation models. At each time step, new observations are available and are assimilated to improve the model parameters (permeability) and the associated state variables (saturation, temperature and pressure). Therefore, the analyzed ensemble provides optimal realizations that are conditioned on all previous data, these ensemble realizations can also be used in a prediction of future production and field planning strategy. Evensen et al. (2007), Bianco et al. (2007) and some other researchers applied EnKF technique to full field models and obtained good history match results. Seiler et al. (2009) discussed three major steps involved in EnKF based history matching workflow;

- Parameterization, identification of most uncertain parameters and at the same time characterize the major uncertainty of the model solution
- A priori error model, based on the initial uncertainty analysis, error model is specified for the selected parameters
- A solution method, it is required to be selected to minimize the prior error

These three steps are equally important and the quality of the EnKF based history matching will depend how accurately these steps are performed. The uncertain

*Some sections of this chapter have been taken from the paper (WHOC11-568) presented at World Heavy Oil Congress Conference 2011, held at Edmonton AB, Canada, on March 15 - 17. (Gul et. al., 2011)

parameters must be selected on the basis of sensitivity and effectiveness. The EnKF is not limited by number of model parameters, because the dimension of the inverse problem is reduced to the number of realizations included in the ensemble. Therefore, the solution is searched for in the space spanned by the ensemble members rather than the high dimensional parameter space, (Evensen et. al., 2007). An initial uncertainty analysis leads to a quantification of the prior uncertainties of the parameters, which is then presented using pdf (probability density function). The specified pdfs then represent our prior belief concerning the uncertainty of a particular parameter selected by parameterization. Geostatistical simulations are used to generate multiple realizations of the model parameters based on the available geological information. The model parameters are generally characterized by a Gaussian distribution with mean equal to the best estimate and standard deviation reflecting the uncertainty spread. Variograms are used to describe the geological continuity of 'homogeneously heterogeneous' properties. Therefore, variograms are typically best suited for establishing continuity of model parameters within layers or facies bodies, (Caers, 2003). Generally, the initial ensemble consists of 30, 50 or 100 realizations of a Gaussian random field with constant mean parameter value (e.g. permeability) and a selected variogram function. The permeability distribution can also be constrained at the measured values from core samples obtained at well locations. The reservoir state variables (e.g. pressure, temperature and saturation) grid cell values are included in the initial ensemble through an initialization using the flow simulator. The production variables, such as oil production rate, steam oil ratio, etc. are needed to update the model state at analysis step, but these variables may contain contaminated data that could result in inconsistent updates, possibly leading to model instabilities. Thus, appropriate production observation errors are added to get rid of the possible data contamination. Observation errors are computed as Gaussian distribution with a mean zero and standard deviation relative to the actual value of the observations.

When an initial ensemble of permeability realizations is generated, the EnKF is used to update the ensemble sequentially in time to honour the new production

measurements at the time they arrive. The EnKF technique for history matching consists of a forward step to generate the forecast ensemble, followed by the updating of state vector to generate the analyzed ensemble, as shown in the Figure 3.1.

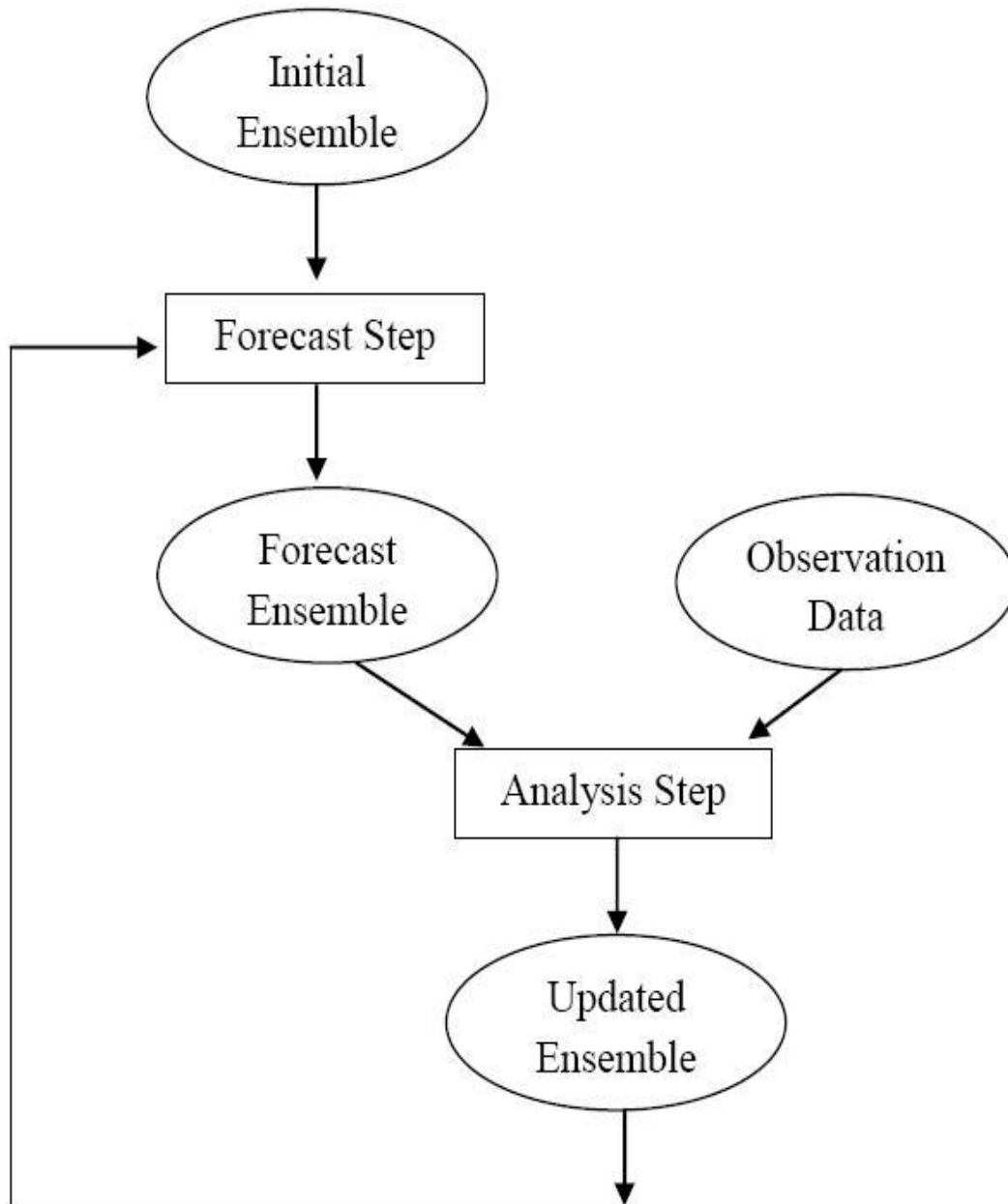


Figure 3.1: EnKF Workflow for History Match Problems, (Seiler et. al. 2009)

The assimilated measurements are considered as random variables having a Gaussian distribution with mean equal to measured value and an error covariance

reflecting the accuracy of the measurement. The updated ensemble is then integrated until the next update step. The result is an updated ensemble of realizations, conditioned on all previous data and thus gives the optimal starting point for predictions of future production, (Seiler et al., 2009).

3.2 Constrained EnKF

Constrained EnKF is widely discussed and applied in history matching process of reservoir simulation models since last couple of years. Due to the nonlinearity of reservoir fluid flow equations and the limited number of ensemble members used to estimate the covariance, new challenges have been commenced in standard EnKF data assimilation technique. A constrained EnKF can be a viable solution to avoid state variables from exceeding feasible bounds, (Oliver and Chen, 2011; Phale and Oliver, 2009; Wang et al., 2009). There are two type of constraints that are incorporated in EnKF technique, namely; Equality and Inequality constraints. Thacker (2007) proposed method for dealing with inequality constraints in the Kalman Filter. Phale and Oliver (2009) adapted that method for updating reservoir model using the EnKF to avoid the problem of non-physical values of state variables. Wang et al. (2009) discussed three methods of constrained EnKF.

1) Naive method:

This method is used to deals with constraints in unconstrained EnKF and set the updated state Y equal to Y_{max} directly if the nonlinear constraint is violated.

2) Projection method:

In this method, states and parameters are updated through the unconstrained EnKF and then constraints are checked for each ensemble member. The ensemble members that violate any constraints are modified by projection so that new states and parameters are contained in constrained space.

3) Accept/ Reject method:

This method checks the violation of all constraints in the forecasted and analyzed states, respectively. Once the simulation run is finished, the first loop regenerates the model error until the forecasted states obey the linear and nonlinear inequality constraints and second loop regenerates the observation error.

In this study, Naive method has been applied to improve the performance of standard EnKF for history matching. We constrained model parameters (grid permeability values) at minimum and maximum limits based on prior geological knowledge. Therefore; if grid permeability value is less than the lower limit, it became the Y_{min} and if the value is higher than upper limit then it became Y_{max} . The constraints of interest in this method are linear inequality constraints of the form

$$m_{\min} \leq m_i \leq m_{\max} \quad (2.26)$$

which is of the type satisfied by reservoir permeability. Where m is the model parameter that represents permeability value at each grid block for all ensemble members. The constraints were checked in forward step after adding model error and after updating state vector in update step. Constraints violation of model parameters can be checked at both points and if a model parameter is on or beyond the boundary of feasible region, then the inequality constraint will be replaced by equality constraint as given below;

$$m_i > m_{\max} = m_{\max} \quad (2.27)$$

$$m_i < m_{\min} = m_{\min} \quad (2.28)$$

3.2.1 Permeability Constrained EnKF

Creating the ensemble of realizations of model parameters mostly initializes the Ensemble Kalman Filter. State variables are assumed to be known for petroleum reservoirs and are provided as a static initial condition to begin with, (Oliver et al., 2011). The uncertainty in state variables is largely a result of uncertainty in model

parameters; therefore, the emphasis is mostly on estimation of model parameters. The constrained EnKF based history match technique studied and implemented here is based on unknown reservoir model parameters, i.e. grid block permeability values. Many authors emphasize the importance of permeability in reservoir engineering and it is considered as a key parameter in reservoir fluid flow calculations, (Yang and Butler, 1992; Birrell and Putnam, 2000; and Albahlani and Babadagli, 2008). However, it is a fact that knowledge about permeability is very limited and exact values can only be known at core hole locations. Because of complex geological depositional environments, permeability changes within reservoir at very short distances in horizontal and vertical directions. Nevertheless, due to enormous research and advancement in geology, geophysics and geostatistical studies, we can obtain a good initial knowledge about subsurface structures. Geologists also provide rock type, shale content and possible fractures and fault information; they study different logs and seismic data to prepare variogram models on which basis different geostatistical simulation tools generate permeability value at all grid locations, (Remy, et. al., 2009).

To avoid the spurious values of permeability after each step in EnKF, permeability was constrained based on prior geological information. Each model has its own minimum and maximum limits; to avoid an unexpected increase or decrease in the grid permeability values that can be caused by the effect of field data noise on the Kalman gain. This technique significantly improved history matching quality in terms of the permeability update, as well as in data assimilation of field measurements.

3.2.2 Temperature Constrained EnKF

The interaction between SAGD steam chamber and vertical heterogeneities can be studied from the vertical temperature observation wells. The vertical observation wells, drilled along the length of each horizontal well as well as between the well pairs, are typically instrumented with numbers of thermocouples spaced throughout the formation. From the study of temperature profile ahead of the

steam chamber, much more information about the location and movement of steam chamber can be gained analogous to pressure transient analysis.

Different numbers of grid block locations were selected in all SAGD models to assimilate the temperature data. In the selection of temperature thermocouple locations, steam chamber was considered as reference: some thermocouple location was selected at the bottom, some at center and some of them at the top of the formation. In this way, chamber growth was characterized which provided the valuable information about the anisotropy and heterogeneity of reservoir. Since the temperature changes occur at different thermocouple locations as a function of time, it is not useful to update those parameters which are not changing at particular update time step. For this reason, temperature observations were constrained as a function of time and updated only for that time when temperature was varying. It is important to note that it is possible to integrate as many thermocouple data as available into closed-loop dynamic history matching using EnKF. For sensitivity analysis, a history match case was run with a SAGD model without temperature observations assimilation.

Chapter 4

Constrained EnKF for Continuous SAGD Reservoir Model Updating - Twin Well SAGD Model*

In previous chapters, we have reviewed the unconventional heavy oil reservoirs, SAGD modeling, history matching techniques and the basic theory of Ensemble Kalman Filter (EnKF). In this chapter and upcoming two more chapters, we will implement and test the constrained EnKF to 3-dimensional SAGD thermal reservoir models. This is a unique study from its prospect that first time EnKF is applied to thermal simulation models and all models are 3-D. Also, for the first time temperature observations are included in data assimilation step to improve the history match results. The advantage of constrained EnKF is demonstrated and the different assimilation parameters are investigated.

In this chapter, the constrained EnKF technique has been implemented for history matching of two synthetic SAGD reservoir models. First model is a Twin Well SAGD (TWSAGD) model with one well pair and contains fine grid population in vertical cross section perpendicular to well direction to investigate the steam chamber growth properly. Second model is a Multi Pair SAGD (MPSAGD) model with two well pairs to investigate the quality of EnKF based history match technique at field level, where adjacent well pairs affect the fluid flow, pressure and temperature responses due to reservoir heterogeneity.

*Some sections of this chapter have been taken from the paper (WHOC11-568) presented at World Heavy Oil Congress Conference 2011, held at Edmonton AB, Canada, on March 15 - 17. (Gul et. al., 2011)

CMG-STARS advanced thermal reservoir simulator was used for the modeling. Synthetic models were built as representative of the heterogeneous oil sands deposits of McMurray formation in Athabasca region, where SAGD technique has unlocked the deep heavy oil and bitumen reserves into economical recovery that cannot be accessible with surface open-pit mining techniques.. Required data were obtained from literature describing the geological features of the formation and technical papers quoting implemented thermal recovery techniques in the area, (Gittens et al., 1992; Mukherjee et. al., 1995; Redford and Luhning, 1999; Edmunds and Gittins, 1993).

4.1 Unconventional Oil Reservoir Fluid and Rock Properties

Oil sands deposits of McMurray formation in Athabasca have a viscosity of more than 1,000,000 cp at reservoir temperature and are categorized as unconventional oil reservoir. All SAGD models in this study possess same reservoir fluid and rock properties, only well configuration and reservoir heterogeneity distribution are different for each model.

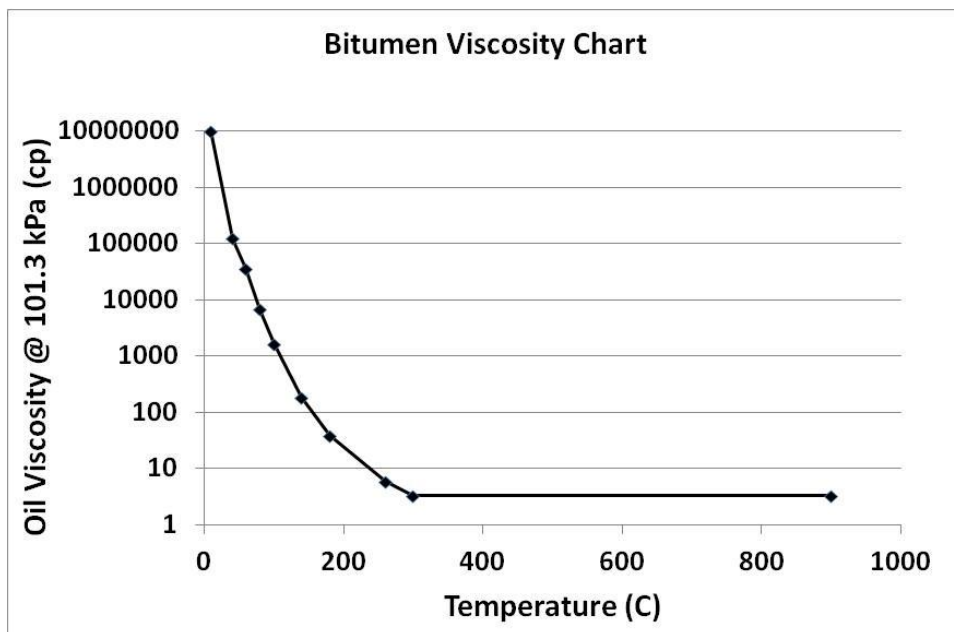


Figure 4.1: Bitumen Viscosity vs Temperature

The fluid model generated to perform the studies, consists of three phases, namely water, oil and dissolved gas. Connate water saturation was assumed 20% and dissolved gas was 10% of total bitumen saturation. Bitumen viscosity was 4 million cp at 16 C initial reservoir temperature and 2600kPa initial reservoir pressure. The relation between oil viscosity and temperature is given in Figure 4.1. Reservoir thickness is about 30 meters and no top gas, bottom water zone or thief zone is present in the reservoir. To prepare the geological model, porosity was assumed to be constant throughout the reservoir (equal to 35%), formation top was assumed at 450 m and permeability values are distributed using a stochastic representation on the basis of the geostatistical method. Relative permeability curves of oil and water verses water saturation are plotted in Figure 4.2 and relative permeability curves of gas and oil are plotted against liquid saturation in Figure 4.3. The permeability data were generated based on the core data of the observation wells and petro-physical well logs along the wellbore of horizontal wells. The geostatistical model was created using the variogram model that honours the distribution and spatial continuity from the available data. SGSim generates a number of equi-probable realizations, honouring the predetermined data (hard data). The natural logarithm of permeability $\ln(k)$ had a Gaussian histogram with mean and variance and the unit of permeability was mDarcy (mD).

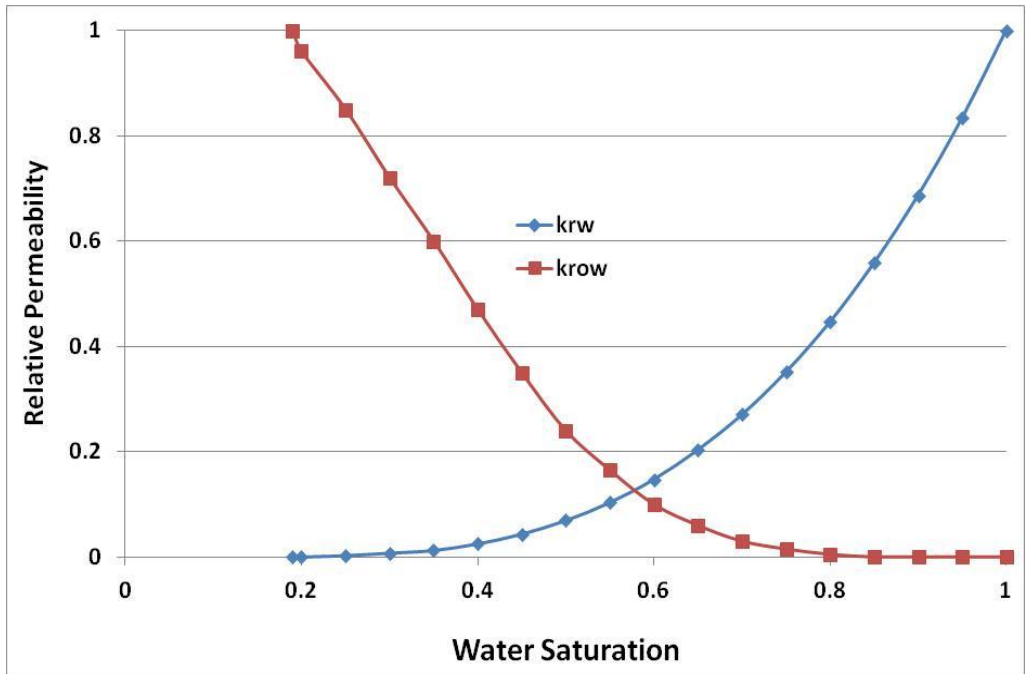


Figure 4.2: Relative Permeability of Oil and Water vs S_w

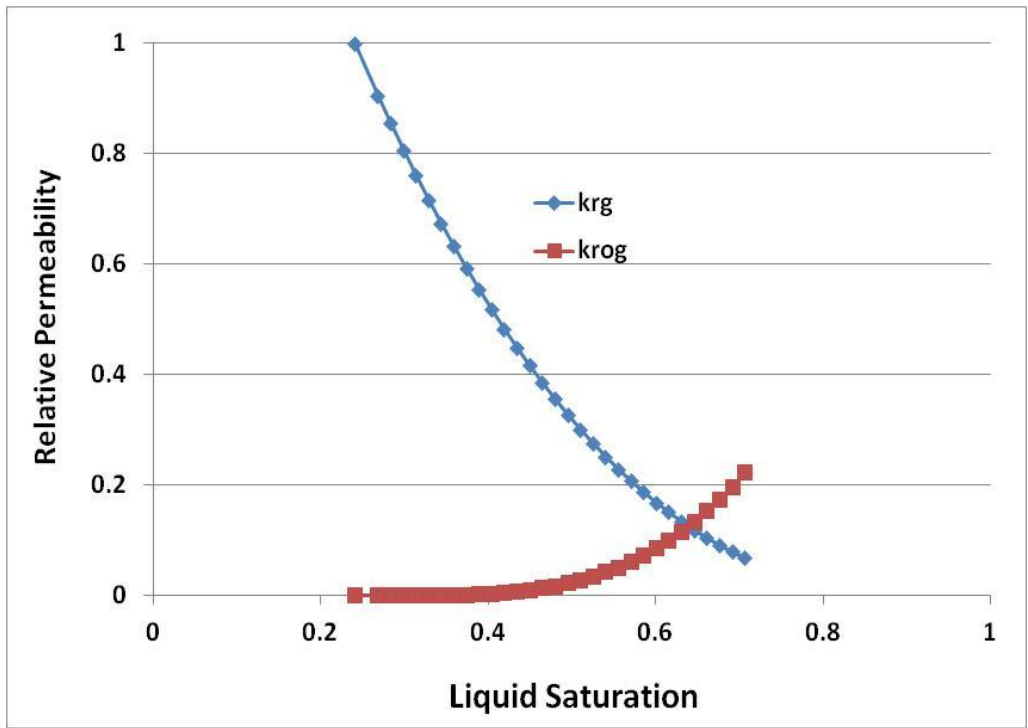


Figure 4.3: Relative Permeability of Gas and Liquid vs S_L

4.2 CASE STUDY - 1: Twin Well SAGD Model and the EnKF Scheme

This model contains 3900 grid blocks and a pair of twin horizontal SAGD wells. The model size is 50 x 3 x 26 blocks with gridblock dimensions of 2 x 200 x 1 m in x, y and z directions, respectively. A 3D model view is shown in Figure 4.4.

In this model, the horizontal well pair is in Y-direction and steam chamber will grow in X-Z cross section. Therefore, the number of grids were increased in both directions and size of each grid was refined as 2m in X-direction and 1m in Z-direction, to observe the steam chamber growth in its proper shape (Gittins et. al., 1992). Production well was located 2 m above the bottom of the formation while injector was completed parallel to the producers with 6 m spacing. The horizontal length of each well was 600 m in y-direction. Steam was injected in injector well at a maximum bottom hole pressure of 5500kPa and a maximum injection rate of 300 m³/d cold water equivalent. Injection steam quality and temperature were 90% and 270 °C respectively. Producer and

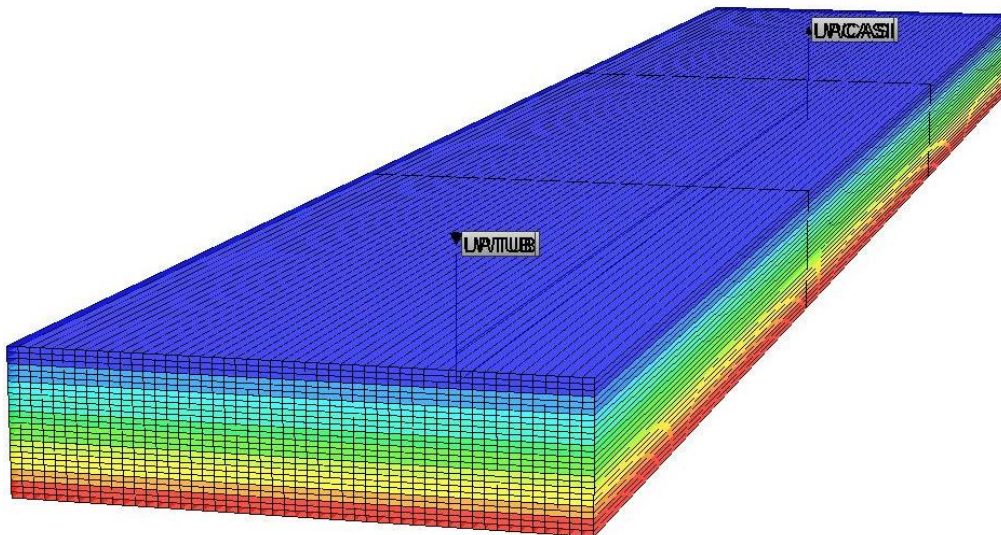


Figure 4.4: 3D view of Twin Well SAGD Model in CMG STARS Simulator

injector wells were initially circulated with 50% steam quality and 320 °C for the first four months to create communication between the wells and allow steam chamber to grow inside the reservoir. Producer well was operated at a minimum bottom hole pressure constraint of 5000 kPa, maximum liquid rate of 300 m³/d and steam rate of 10 m³/d. The reservoir rock and fluid properties are given in table 4.1

Table 4.1: TWSAGD Model Reservoir Properties

Permeability	Heterogeneously Distributed
Porosity	35%
Number of component	3 (Water, Bitumen and Dissolved Gas)
Connate Water Saturation	20%
Reservoir Initial Temperature	16 C
Reservoir Initial Pressure	2600 kPa
Bitumen viscosity	4,000,000 cp @ 16 C
Dissolved Gas in Bitumen	10% of total Bitumen Saturation
Injection Fluid	Steam
Steam Quality	90%
Injection Temperature	270 C

Stochastic simulation was used to generate several realizations of permeability field and represented the uncertainty in the property model. The realizations were conditioned to the core data and honour the trend and correlation of well log data. The initial ensemble of permeability realizations were generated using the Sequential Gaussian Simulation method SGSim [Deutsch and Journal (1998)]. The mean permeability value was taken at natural logarithm (ln) scale as 8.4 and

variance of 0.1 from core data. The spherical variogram model was selected to search simulated values with a range of 20, 3 and 10 grid blocks in the maximum, median and minimum correlation ranges respectively and zero degree angles for all directions. In Figure 4.5, we plot the special distribution of the reference permeability field (left column), and mean of initial ensemble of 30 permeability realizations (right column) of TW-SAGD model with a range from 2500 md to 7200 md values. The three cross sections between X-Z directions are plotted;

For computer assisted history matching, field observed data (oil rate, steam oil ratio and temperature observations) were prepared by using reference permeability values in simulation model and simulated dynamic data was considered as benchmark case. Measurements of oil rate and steam oil ratio (SOR) at production wells and temperature sensors data at observation wells were available at the end of each month upto 15 years. Observed data can be directly read from the file of benchmark case for history matching. The history matching was performed for a period of 9 years and the observed field data were used for assimilation every year, from Dec `10 to Dec `19. The measurement covariance matrix (R values in ϵ_k^d matrix) was selected as 1 m³, 0.01 and 1 °C for oil rate, SOR and temperature, respectively. The model covariance matrix (Q values in ϵ^m matrix) was selected as 1.0E⁻⁴ for all grid blocks.

4.3 Twin Well SAGD Model Results

The constrained EnKF based on naive method has been applied to unconventional TWSAGD thermal reservoir model is presented here. The process of data assimilation and permeability update affect each other because they are in a closed loop. Quality of results obtained by the CEnKF based history match technique will be evaluated by comparing the after history match results with the reference/benchmark data.

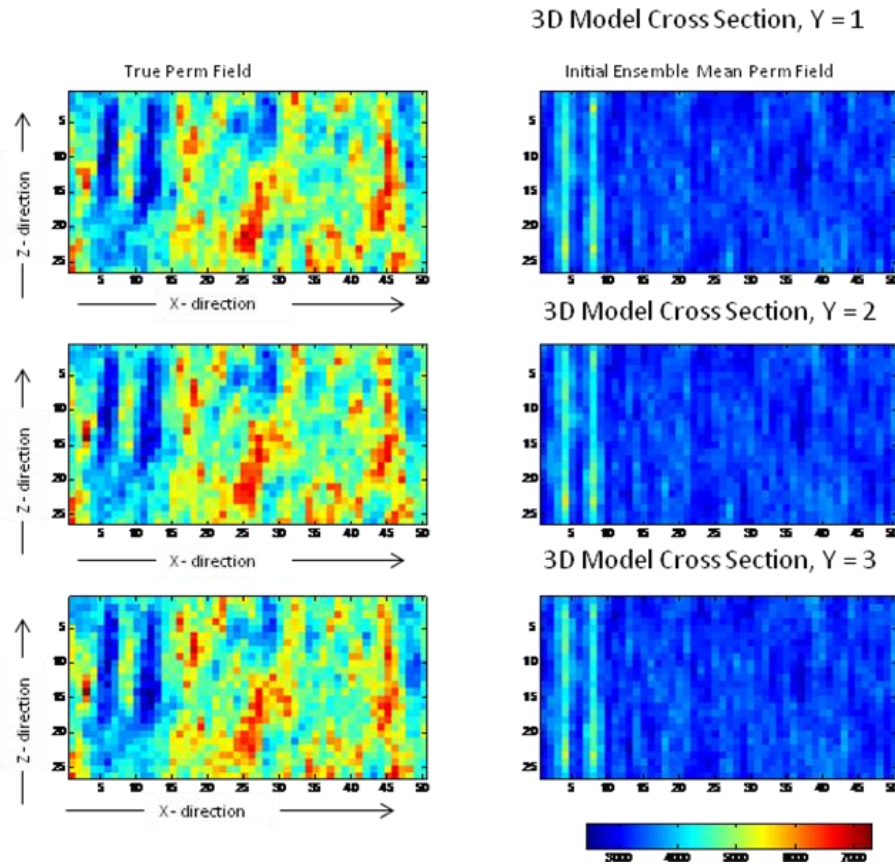


Figure 4.5: TWSAGD model X-Z cross sections, True Perm Case (left col.), and Initial Mean Perm Case (right col.)

4.3.1 Model Parameter Update

As discussed, model parameters are considered as static in nature and will not change with respect to time. But they are only known at core hole locations or near well bore. In this study, permeability is selected as tuning parameter in history matching process. Permeability vector of TWSAGD model has been tuned through Kalman gain at each update step during sequential data assimilation.

Updated mean permeability field of TW-SAGD model (Figure 4.6, right column) is improved significantly after history match process through Ensemble Kalman Filter technique. Updated mean permeability field is close to reference case as compared to the initial ensemble mean permeability field. In this model, geostatistically generated permeability field has uniform distribution whereas

updated mean permeability field contains plausible information about reservoir heterogeneity distribution throughout the reservoir. The high permeability and low permeability zones are also identified by CEnKF after updating model parameters upto 10 years. Visual comparison also suggests much improvement was obtained with the constrained EnKF method.

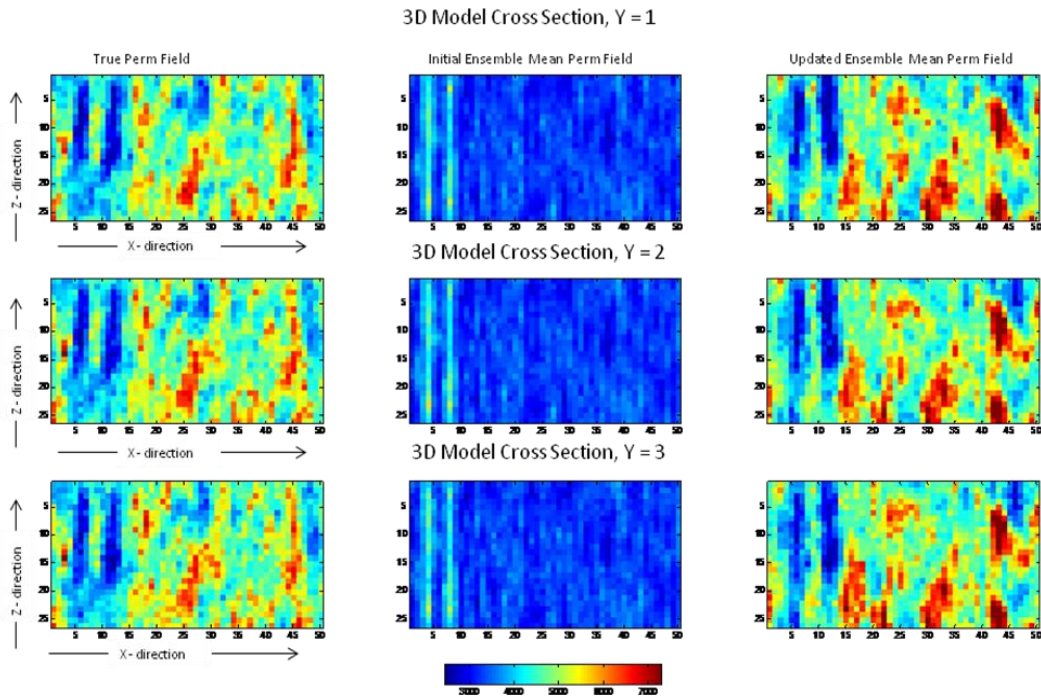


Figure 4.6: TWSAGD model X-Z cross sections, True Perm Case (left col.), Initial Mean Perm Case (mid col.) and Updated mean Perm Case (right col.)

4.3.2 Production Parameters Match

The history match results of production parameters from TWSAGD model is shown in Figure 4.7 and Figure 4.8, where oil production rate and SOR are plotted. Each figure contains two plots. Top plot represents the after history match predictions obtained by using updated permeability in simulation starting from time zero. Bottom plot represents before history match predictions forecasted using initial permeability in simulation. The redline curve represents the benchmark case result and green curves represent 30 ensemble members prediction results. The black vertical lines on both plots are showing the range of

minimum and maximum values of that parameter. In top plots, cyan vertical arrow indicates history match start date and pink vertical arrow indicates history match end date.

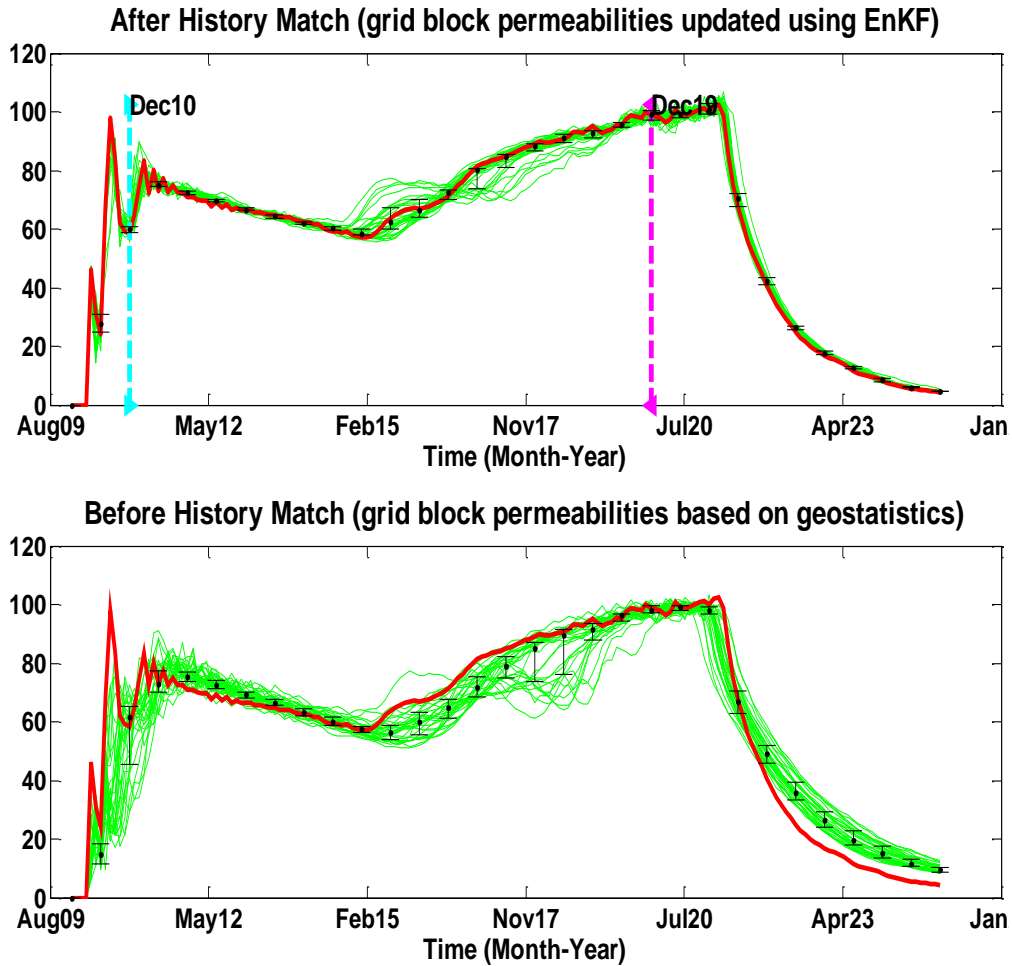


Figure 4.7: Field Oil Production Rate, m3/d, TWSAGD Model

The predictions of field oil production rate for TWSAGD model is obtained by running simulator from time zero. After history match, the oil production rate predictions are quite good from the beginning as the spread in ensemble is centered around the observation. The predictions of Cumulative SOR for TWSAGD model is a good example of improvement in predictions after history matching through CEnKF technique. All members of the ensemble move closer to the observations and uncertainty is reduced significantly.

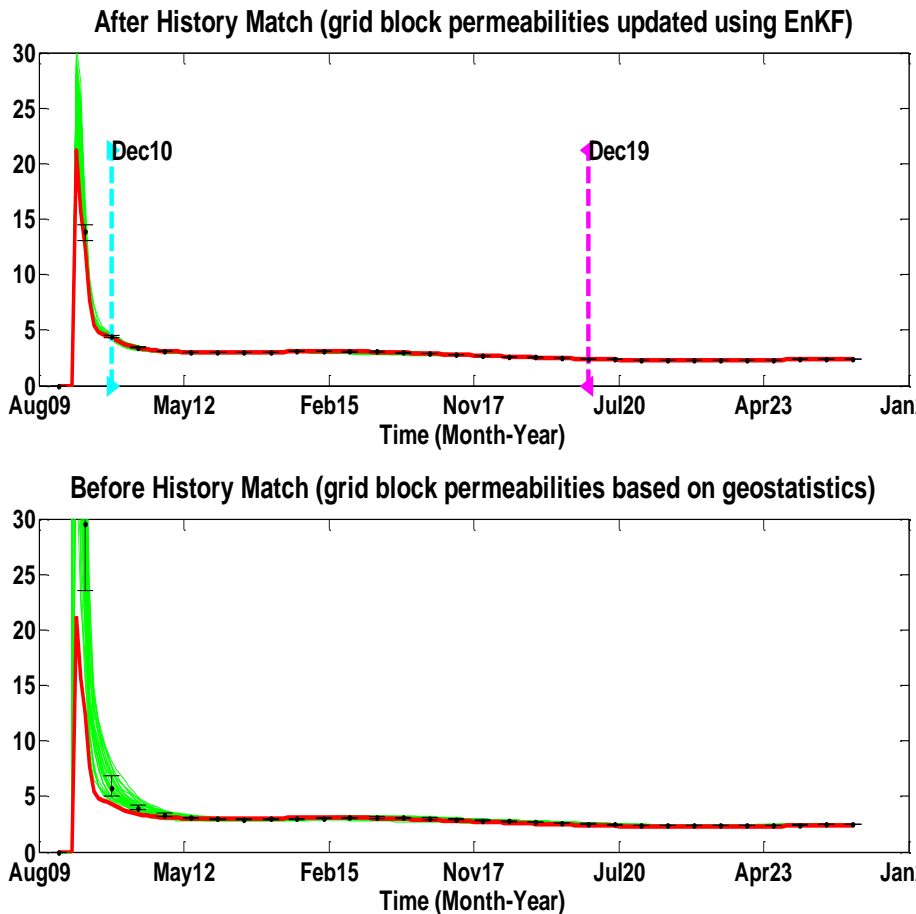


Figure 4.8: Cumulative Steam Oil Ratio, TWSAGD Model

4.3.3 Importance of Temperature Observations on History Matching Results

Figure 4.9 and Figure 4.10 illustrate the predictions of temperature observations for TWSAGD model. Significant reduction in uncertainty of temperature observations is observed after update of model parameters. It can be noticed from the resulting plots that the uncertainty is higher in temperature predictions as compared to production variables in before history matching plots of TWSAGD model. Because the mean of geostatistically generated permeability field for this case study is higher than 3000 md and at this average permeability, production fluids are less affected by heterogeneities of single facies formation. But steam

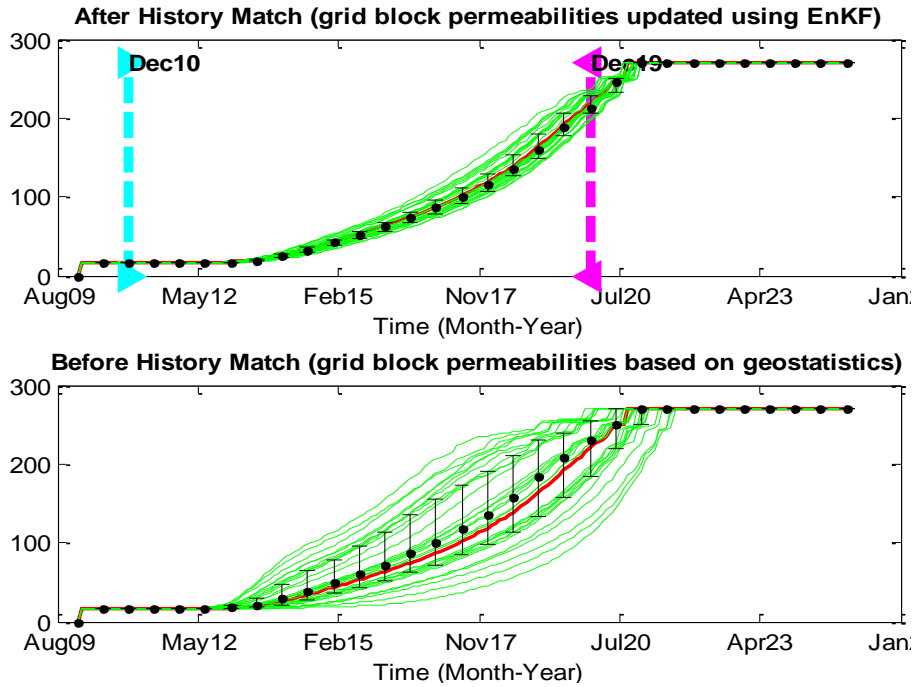


Figure 4.9: Reservoir Temperature at grid location 9, 3, 21, TWSAGD Model

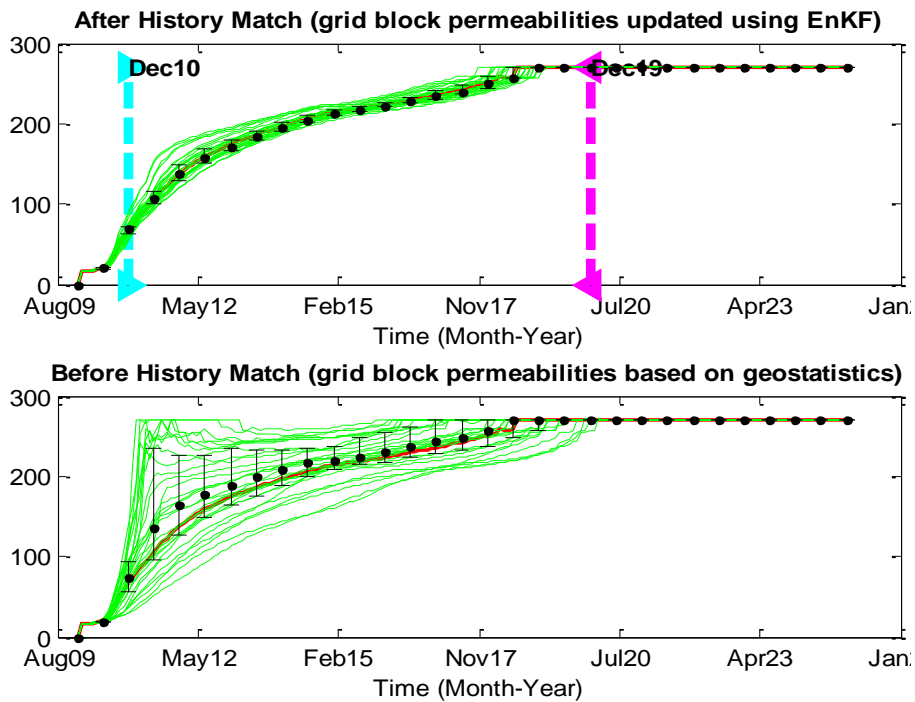


Figure 4.10: Reservoir Temperature at grid location 21, 3, 17, TWSAGD Model

chamber growth is too sensitive to permeability variations and therefore; temperature observations assimilated and estimated more reliable permeability distribution throughout the reservoir.

Gotawala and Gates (2008) summarized the rise rate data for SAGD steam chambers from field operations. These rise data were strongly dependent on oil viscosity which in turns is a function of the steam temperature. Prediction of steam chamber rise or length of steam fingers at the edge of steam chamber is usually done through temperature measurements obtained from thermocouples at many locations at different depths within observation wells. However, inclusion of these data for direct characterization of reservoir heterogeneity along with production data dynamically, has not been done to the knowledge of the author. During numerical simulation, the reservoir heterogeneity plays an important role in steam chamber/finger growth and hence the production. Incorrect representation of reservoir heterogeneity derived using only available core data may lead to false prediction of temperature as well as steam chamber rise and areal shape. This is evident from Figure 4.9 and Figure 4.10 where generated ensembles shows uncertainty in temperature predictions at grid locations 9, 3, 21 and 21, 3, 17 in twin well SAGD model. Moreover, accurate prediction of temperature in the reservoir using well characterized model helps in efficient steam trap control, generally achieved by adjusting the fluid withdrawal rate from the production well such that the temperature of the produced fluid remains below the steam saturation temperature by a preset subcooling temperature. Therefore, we have included temperature measurements in dynamic parameter updates in CEnKF.

The history matching process was constrained dynamically with temperature measurements at grid blocks 9, 3, 21 and 21, 3, 17 in TWSAGD model using temperature constrained EnKF technique discussed in section 2.4.2.2. This in turn constrains the steam chamber areal shape and rise rate. Temperature observation data has been compared at 3rd update step during history match (at the middle of steam chamber growth). Spatial distribution of the steam chamber growth height

has been compared for true, initial and updated permeability distribution in Figure 4.11 for TWSAGD model. It is evident from the figure that inclusion of temperature from observation wells has great potential in providing better insight of steam chamber propagation. Accurate information about the location and movement of steam chamber can be derived from updated ensemble model with lower uncertainty.

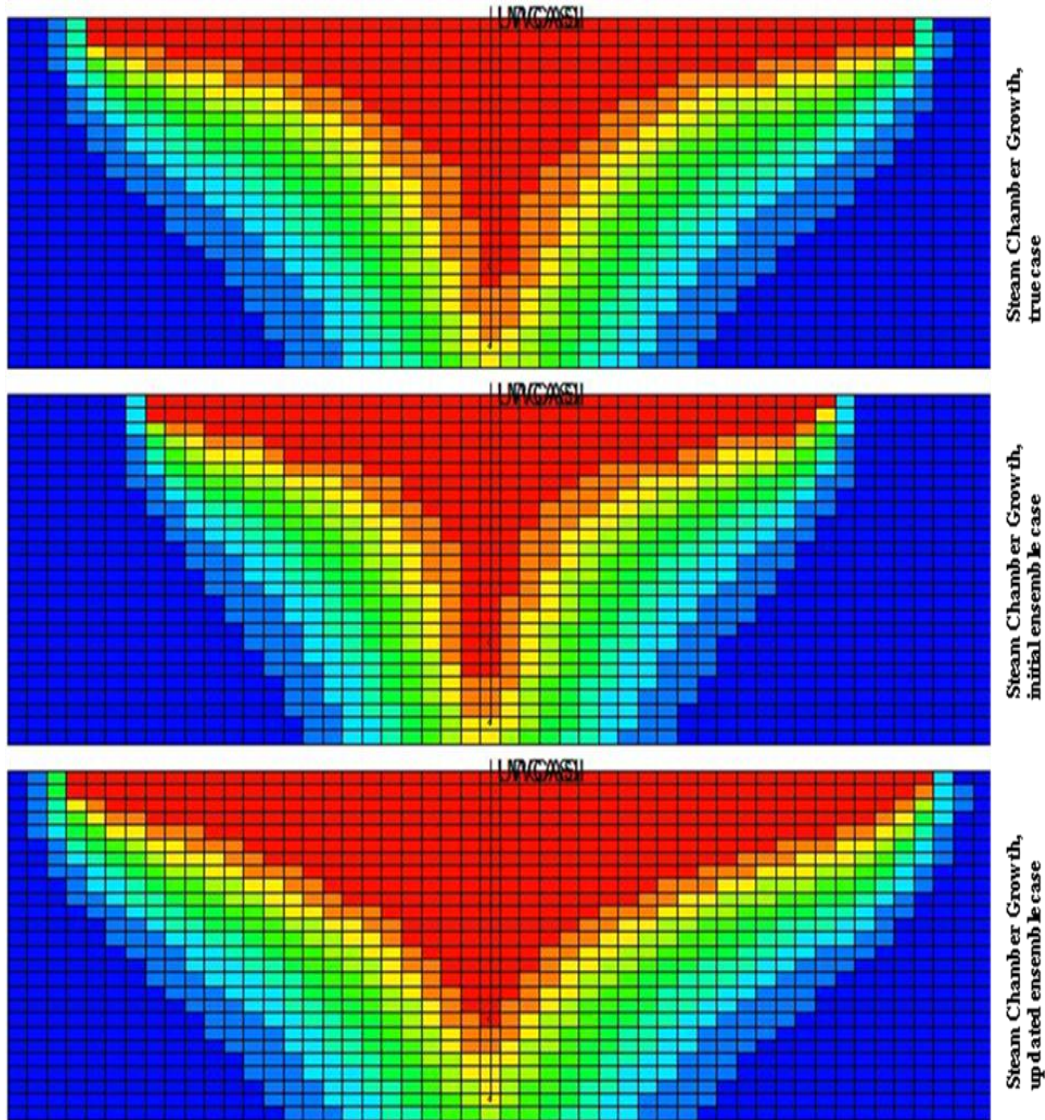


Figure 4.11: 3D model cross sections, Steam Chamber Growth in True Case (top), Steam Chamber Growth in Initial Ensemble Case (mid) and Steam Chamber Growth in Updated Ensemble Case (bottom)

4.3.4 Ranking of Realizations

During ranking the geological realization, few geological realizations are selected based on corresponding target percentile of the production response. There are different methods to rank the geological realization. The static method suggested by previous researchers (McLennan and Deutsch, 2005; Deutsch and Srivinasan, 1996) such as volumetric method (net oil in place and original oil in place), statistical measure (average properties), global connectivity and local connectivity do not incorporate the dynamic response from injection, production and observation wells. On the other hand, dynamic method so far has not been feasible in terms of computational time due to time associated with running detailed flow simulations for multiple realizations, and that too with multiple well pads. Dynamic ranking methods such as tracer production data and streamline simulations (Saad et al., 1996; Ates et al., 2005; Gilman et al., 2005) also rely on flow-physics approximations and thus undermine the geological uncertainty due to inherent simplified assumptions. The advantages of EnKF in history matching and geological characterization can replace the existing methods for ranking of realization (ensemble members).

The number of realizations used in SAGD models is 30, which is a reasonable number for the Constrained Ensemble Kalman filter. Quality of history match results can be improved if the number of realizations are increased but at the cost of a larger computational time for a single history match run. Each realization has its own uncertainty value and the error reduction is independent from rest of realizations after the history match. Hence, ranking of realizations can also be used as a useful tool to evaluate the performance and contribution of each realization towards the model parameter update at the end of the history matching process.

In this work, we have selected a different technique to rank geostatistical realizations after history match process as described by Ljung, L. (1999) and Chitrlekha et al. (2010). In this technique, the geostatistical realizations are

ranked by two methods, a) weighted mean square error and b) weighted R^2 . Weighted mean square error (WMSE) graph represent the deviation of the dynamic parameters from the benchmark case. The first realization is the best realization and the last realization has least match with benchmark case data. Figure 4.12 shows the WMSE graph;

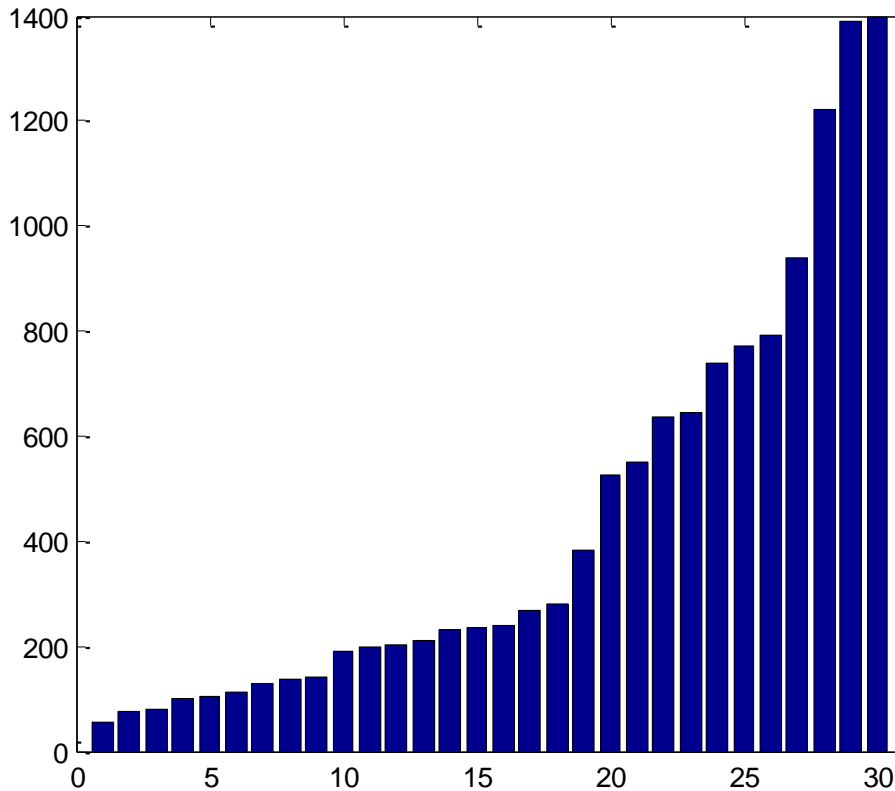


Figure 4.12: Weighted Mean Square Error (WMSE), TWSAGD Model

Weighted R^2 (WR^2) graph represent deviation of each realization from true case in terms of percentage. The realizations close to 1.0 are best fit realization and decreasing down side showing more uncertainty. From the figures mentioned above, most of the realizations show around 95% fit or more and hence significantly reduce the uncertainty in modeling and reservoir predictions. Figure 4.13 shows WR^2 graph;

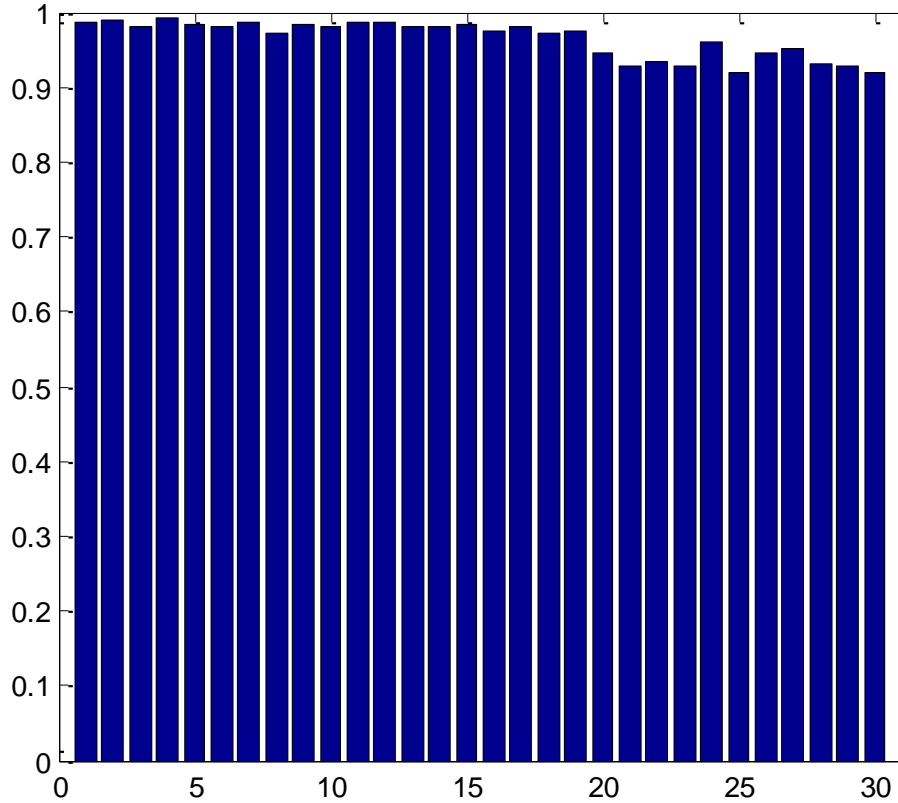


Figure 4.13: Weighted R Square (WR2) Graph, TWSAGD Model

4.4 CASE STUDY - 2: Multi Pair SAGD Model

MPSAGD (Multi Pair SAGD) model contains 2500 grid blocks and two pairs of twin horizontal SAGD wells. The dimensions of the model are 50 x 10 x 5 grid blocks which are uniformly distributed in x, y and z directions. Figure 4.14 depicts the model dimensions and well locations.

Production wells in this model are located 12 ft above the bottom of the formation while injectors are completed parallel to the producers with 25 ft spacing. The pairs are nominally spaced 300 ft apart and the completion length of each well is 3500 ft. Steam is injected in each injector well at a maximum bottom hole pressure of 500 psi and a maximum injection rate of 1000 BPD cold water equivalent. Injection steam quality and temperature are 95% and 550 °F respectively. Producer wells are shut-in for the first six months to allow steam

grow inside the reservoir and then opened at a minimum bottom hole pressure constraint of 50 psi.

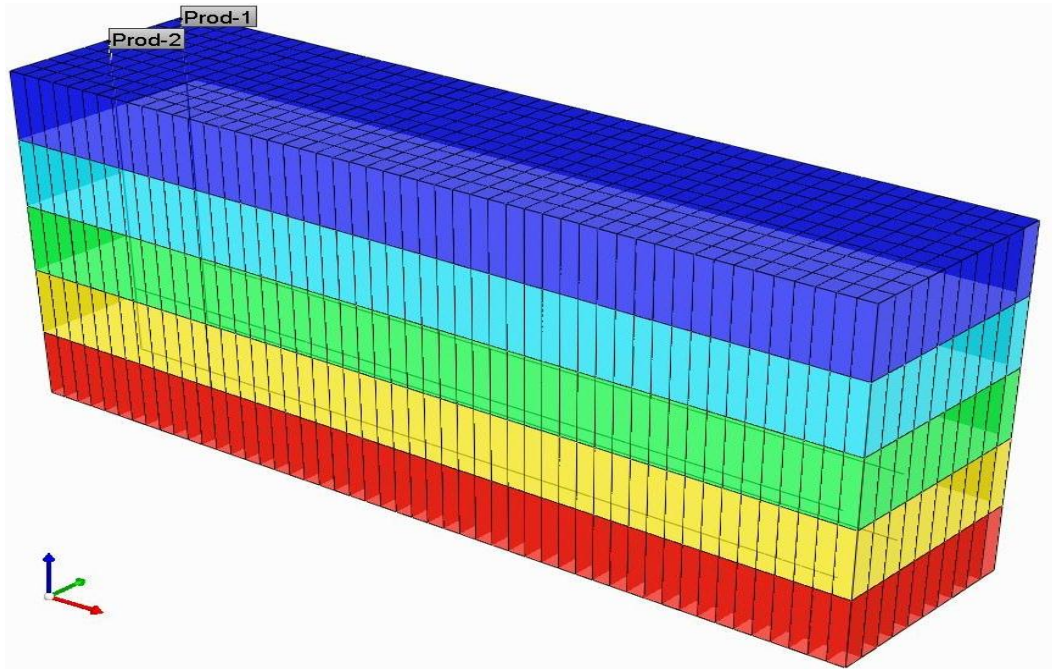


Figure 4.14: A cross section 3D view of MPSAGD Model showing the location of wells

The reservoir fluid and rock properties for MPSAGD model are given in table 4.2

Table 4.2: MPSAGD Model Reservoir Properties

Grid dim. in x, y, z-dir.	80ft x 100ft x 25ft
Porosity	35%
Horizontal Perm (k_h)	Heterogeneous
Vertical Perm (k_v)	$0.5*k_h$
Number of component	3 (Water, Bitumen and Dissolved Gas)
Connate Water Saturation	20%
Reservoir Initial Temperature	70 °F

Reservoir Initial Pressure	150 psi
Bitumen viscosity	2,000,000 cp @ 70 °F
Dissolved Gas in Bitumen	1% of total Bitumen Saturation
Formation Heat Capacity	35 BTU/(hr.ft ³ .F)
Thermal Conductivity	24 BTU/(hr.ft.F)
Injection Fluid	Steam
Steam Quality	95%
Injection Temperature	550 °F

The initial ensemble of permeability realizations were generated using the Sequential Gaussian Simulation method SGSim, (Deutsch and Journal, 1998). The permeability values were taken at natural logarithm (ln) scale from core data. The spherical variogram model was selected to search simulated values with a range of 20, 5 and 1 grid blocks in the maximum, median and minimum correlation ranges respectively and zero degree angles for all directions. Figure 4.15 and Figure 4.16 depict the reference permeability field and core hole locations where hard data of the reservoir were available. Figure 4.17 depicts the mean of initial ensemble of 30 permeability realizations.

For computer assisted history matching, field observed data (oil rate, steam oil ratio and temperature) were prepared by using reference permeability values in simulation model and simulated dynamic data was considered as benchmark case. Measurements of oil rate and steam oil ratio (SOR) at production wells and temperature sensors data at observation wells were available at the end of each month for upto 15 years. Observed data can be directly read from the file of benchmark case for history matching. The history matching was performed for a

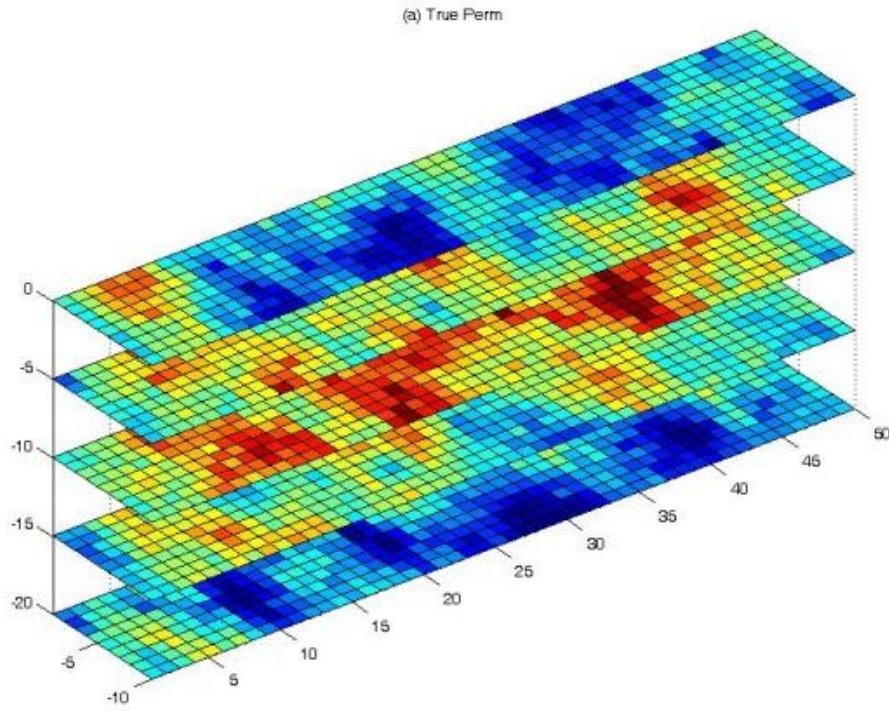


Figure 4.15: Reference Permeability Field (md) for MPSAGD Model

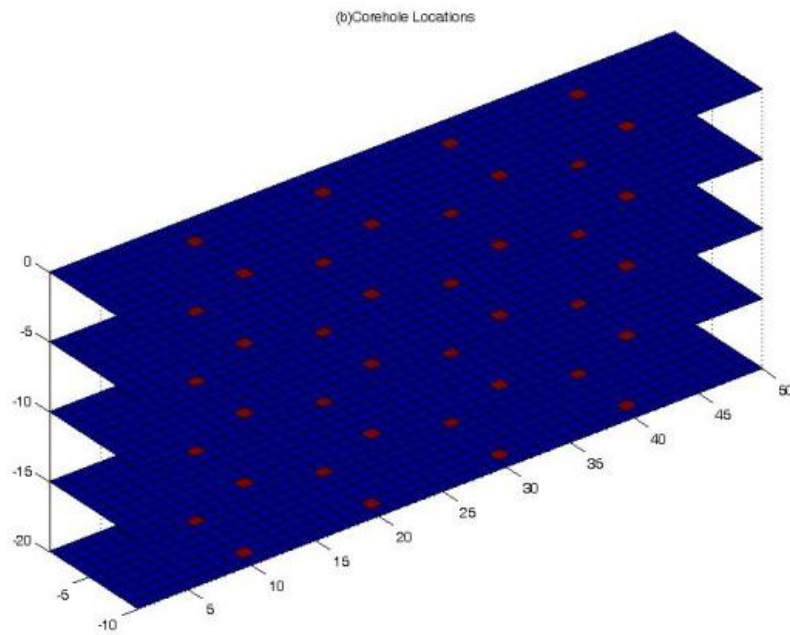


Figure 4.16: Corehole Locations where hard data is available for MPSAGD Model

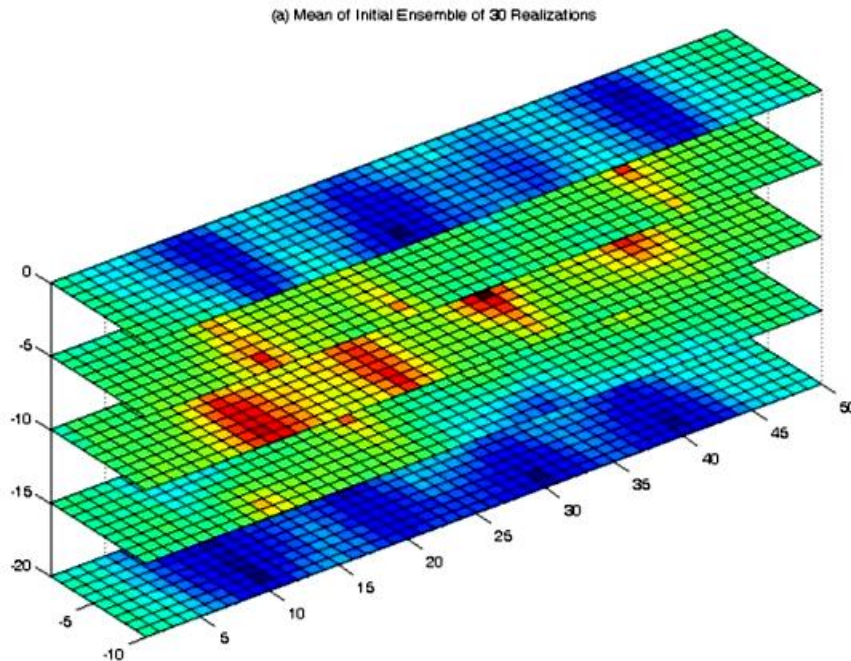


Figure 4.17: Initial Mean Permeability (md) for MPSAGD Model

period of 3 years and the observed field data were used for assimilation every six months, from Mar `04 to Mar `07. The measurement covariance matrix (R values in ε_k^d matrix) was selected as 10 STB, 0.001 and 5 F for oil rate, SOR and temperature, respectively. The model covariance matrix (Q values in ε^m matrix) was selected as $1.0E^{-4}$ for all grid blocks.

4.5 Multi Pair SAGD Model Results

The constrained EnKF based history match technique has been applied to MPSAGD model and the results obtained at the end of data assimilation process are presented here.

4.5.1 Model Parameter Update

As discussed in previous case study, the model parameter which was updated in analysis step is permeability, which mainly controls the reservoir heterogeneity. Kalman gain was computed through covariance matrices at each analysis step of

CEnKF based history matching process and MPSAGD model was tuned through Kalman gain. The MPSAGD model was constrained with minimum permeability range of 1500 md and maximum permeability range of 4000 md. Figure 4.18 depicts the updated mean permeability field of MPSAGD model;

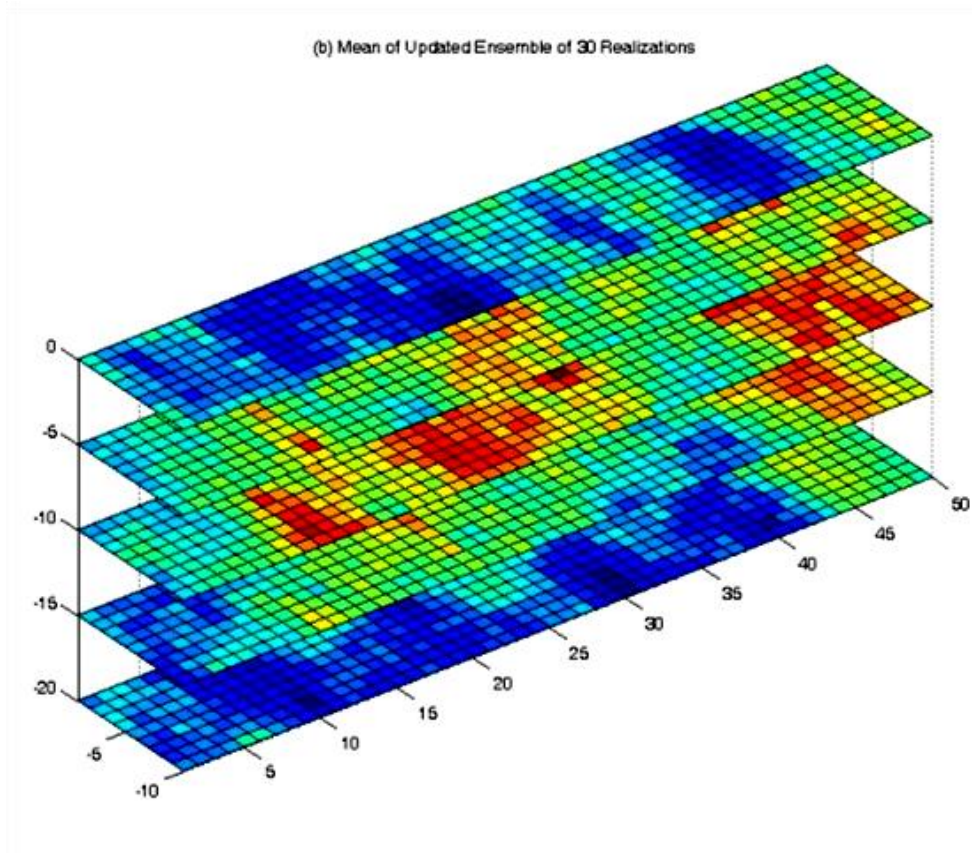


Figure 4.18: Updated Mean Permeability Field of MPSAGD Model

As shown in figure, after history match process, the updated mean permeability field of MPSAGD model is improved and reflect many aspects of true permeability field. The initial ensemble mean permeability field shows more lower values in first and last layers and remaining three layers contain average permeability values which can lead to false predictions, as will be shown in next section. After history matching, heterogeneity distribution of MPSAGD model is closed to reference case.

4.5.2 Dynamic Parameter Match

The production oil rate, steam oil ratio and temperature observations were assimilated in history match process and updated parameters are plotted in following figures. The plots of dynamic parameters presented here contain same features as discussed in section 3.2.2.2. The production oil rate predictions after and before history match with measurement data are plotted in Figure 4.19

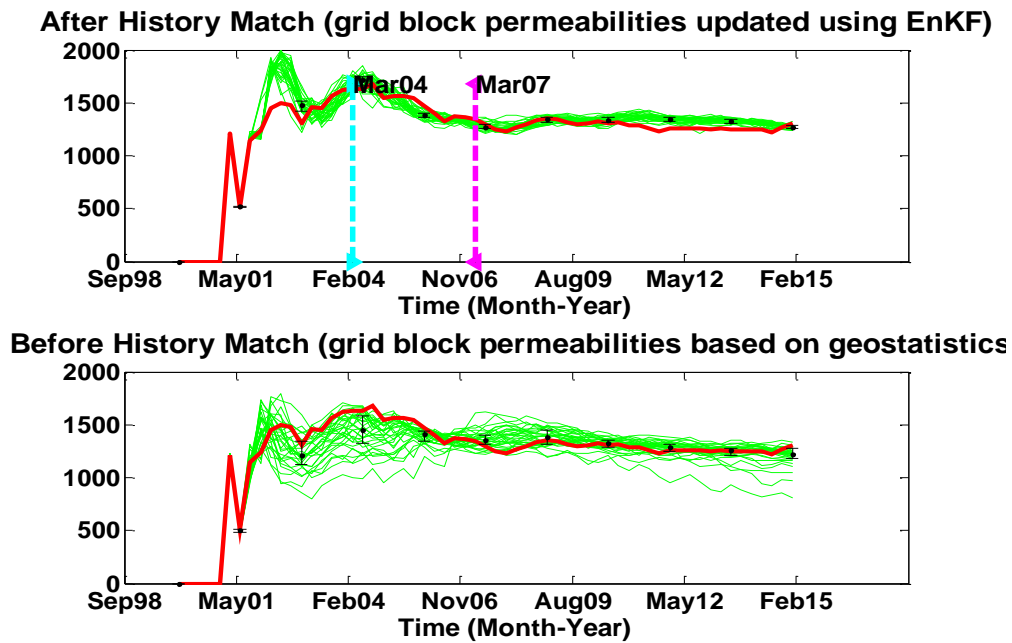


Figure 4.19: MPSAGD Model Field Oil Production Rate (BPD)

After history match plot (upper plot), shows initially a high peak in all assimilated predictions but quickly all ensemble members' forecast is centered around the measurement data. Cumulative steam oil ratio (CSOR) is shown in Figure 4.20

In Figure 4.20, after history match plot, predictions of CSOR are quite good from the beginning as the spread in ensemble is centered around the observation data. The uncertainty in this parameter is reduced significantly. Two sensor locations were used in assimilation process to update model parameters of MPSAGD model, both temperature observations are depicted in Figure 4.21 and Figure 4.22

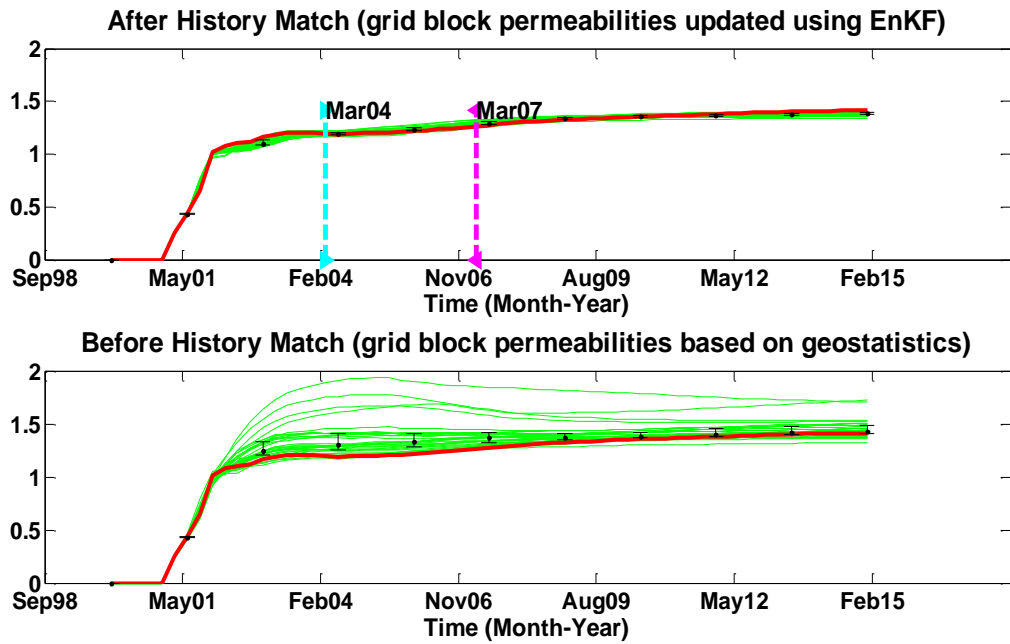


Figure 4.20: MPSAGD Model Cumulative Steam Oil Ratio (CSOR)

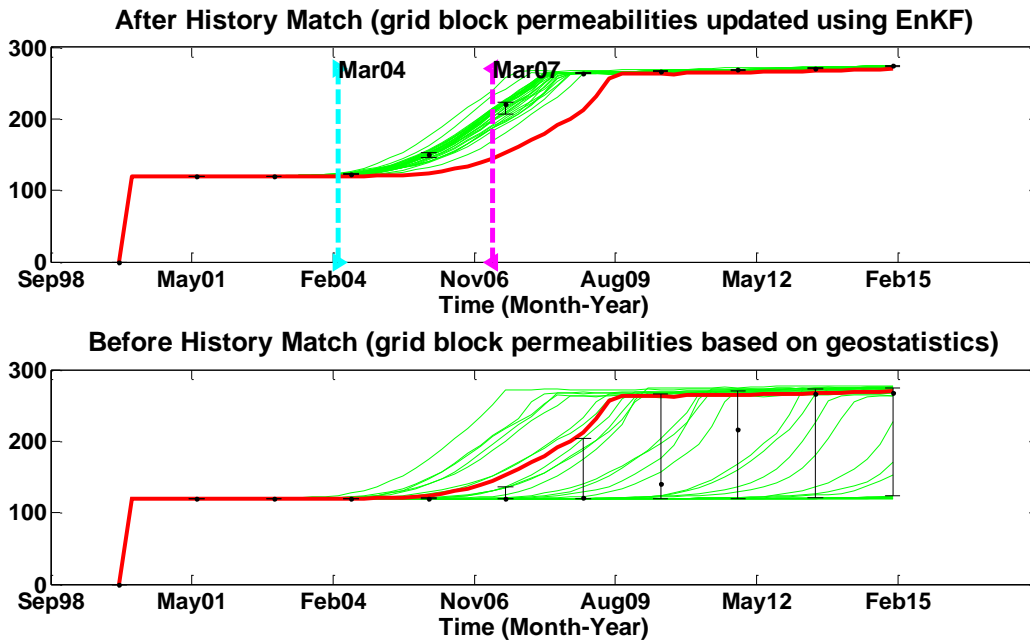


Figure 4.21: Reservoir Temperature (°F) at sensor location 30, 5, 1

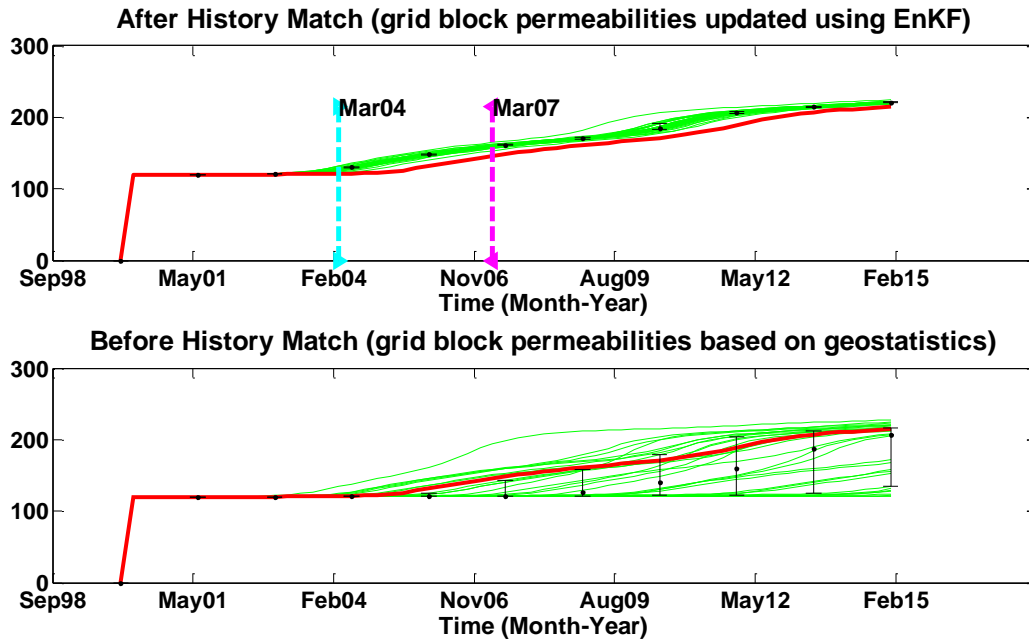


Figure 4.22: Reservoir Temperature (°F) at sensor location 30, 2, 3

Both figures illustrate the predictions of temperature observations for MPSAGD model. Significant reduction in uncertainty is observed after data assimilation process. As noted in case study-1, here too, the uncertainty in before history match predictions is higher in temperature observations as compared to production parameters (Oil Rate and CSOR). Hence, we emphasize to include temperature observations in assimilation process in order to obtain better model parameters update. We will show some more cases and comparison in upcoming chapters.

4.5.3 Ranking of Realizations

Initial ensemble for MPSAGD model was generated with 30 number of realizations and updated during CEnKF based history matching process. The ranking methods and procedure as defined in section 4.3.4 are applied here too. Figure 4.23 is showing the weighted mean square error graph and Figure 4.24 is showing the weighted R square graph as below

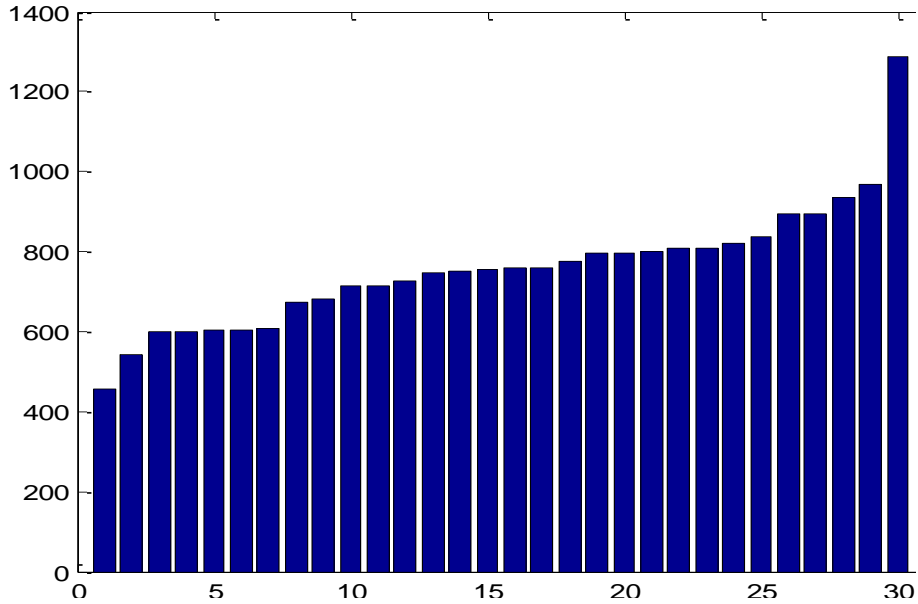


Figure 4.23: Weighted Mean Square Error (WMSE), MPSAGD Model

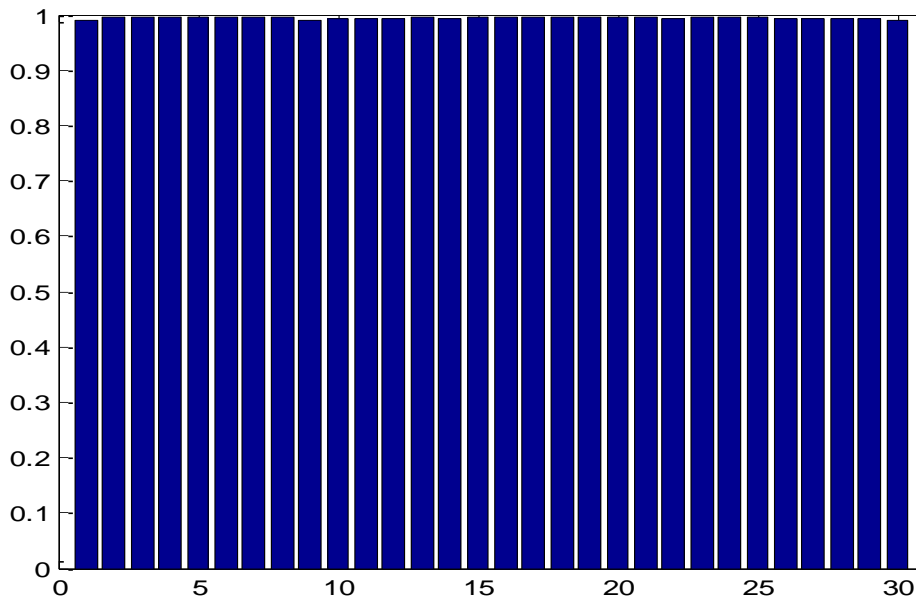


Figure 4.24: Weighted R Square (WR²) Graph, MPSAGD Model

WMSE graph illustrate that the best realization contains the mean square error of 400 approximately by weighting all four assimilation parameters, whereas the least match realization contains approximately 1400 mean square error. This shows that still there is some error and uncertainty present in updated ensemble, even after history match. That proves the basic stochastic modeling ideology, we

can reduce the uncertainty but cannot eliminate it 100%. WR^2 graph illustrates that the assimilated parameters are matching with reference case more than 95% that shows the quality of history matching.

Chapter 5

Constrained EnKF for Continuous SAGD Reservoir Model Updating - Single Well SAGD Model*

The second case has been prepared to study a new technique in SAGD reservoirs known as single well SAGD or SW-SAGD, (McCormack et. al., 1997; Singhal et. al., 2000). This technique is very useful in relatively thin bitumen / heavy oil reservoirs, where reservoir thickness is less than 25m, (Siu et. al., 1990). Moreover, it is cost effective technique to reduce the capital expenditure (CAPEX) by drilling only one horizontal well instead of twin wells as suggested by Butler et al. (1981). Consequently, a single horizontal well is drilled at bottom of reservoir in which steam is injected via tubing at the toe and oil is produced through the annulus (at the heel).

In this chapter, we have one case study (i.e. SWSAGD model) but ran with two cases and have two results. In the first case, CEnKF applied to SWSAGD model where model parameters were updated with production parameters as well as temperature observations. In the second case, CEnKF applied to SWSAGD model with same initial reservoir parameters but model parameters were updated without temperature observations, only production variables were used to assimilate history match data and updated model parameters. Later, we will compare both cases to check whether temperature observations have some contribution in model parameters' update or not.

*Some sections of this chapter have been taken from the paper (WHOC11-568) presented at World Heavy Oil Congress Conference 2011, held at Edmonton AB, Canada, on March 15 - 17. (Gul et. al., 2011)

5.1 Single Well SAGD Reservoir Model with Hybrid Grids

SWSAGD Model dimensions are 25 x 20 x 6 grid blocks in X, Y and Z directions respectively. Cartesian grids of the model have been refined locally throughout the horizontal section of wellbore with hybrid grid refinement as 5 x 4 x 1, to simulate near wellbore fluid flow appropriately. Figure 5.1 depicts 3D SW-SAGD thermal reservoir model dimensions and the well location.

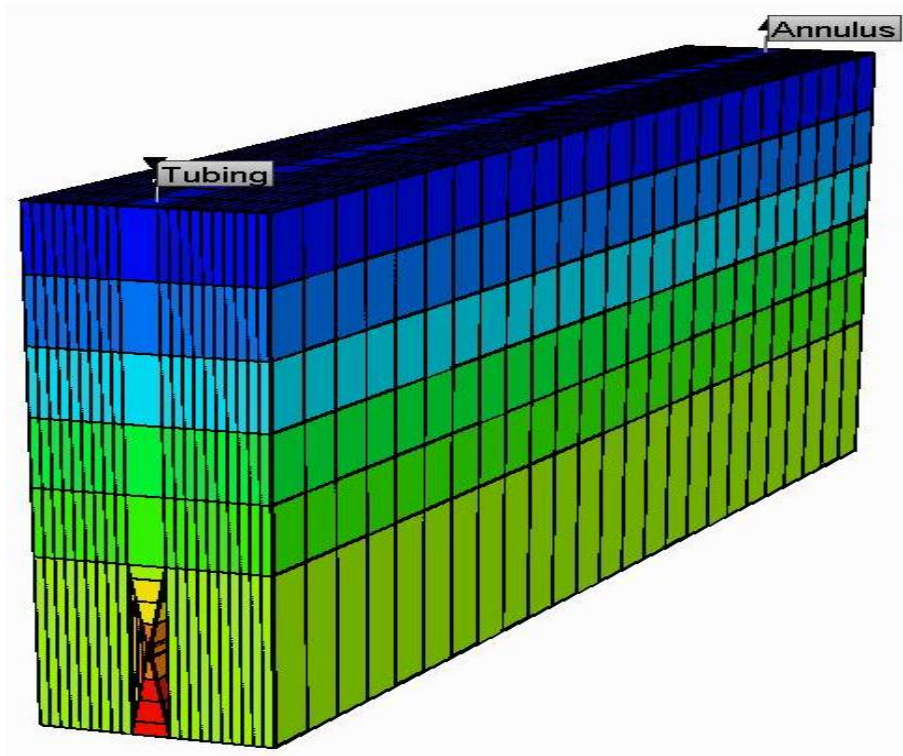


Figure 5.1: 3D view of Single Well SAGD Model in CMG STARS Simulator

The single horizontal well was discretized into two independent strings, namely tubing and annulus. Strings are equal in length and are placed directly end to end, tubing string acts as injector and annulus string as producer. Steam was injected through tubing at maximum bottom hole pressure of 500 psi and 70 m³ cold water equivalent. After six months, injection rate of steam is increased to maximum 100 m³/d cold water equivalent and maximum bottom hole pressure of 800 psi. Injection steam quality and temperature are 95% and 300 °C respectively. Producer well was constrained at maximum liquid production rate of 100 m³/d

and minimum bottom hole pressure of 500 psi throughout the simulation run. The reservoir fluid and rock properties for MPSAGD model are given in table 5.1

Table 5.1: SWSAGD Model Reservoir Properties

Length in x, y, z-dir.	500m x 70m x 15m
Porosity	35%
Horizontal Perm (k_h)	Heterogeneous
Vertical Perm (k_v)	$0.2*k_h$
Number of component	3 (Water, Bitumen and Dissolved Gas)
Connate Water Saturation	15%
Reservoir Initial Temperature	16 °C
Reservoir Initial Pressure	200 psi
Bitumen viscosity	1,000,000 cp @ 16 °C
Dissolved Gas in Bitumen	10% of total Bitumen Saturation
Formation Heat Capacity	2E6 J/(m ³ . C)
Thermal Conductivity	5E4 W/ (m. C)
Injection Fluid	Steam
Steam Quality	95%
Injection Temperature	300 °C

Similar to the previous chapter case studies, SGSim was applied to generate initial ensemble of permeability realizations using the same geostatistical parameters as reference case. All realizations were conditioned with hard data. The spherical variogram model was selected to search simulated values with range of 10, 03 and

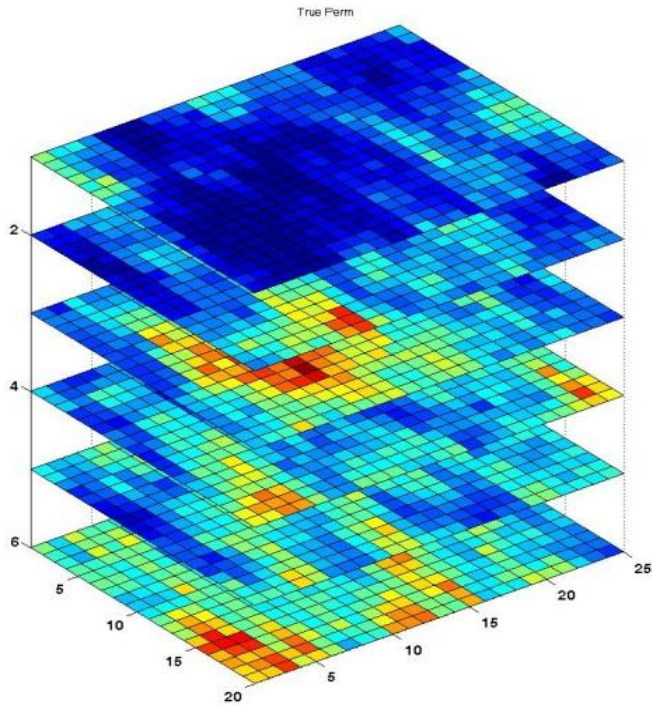


Figure 5.2: Reference Permeability Field (md), SWSAGD Model

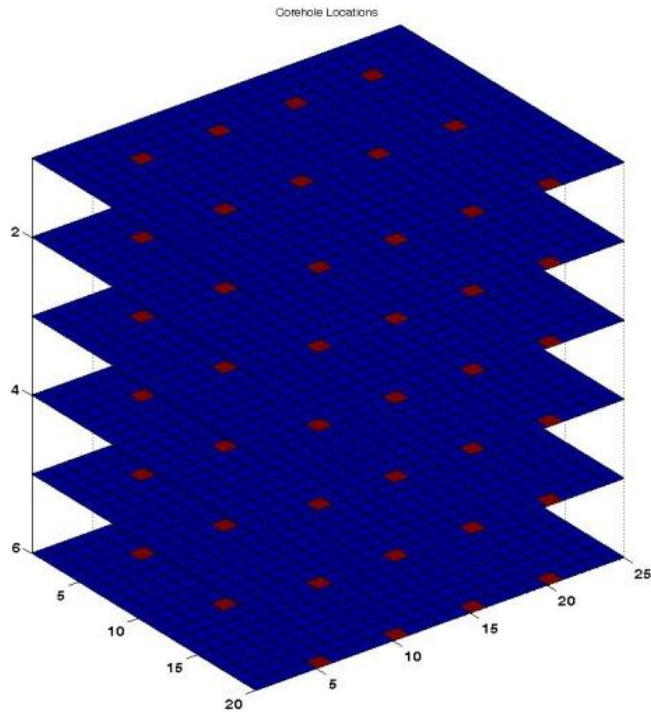


Figure 5.3: Corehole Locations where hard data is available SWSAGD Model

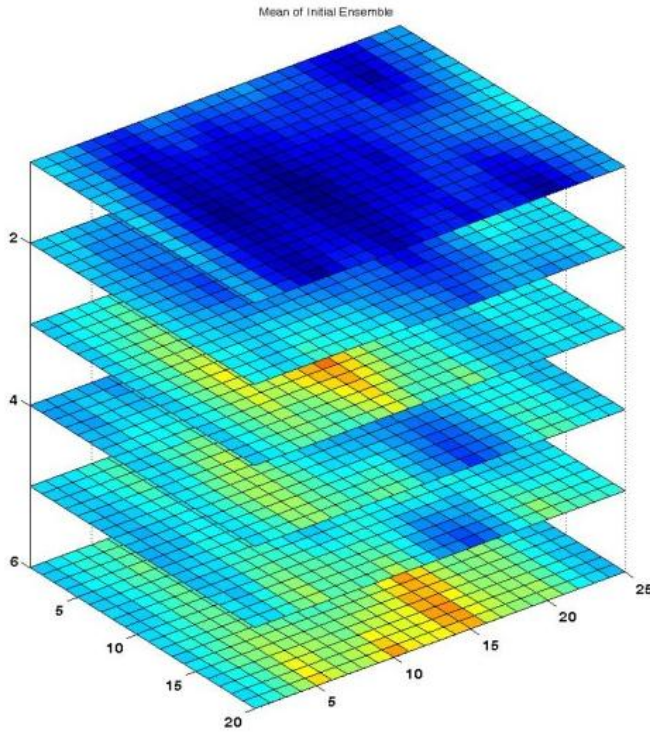


Figure 5.4: Initial Mean Permeability Field (md), SWSAGD Model

01 grid blocks in the maximum, median and minimum correlation ranges respectively and zero degree angles for all directions. Figure 5.2 and Figure 5.3 depict the reference permeability field and core hole locations where hard data of the reservoir were available. Figure 5.4 depicts the mean of initial ensemble of 30 permeability realizations.

For computer assisted history matching, field observed data were prepared in a similar way as the previous case studies in chapter 4. Measurements of oil rate and SOR at production wells and temperature sensors data at observation wells were available at the end of each month for upto 12 years. Observed data can be directly read from the file of benchmark case for history matching. The history matching was performed for a period of 2 years and the observed field data was assimilated at every six months interval, starting from Dec `03 to Dec `05. The measurement covariance matrix (R values in ε_k^d matrix) was selected as 1 m^3 , 0.1

and 5 °C for OR, SOR and Temperature, respectively. The model covariance matrix was selected as $1.0E^{-4}$ for all grid blocks (Q values in ϵ^m matrix).

5.2 Case - 1: Single Well SAGD Model Results

The CEnKF method applied to single well SAGD model to perform computer assisted history matching with production variables (oil rate and CSOR) and temperature observations to update model parameters.

5.2.1 Model Parameter Update

Grid block permeability values were updated as model parameters during analysis step of CEnKF technique. Figure 5.5 depicts the updated mean permeability field of single well SAGD (SWSAGD) model

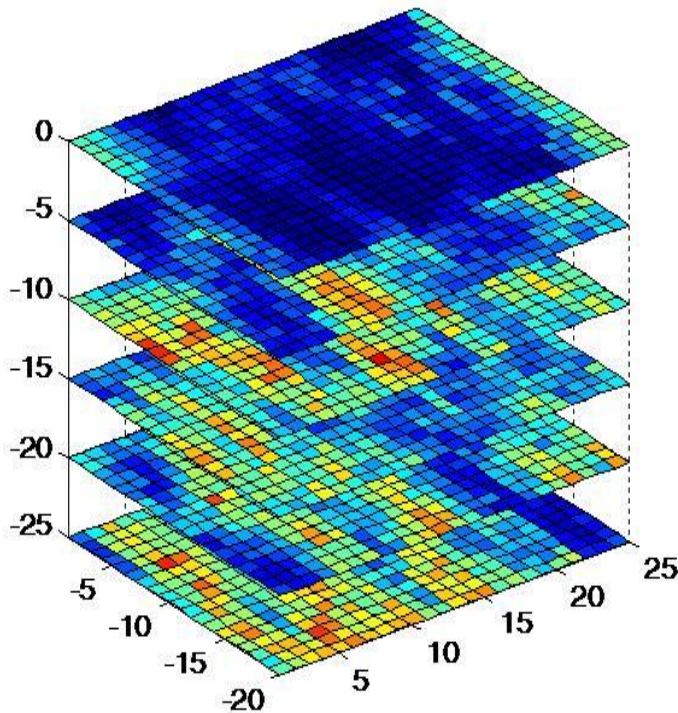


Figure 5.5: Updated Mean Permeability of 30 realizations, SW-SAGD Model

The updated mean permeability field has close resemblance with reference permeability field as shown in Figure 5.5. Low and high permeability regions are

clearer in updated mean permeability as compare to initial ensemble mean permeability; this information helps in steam chamber growth and to locate potential barriers.

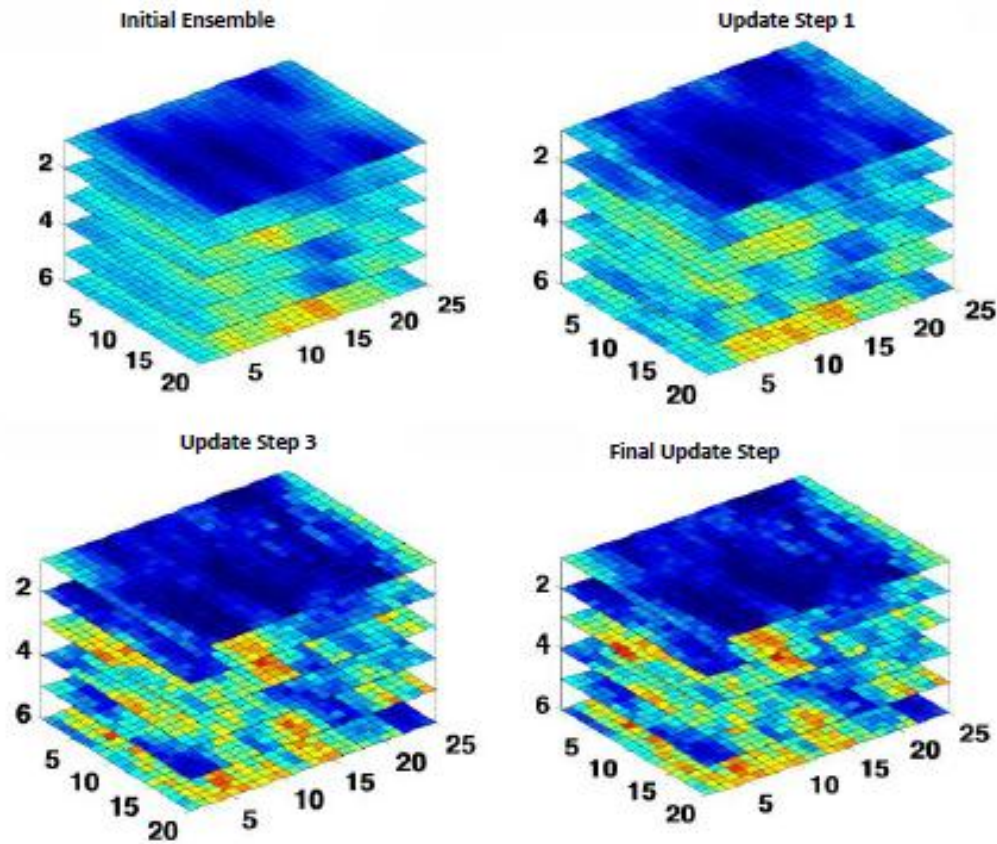


Figure 5.6: Permeability field update at different time steps, SWSAGD Model

Figure 5.6 depicts the permeability update at different time steps. Major changes occur in permeability update at the first two or three time steps, since initial ensemble contains a lot of uncertainty and the Kalman filter is designed to compensate error through the Kalman gain vector as given in equation (2.25). This permeability update will help in reservoir characterization and future field development.

5.2.2 Dynamic Parameter Update

In the first case, all available measurements were used to assimilate data and the assimilated parameters were oil production rate, cumulative steam oil ratio, and temperature observations. Plot features are already discussed in chapter 4, figures with same plot features were produced here too. Figure 5.7 shows the oil production rate predictions after and before history match process. The initial ensemble generated for SWSAGD model predicts under-estimate to oil production rate and predict over-estimate to CSOR. But after history matching process both parameter predictions are quite good from beginning as the spread in ensemble is centered around the observation. The predictions of temperature parameters are depicted in Figure 5.9 and Figure 5.10. Once again, temperature observations contain huge uncertainty before history matching and after successful data assimilation process, uncertainty reduced to its minimum level.

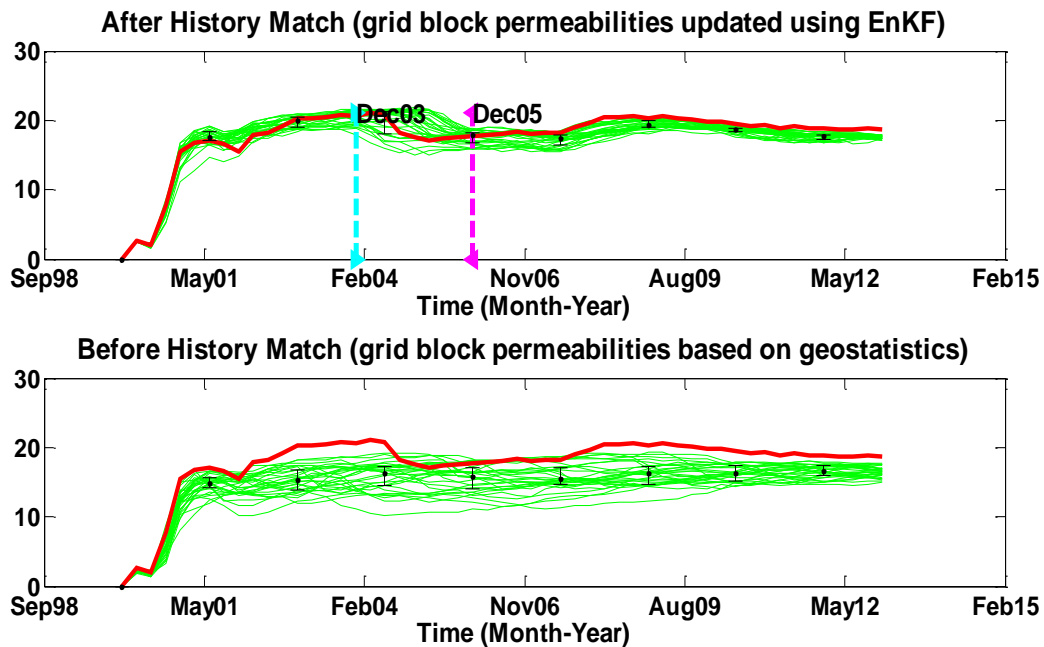


Figure 5.7: Field Oil Production Rate (m3/d) , SWSAGD Model

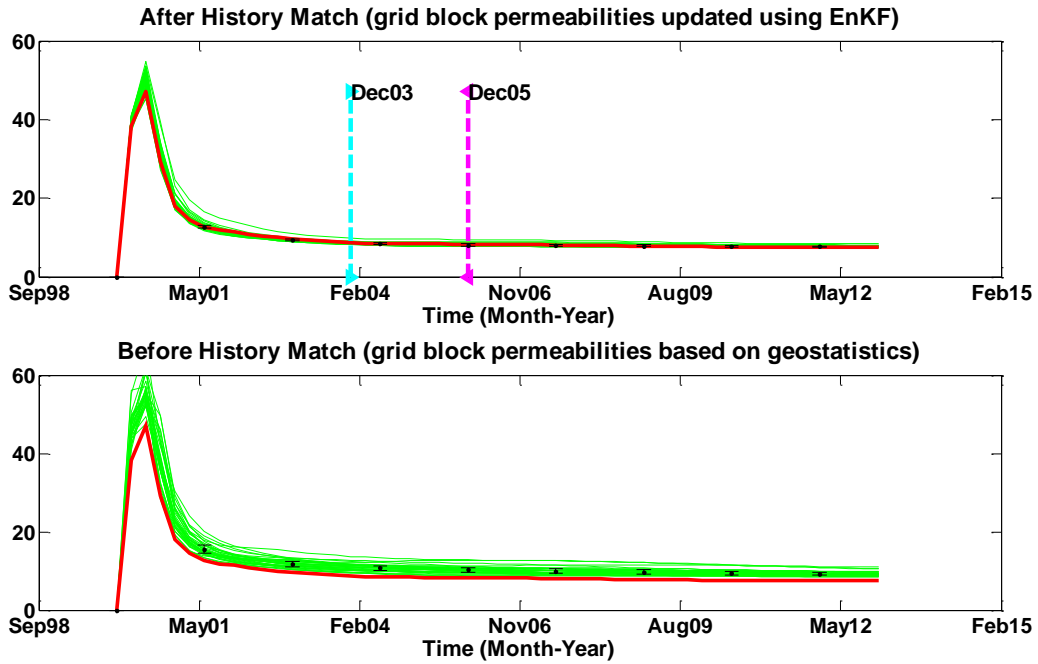


Figure 5.8: Cumulative Steam Oil Ratio, SW-SAGD Model

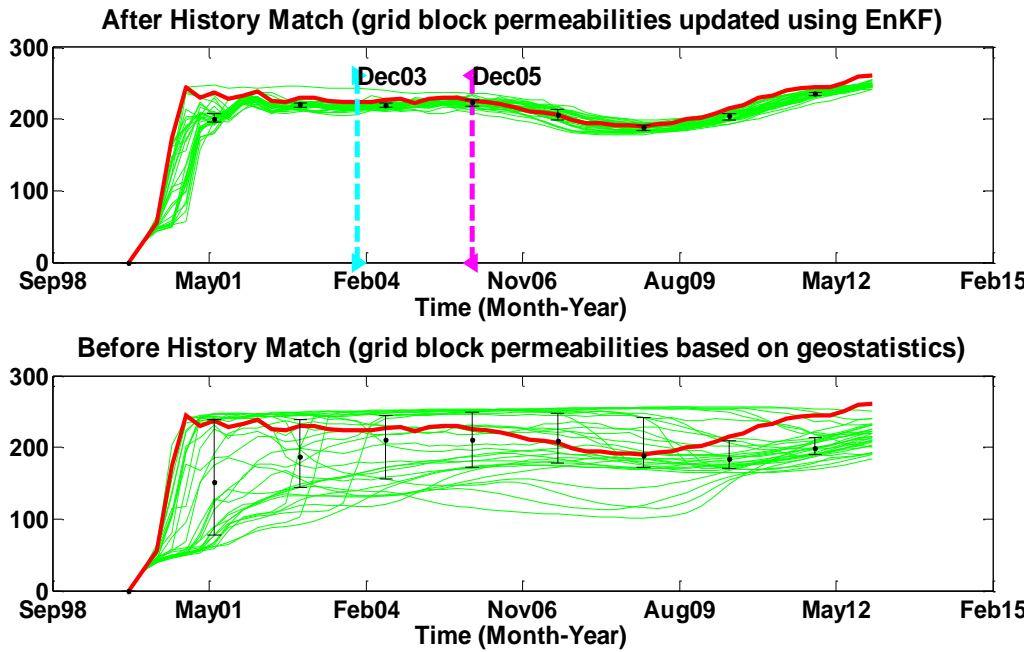


Figure 5.9: Reservoir Temperature (C) at grid location 12, 11, 6, SW-SAGD Model

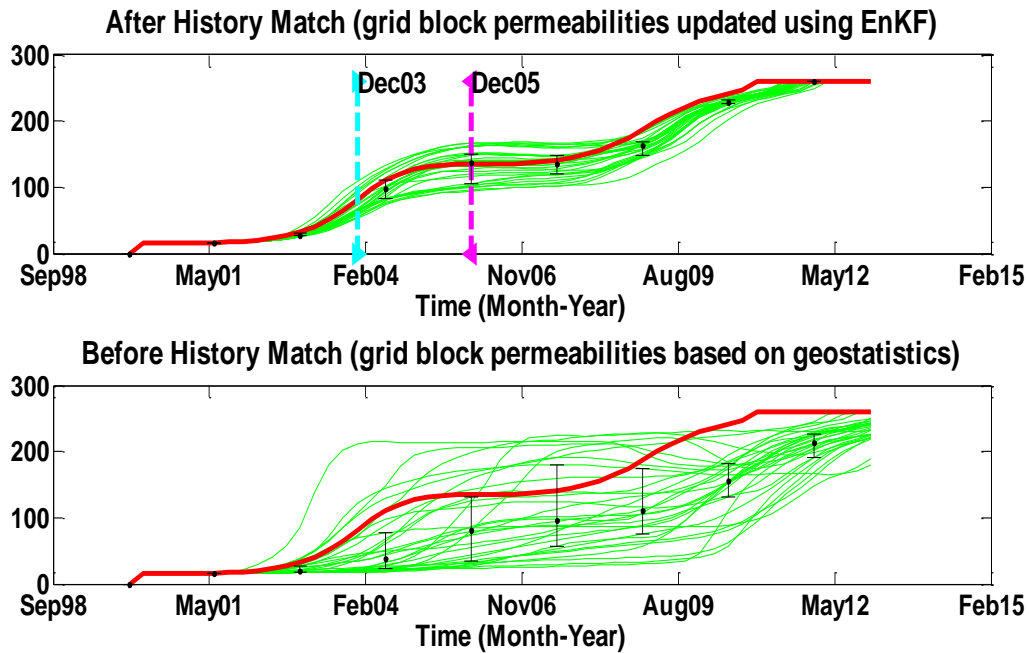


Figure 5.10: Reservoir Temperature (C) at grid location 12, 16, 4, SW-SAGD Model

5.2.3 Ranking of Realizations

The number of realizations generated for CEnKF based history matching of SWSAGD model is 30, to properly calculate covariance matrices for kalman gain calculation within minimum computational time. The realizations were ranked by WMSE method and quality of individual realization was evaluated by WR^2 method. Both methods are described in chapter 3, here we present the results. Figure 5.11 illustrates the WMSE graph and Figure 5.12 illustrates the WR^2 graph. The best realization of SWSAGD model which matches closely to all dynamic parameters contain 200 mean square error and least matched realization contains 1200 mean square error. Whereas the quality of history matching of all realizations is more than 90% as provided by WR^2 graph, Figure 5.12.

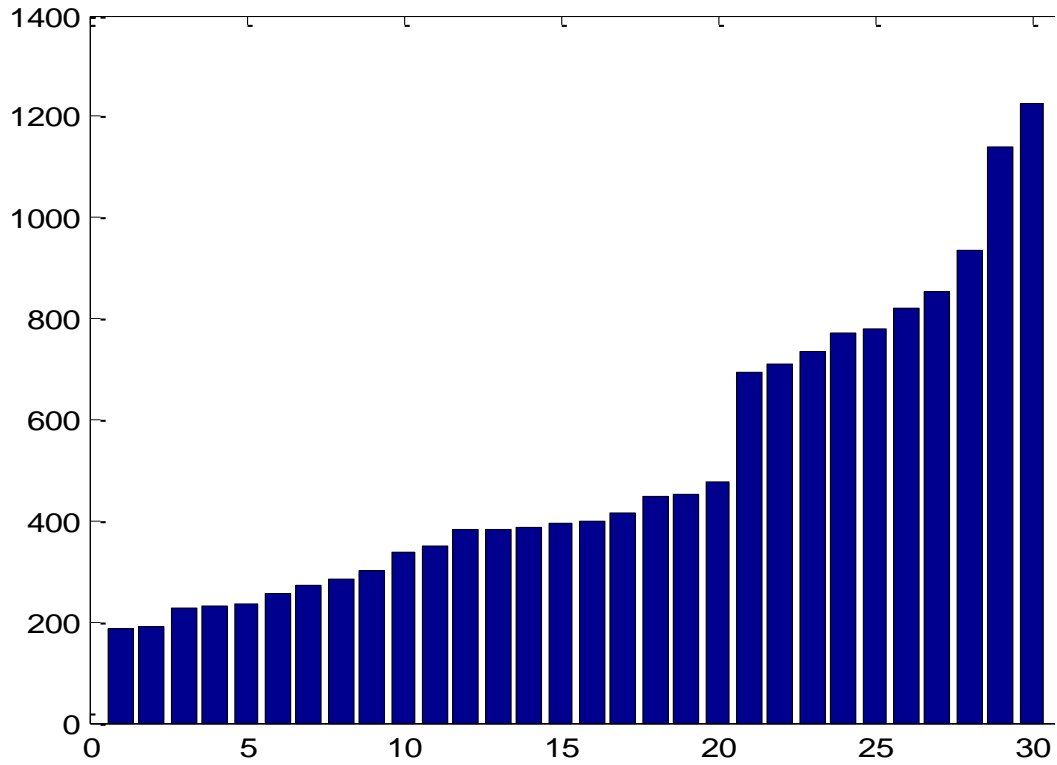


Figure 5.11: Weighted mean square error (WMSE), SW-SAGD Model

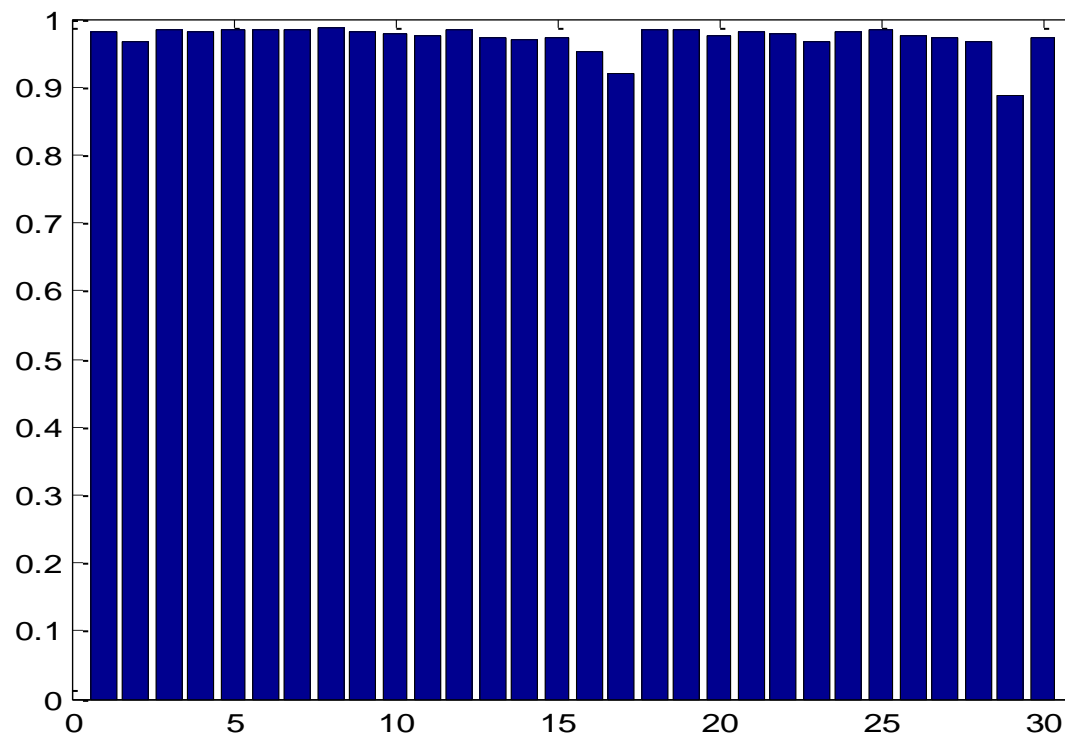


Figure 5.12: Weighted R Square (WR²), SW-SAGD Model

5.3 Case - 2: Single Well SAGD Model Results

In second case, the CEnKF method applied to same SWSAGD model defined in section 5.1 to perform computer assisted history matching with only production variables (oil rate and CSOR) and temperature observations were excluded in analysis step to update model parameters.

5.3.1 Model Parameter Update

For model parameter estimation in unconventional oil reservoirs, a comparative study was carried out to examine the importance of measurement data included in assimilation process during computer assisted history matching process. Figure 5.13 depicts the updated mean permeability field obtained after history matching process without including temperature observations in assimilation process.

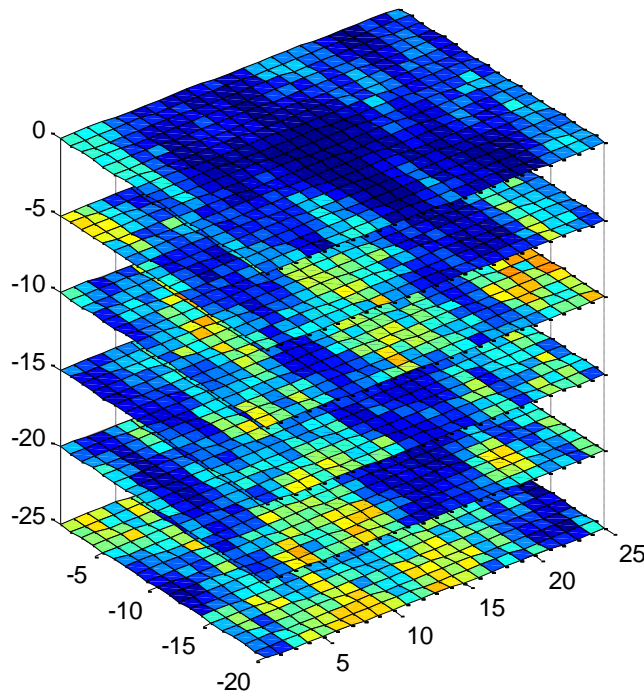


Figure 5.13: Updated mean permeability (md) without temp observations in history matching process, SW-SAGD Model

For better comparison, both cases are shown together in Figure 5.14 given below,

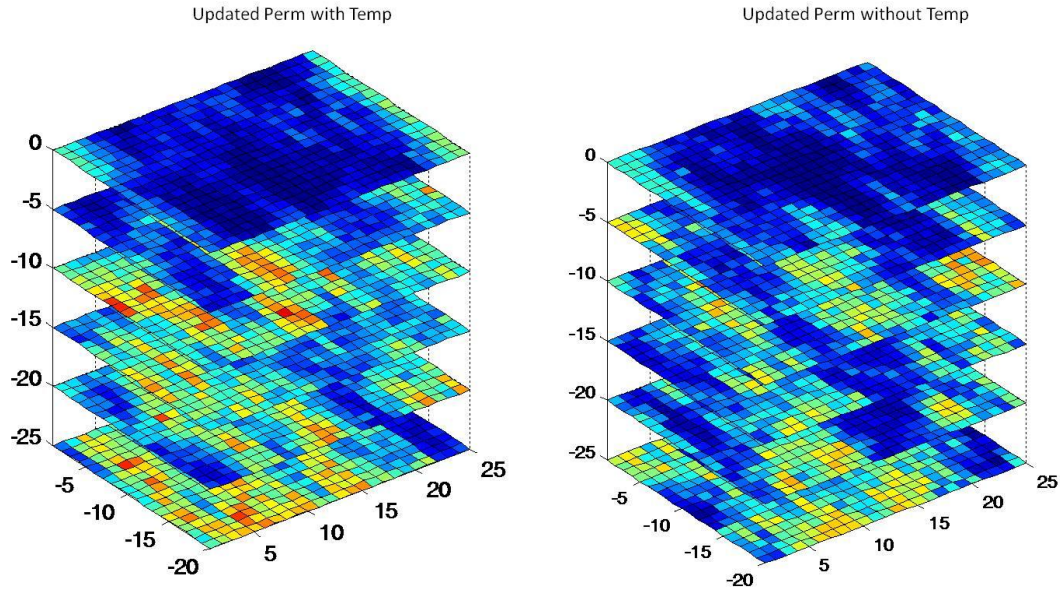


Figure 5.14: Comparison between Permeability Update of two cases, SWSAGD Model

Figure 5.14 represents the comparison between two cases. It shows that without including temperature observations in the history match process, the permeability update is underestimated. On the other hand, in the case-1 when observations from two thermocouples have been included in the history match process, the permeability estimation are close to that of reference case and results into better characterization of reservoir heterogeneity.

5.3.2 Dynamic Parameters Match

As mentioned earlier, in case-2 of SWSAGD model history matching process, only production variables were used in assimilation process. Figure 5.15 depicts the predictions of oil production rate and Figure 5.16 depicts the cumulative SOR achieved by running simulation with updated permeability realizations starting from beginning of SWSAGD model.

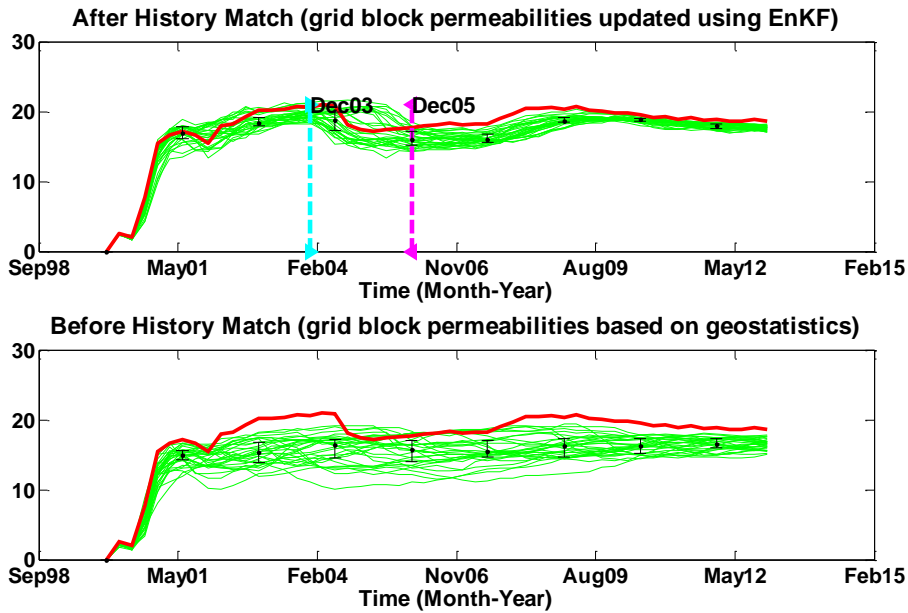


Figure 5.15: Field Oil Production Rate (m3/d), SW-SAGD Model

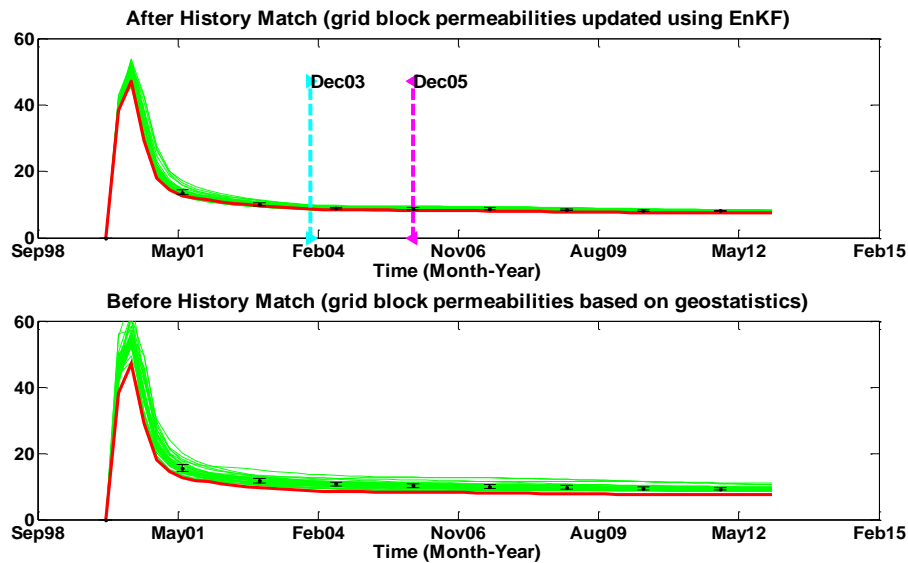


Figure 5.16: Cumulative Steam Oil Ratio, SWSAGD Model

Both production variables are showing an acceptable match between field measurements and model predictions. The uncertainty is reduced equally in this case as we observed in previous case.

5.3.3 Ranking of Realizations

In case-2 of SWSAGD model, the number of realizations was same as in case-1, (i.e. 30 realizations). Figure 5.17 depicts the WMSE graph and Figure 5.18 depicts the WR^2 graph.

The best realization after history matching process contains approximately 50 mean square error weighted by two production variables and least matched realization of SWSAGD model contains approximately 1600 mean square error. This shows a higher uncertainty range as compare to case-1, in which the range of uncertainty was 200 to 1200. This is because of the temperature observations, which play an important role in reduction of uncertainty from model parameters which regenerate the dynamic variables after the last update step in history matching process.

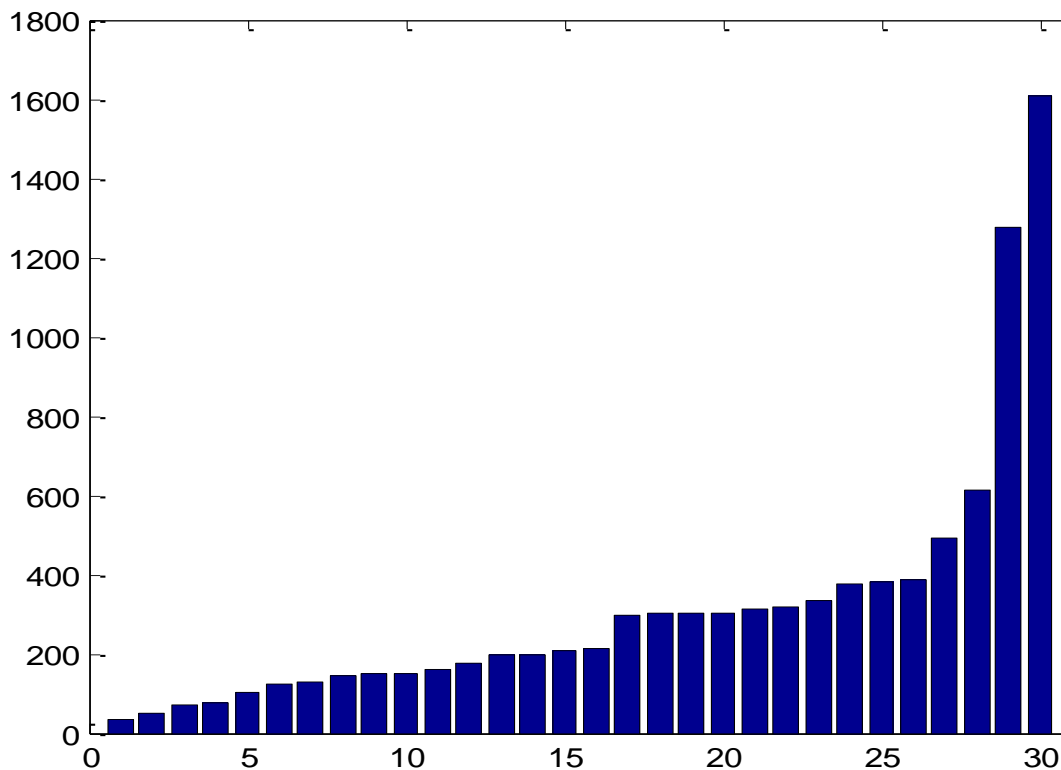


Figure 5.17: Weighted mean square error (WMSE), SWSAGD Model

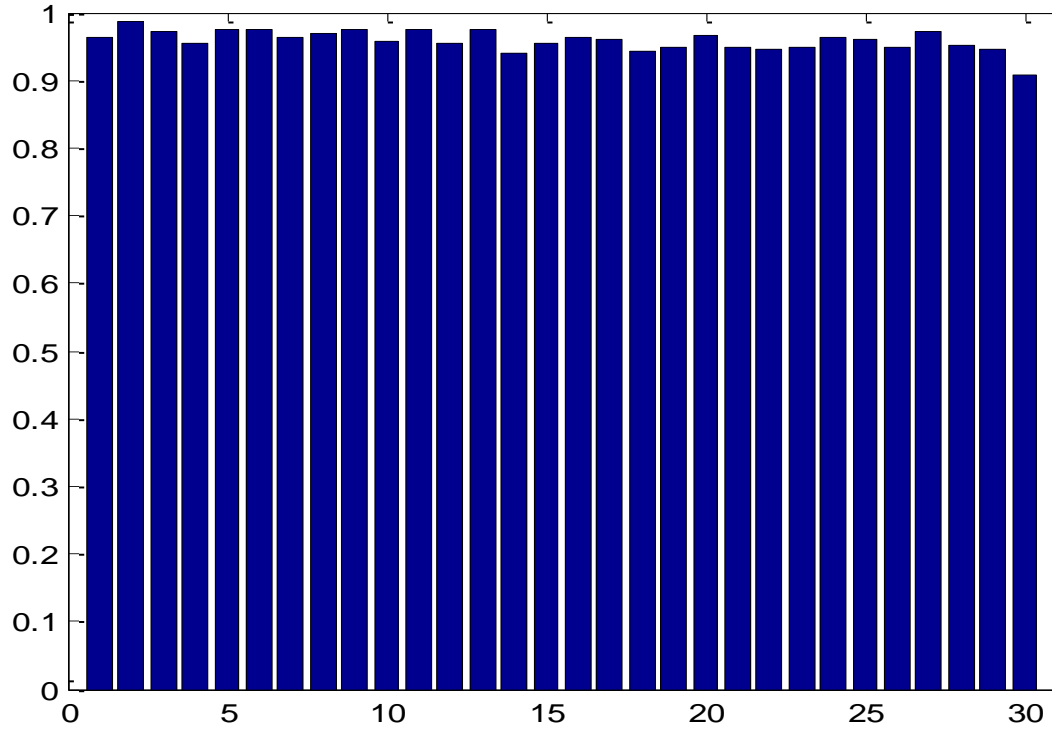


Figure 5.18: Weighted R Square (WR²), SWSAGD Model

Chapter 6

Constrained EnKF for Continuous SAGD Reservoir Model Updating - Multilateral Wells SAGD Model

Advancement in drilling technology allowed to drill and case multilateral well branches in different directions. Multilateral wells increase the primary production through improving the reservoir exposure and enhancing recovery, similarly as horizontal wells. However; the key advantage of multibranch wells over horizontal wells is leading to reduction in overall cost spending on field development. In SAGD operations, multilateral wells can provide means to produce more oil at an economic cost. Gadelle and Renard, (1999) described six common types of multilateral wells, as given below

1. Cluster multibranch well; slanted or curved branches drilled with different azimuths
2. Stacked multibranch well;
3. Multidrain or multilateral well; composed of several horizontal arms drilled from same horizontal drains
4. Re-entry laterals from a vertical well;
5. 3-Dimensional well;
6. Dual opposing laterals

In this chapter, we have two models of multilateral wells and both models contain reservoir properties of Athabasca oil sands deposit, as described in chapter 3. SAGD process is considered as enhanced oil recovery method for both models

and CEnKF based history match technique was applied to assimilate dynamic data and update the model parameters.

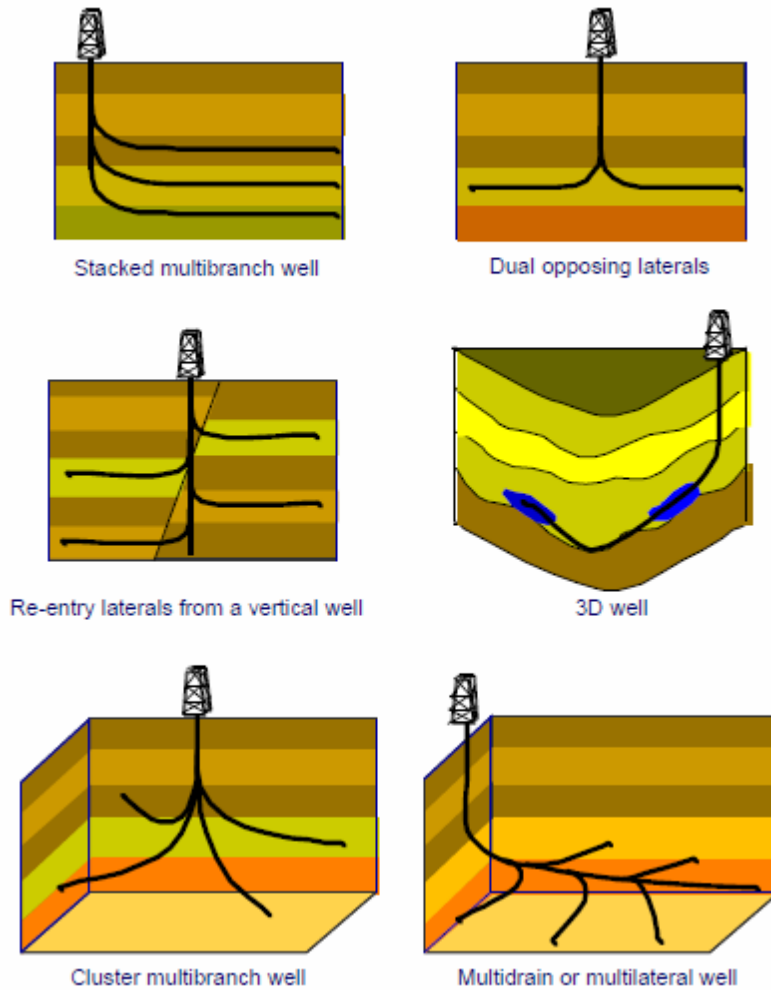


Figure 6.1: Various types of advanced wells, (Gadelle and Renard, 1999)

6.1 Twin Multilateral Wells SAGD Model With Parallel Branches

The first case of multilateral well SAGD model is presented here. The well architecture was of 'Stacked Multibranch Well' type as discussed above. Three well branches were generated for both wells (injector and producer) with 450m length, 60m spacing and 6m vertically separated. Model dimensions were 20 x 13 x 6 grid blocks in X, Y and Z directions, respectively. To obtain higher resolution

near wellbore region of SAGD well pairs, a LGR (Local Grid Refinement) was introduced. The resolution inside the selected area was divided by a factor of 3 x 3 x 3. Figure 6.2 depicts the resulting LGR in the near wellbore region of the multilateral well model.

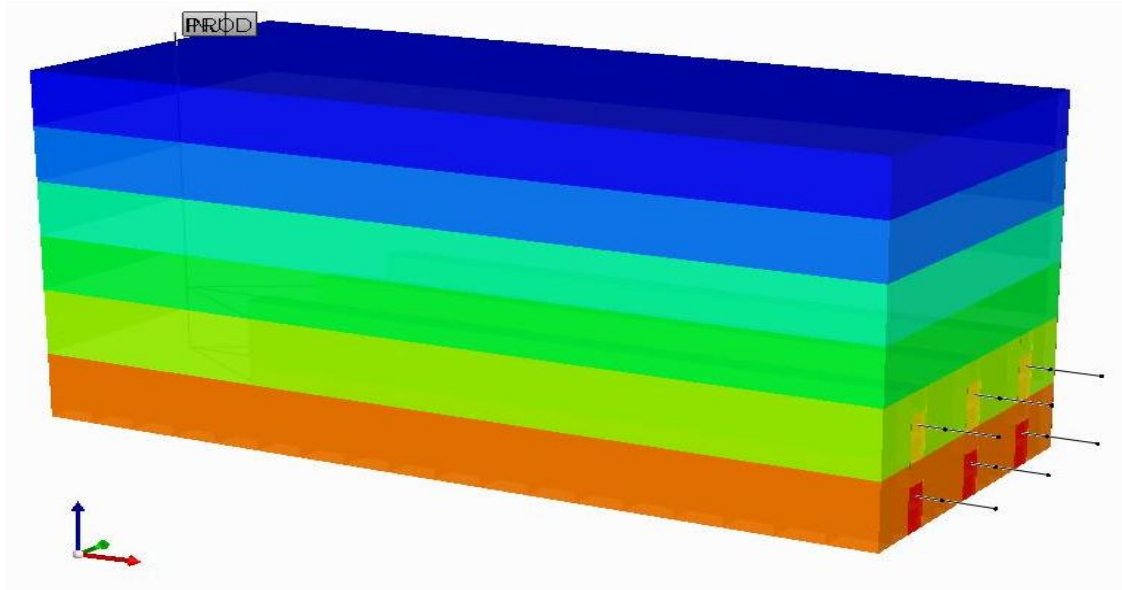


Figure 6.2: Various types of advanced wells, (Gadelle and Renard, 1999)

To initialize the communication between well pairs, electrical heating at 270 °C was applied through the casing pipe of each branch for four months. After that period, steam was injected through injector multibranches well at the rate of 500 m³/d maximum cold water equivalent and 6500 kPa maximum injection BHP. Steam quality was 0.9 and temperature was 270 °C. Reservoir fluid was produced through producer well constrained at 500 m³/d of maximum liquid rate and 5500 kPa minimum BHP. The reservoir fluid and rock properties for Multilateral Well SAGD model are given in table 6.1

Table 6.1: Twin MLW-SAGD Model Reservoir Properties

Length in x, y, z-dir.	500m x 200m x 32m
Formation Top	500m

Porosity	36%
Horizontal Perm (k_h)	Heterogeneous
Vertical Perm (k_v)	$0.3828*k_h$
Number of component	3 (Water, Bitumen and Dissolved Gas)
Connate Water Saturation	20%
Reservoir Initial Temperature	12 °C
Reservoir Initial Pressure	2700 kPa
Bitumen Molar Density	1688 gmole/m ³
Bitumen viscosity	2,000,000 cp @ 12 °C
Dissolved Gas in Bitumen	10% of total Bitumen Saturation
Formation Heat Capacity	2.35 E+6 J/(m ³ . C)
Thermal Conductivity	6.6 E+5 W/ (m. C)
Injection Fluid	Steam
Steam Quality	95%
Injection Temperature	270 °C

The permeability distribution was generated similarly as describe in previous two chapters with 7.8 mean log permeability and 0.85 variance to generate initial ensemble of 30 realizations to perform history match technique. Spherical variogram model was applied with 15, 05 and 01 grid blocks in maximum, medium and minimum correlation ranges, respectively and zero degree angles for all directions. Figure 6.3 depicts the reference permeability field and Figure 6.4 depicts the mean of initial ensemble of 30 permeability realizations.

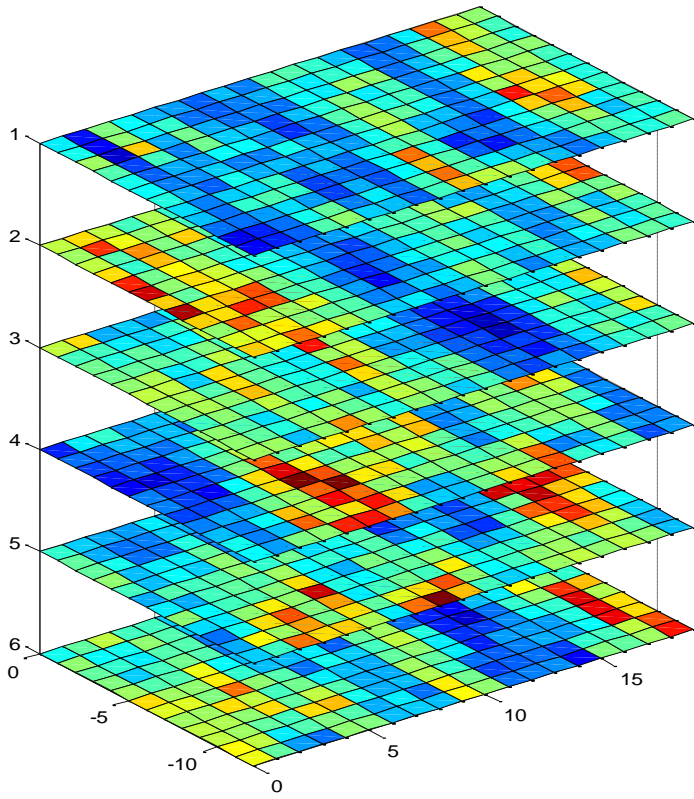


Figure 6.3: Reference Permeability Field of MLW-SAGD Model

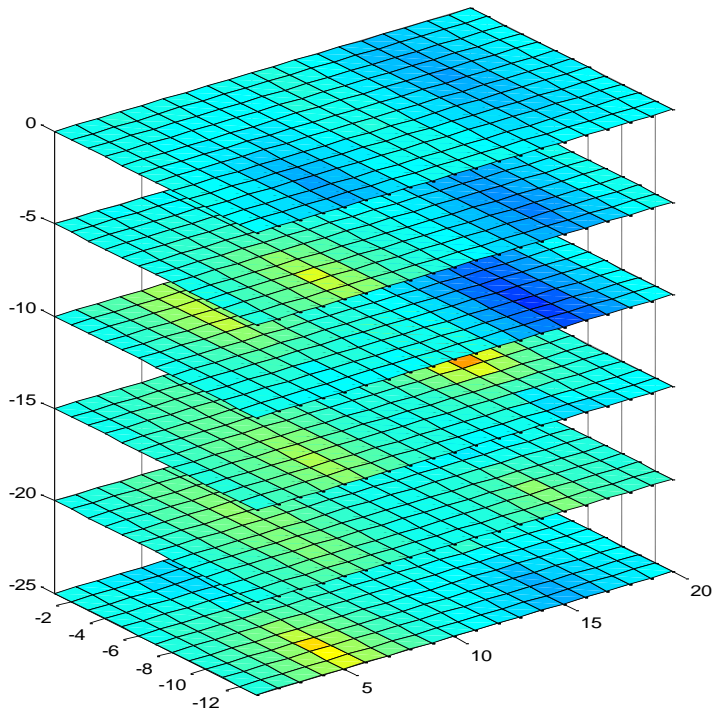


Figure 6.4: Initial Mean Permeability Field of 30 Realizations

EnKF based history match technique was applied to assimilate the observed and predicted data to estimate the model parameters. Field measurements of oil production rate, SOR, and temperature observations were available for 20 years, out of it ten years were used to assimilate data at the end of each year from Dec '96 to Dec '06 and rest of observed data of nine years were used to match with the model predicted variables on the basis of estimated model parameters. The measurement covariance matrix (R values in ε_k^d matrix) was selected as 1 m³, 0.01 and 1 °C for oil rate, SOR and temperature observations, respectively. The model covariance matrix was selected as 1.0E⁻⁴ for all grid blocks (Q values in ε^m matrix).

6.2 Multilateral Wells SAGD Model Results

The results presented here are obtained by applying constrained EnKF based history matching technique to multilateral wells SAGD model.

6.2.1 Model Parameters Update

The reservoir heterogeneity was characterized by generating number of stochastic realizations of permeability field with available geological data. During the history matching process, initial ensemble of permeability realizations were updated by assimilating the field measured data with model predictions. The Multilateral Well SAGD model was constrained with minimum permeability range of 1000 md and maximum permeability range of 4000 md. Figure 6.5 depicts the updated mean permeability field.

The updated mean permeability field shows overestimated values in some parts of model. It can be difficult to get an overall picture of the updates of model parameters by scrolling through the 30 different geostatistical realizations, layer by layer. The applied changes are maybe best analysed by comparing the initial updated mean permeability fields.

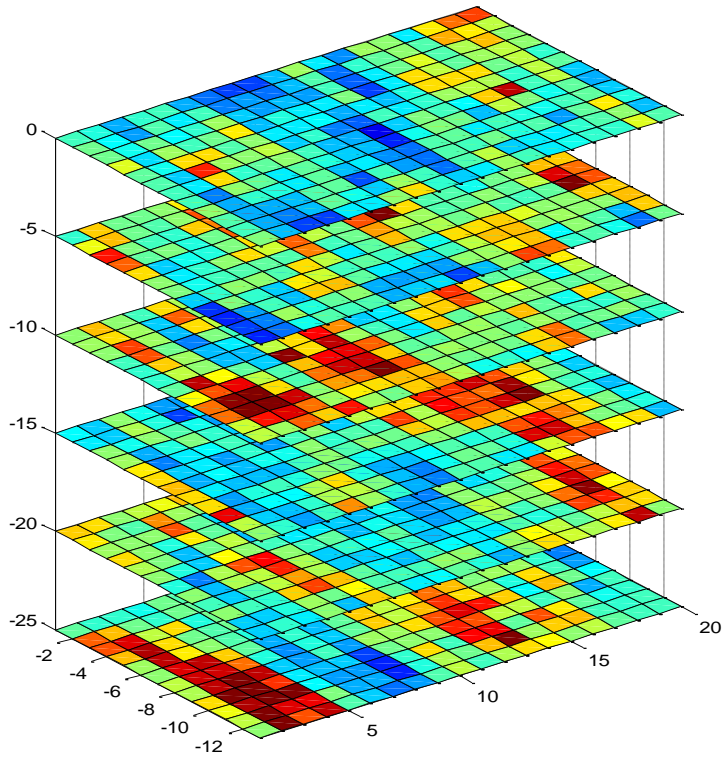


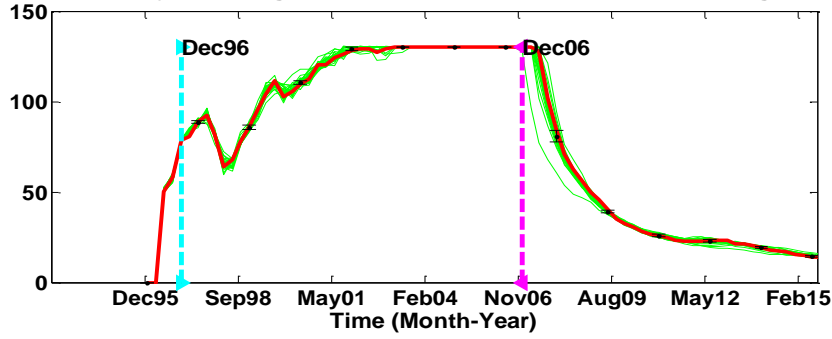
Figure 6.5: Updated mean permeability field, MLWSAGD model

6.2.2 Dynamic Parameters Match

The CEnKF based history matching method was applied to assimilate data obtained from Multilateral Well SAGD model. The assimilated parameters are oil production rate, cumulative steam oil ratio and temperature observations. Figure 6.6 to Figure 6.9 are given below to show the after and before history match plots of all above dynamic parameters.

In multilateral well SAGD model, before history match plots, production parameters contain a huge uncertainty along with temperature observations which we couldn't observe in previous cases. This is because the permeability distribution in this case, starts from 1000 md and at this range production fluids are affected greatly by reservoir heterogeneity. Constrained EnKF on other hand, matched all parameters in excellent way and uncertainty was remained negligible in production parameters and very low in temperature observations.

After History Match (grid block permeabilities updated using EnKF)



Before History Match (grid block permeabilities based on geostatistics)

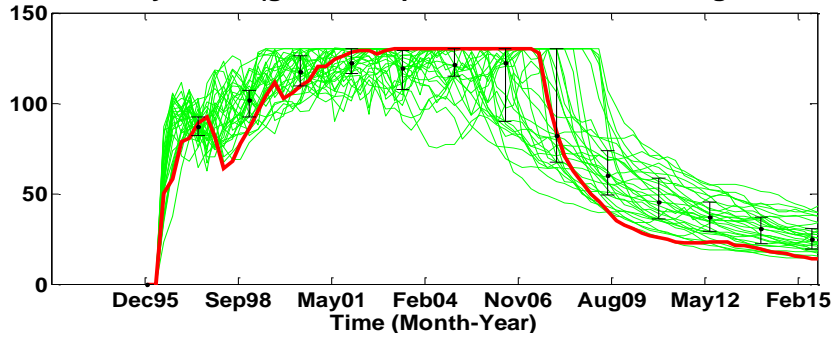
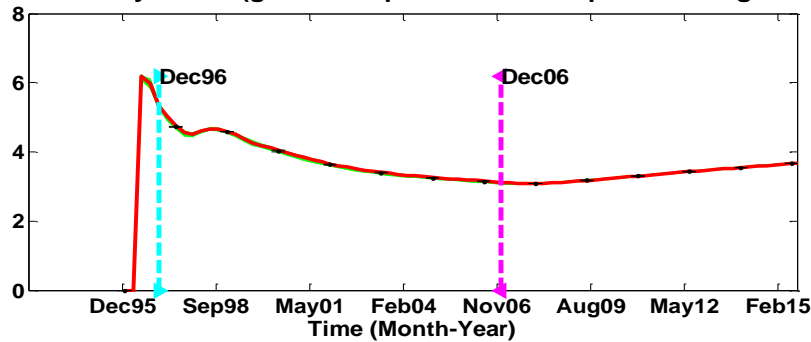


Figure 6.6: Field Oil Production Rate, m^3/d , MLWSAGD Model

After History Match (grid block permeabilities updated using EnKF)



Before History Match (grid block permeabilities based on geostatistics)

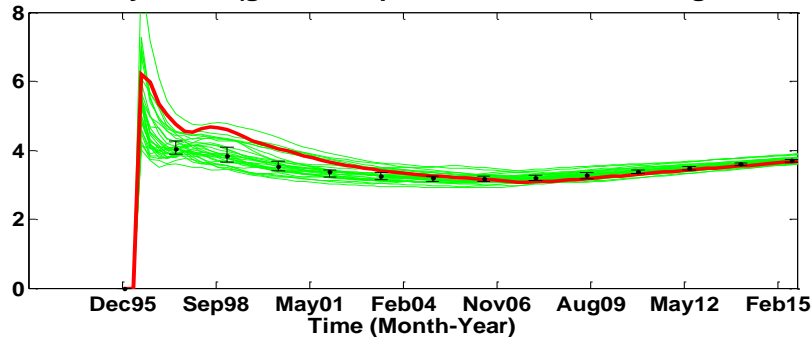


Figure 6.7: Cumulative Steam Oil Ratio, MLWSAGD Model

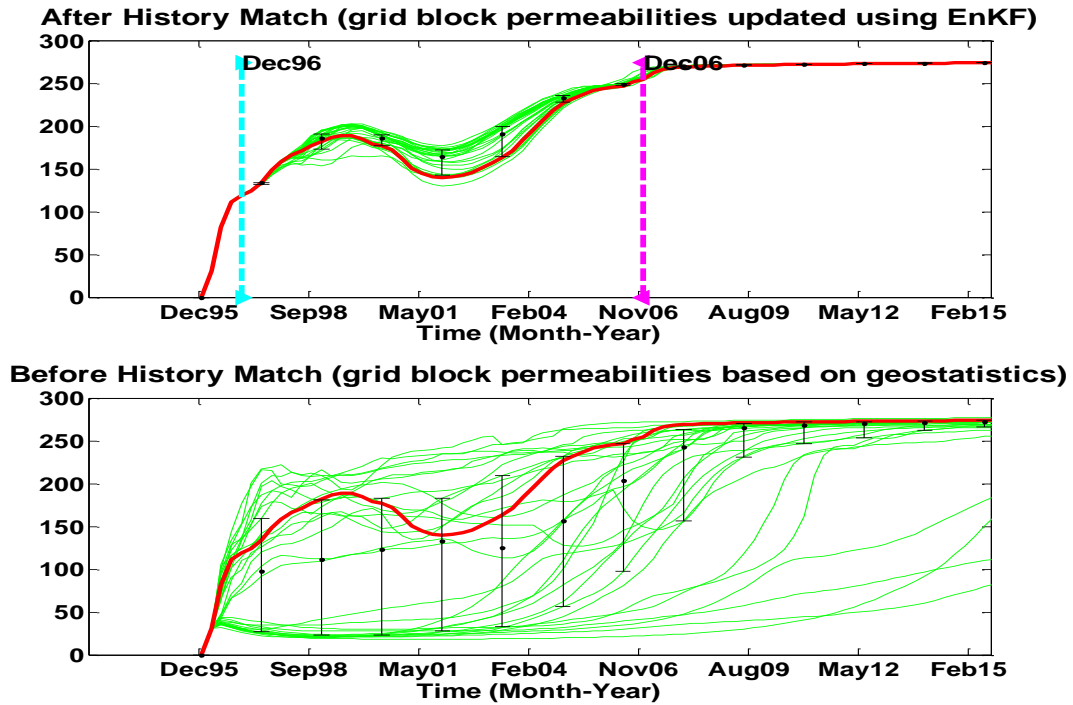


Figure 6.8: Reservoir Temperature ($^{\circ}\text{C}$) at grid location 20, 7, 6, Twin MLW-SAGD Model

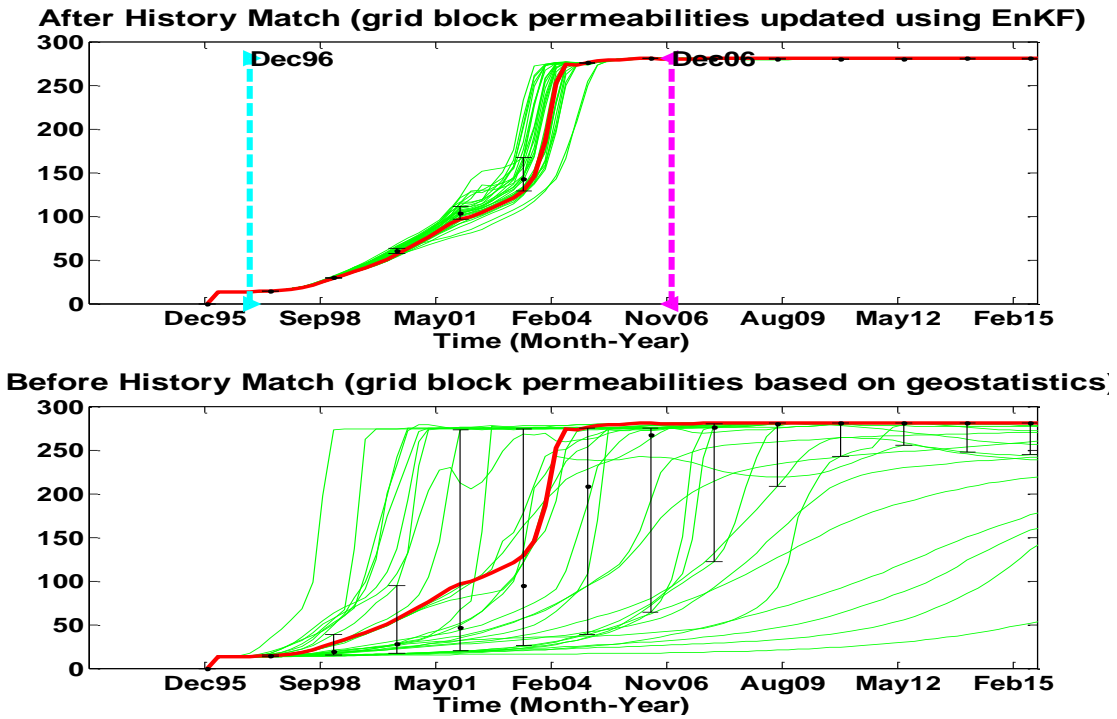


Figure 6.9: Reservoir Temperature ($^{\circ}\text{C}$) at grid location 5, 2, 2, Twin MLW-SAGD Model

6.2.3 Ranking of Realizations

The number of stochastic realizations generated to perform CEnKF based history matching technique were 30 and all realizations were updated with kalman gain vector at each time step along with available field measurements. At the last analysis step, the updated grid permeability values were used to generate all dynamic parameters from beginning and matched with field measurements. On the basis of data match between simulated predictions and field measurements, we ranked all realization. There are two methods to rank the updated realizations, namely; WMSE and WR^2 . These two methods already have been explained in chapter 4; here we will discuss the results.

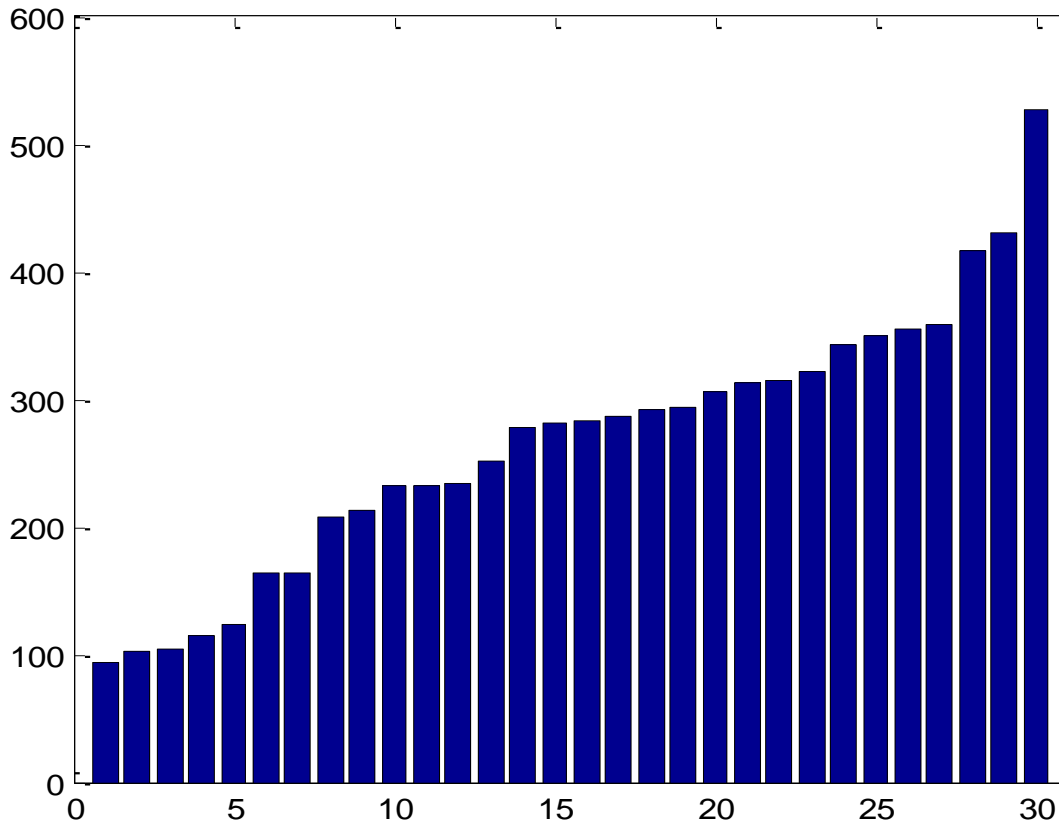


Figure 6.10: Weighted Mean Square Error (WMSE), MLWSAGD

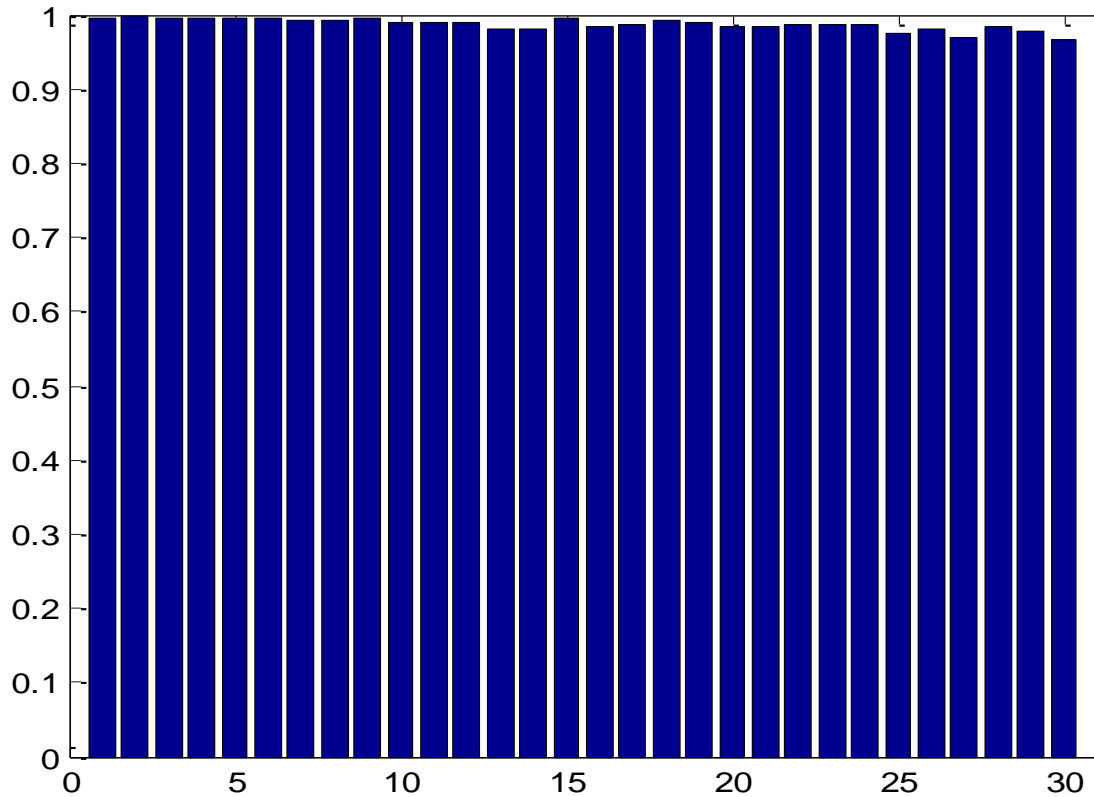


Figure 6.11: Weighted Root Square (WR²), MLWSAGD Model

Since all dynamic parameters match field data very well as shown in Figure 6.6 to Figure 6.9, therefore; the weighted mean square error (WMSE) of every realization in Figure 6.10 is low enough and uncertainty ranges from 100 mean square error to 500 mean square error. All the realizations are matching with reference case to almost 99% in weighted R square (WR²) Figure 6.11. This is the best case of history matching.

6.3 Single Multilateral Well SAGD Model

Single well SAGD model is discussed in chapter 4, where one horizontal well was drilled in oil sands deposit and later on steam was injected through tubing and oil was produced through annulus. A similar technique has been applied to multilateral well technology, from a vertical well, four horizontal branches were drilled in four different directions, called 'Cluster Multibranch Well' as shown in Figure 6.1. Model dimensions are 20 x 20 x 10 grid blocks in X, Y and Z

directions, respectively. Four branches of multilateral well were drilled horizontally with 500m length and 4m above from bottom of the formation. Each horizontal branch was discretized into two independent strings, namely tubing and annulus. Tubing strings act as injector and annuli strings as producer. Figure 6.12 illustrates the 3D view of single MLW-SAGD model dimensions and well location

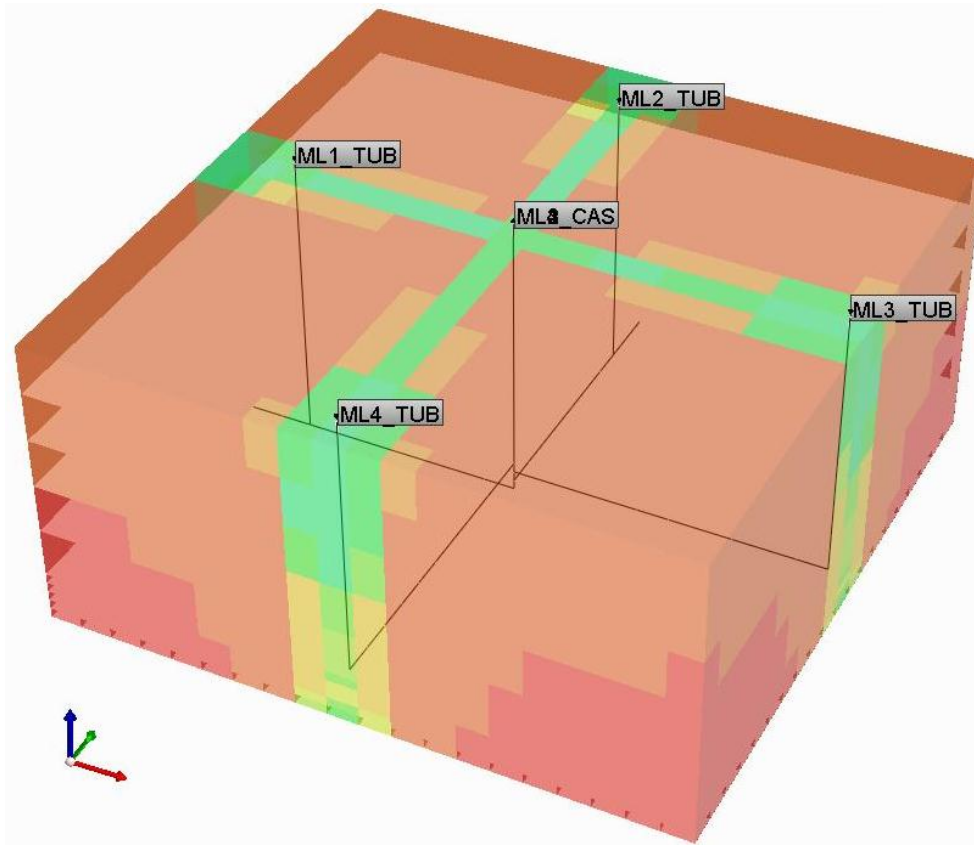


Figure 6.12: 3D view of single MLW-SAGD model with four branches

Electrical heating were applied through casing pipe of four branches at 300 °C for first six months to initialize the movement of reservoir fluid which is dead at reservoir temperature and pressure. After six months, steam was injected through tubing string connected to well head at the rate of 500 m³/d maximum cold water equivalent and 5000 kPa maximum injection BHP. Steam quality was 95% and steam temperature was 325 °C. Reservoir fluids were produced through annulus at the rate of 500 m³/d of maximum oil rate and 500 kPa minimum BHP. The

reservoir fluid and rock properties for single MLW-SAGD model are given in table 6.2

Table 6. 2 Single MLW-SAGD Model Reservoir Properties

Length in x, y, z-dir.	1000m x 1000m x 30m
Formation Top	750m
Porosity	30%
Horizontal Perm (k_h)	Heterogeneous
Vertical Perm (k_v)	$0.3828*k_h$
Number of component	3 (Water, Bitumen and Dissolved Gas)
Connate Water Saturation	10%
Reservoir Initial Temperature	24 °C
Reservoir Initial Pressure	2000 kPa
Bitumen Molar Density	1960 gmole/m ³
Bitumen viscosity	1,000,000 cp @ 24 °C
Dissolved Gas in Bitumen	10% of total Bitumen Saturation
Formation Heat Capacity	3.5 E+6 J/(m ³ . C)
Thermal Conductivity	7.5 E+5 W/ (m. C)
Injection Fluid	Steam
Steam Quality	95%
Injection Temperature	325 °C

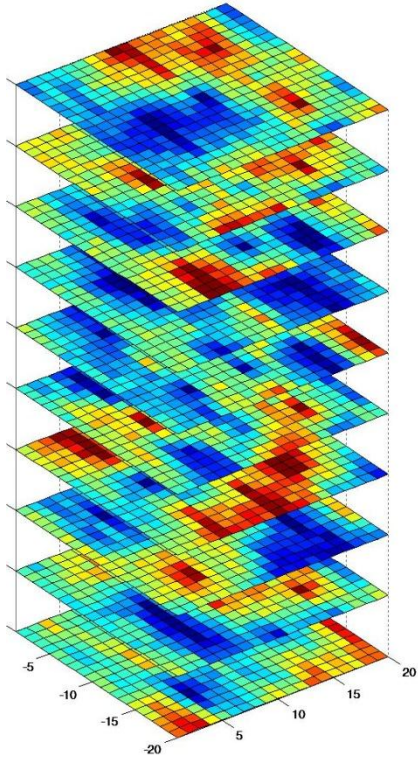


Figure 6.13: Reference permeability field of single MLW-SAGD model

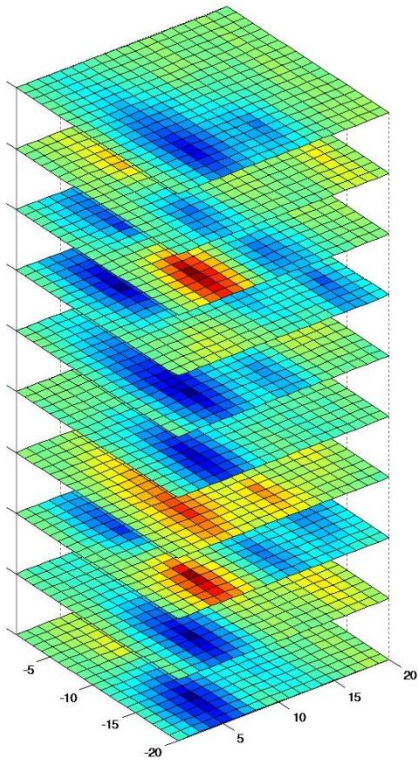


Figure 6.14: Initial mean permeability field of single MLW-SAGD model

Figure 6.13 depicts a reference permeability map of a 3D single MLW-SAGD model. Similar to the previous case, SGSim was applied to generate initial ensemble of permeability realizations using the same geostatistical parameters as reference case. All realizations were conditioned with hard data. The spherical variogram model was selected to search simulated values with range of 10, 10 and 05 grid blocks in the maximum, median, and minimum correlation ranges respectively and zero degree angles for all directions. Figure 6.14 depicts the mean of initial ensemble of 30 permeability realizations.

For computer assisted history matching, field observed data were prepared in a similar way as the previous case, measurements of oil rate and SOR at production wells and temperature sensors data at observation wells were available at the end of each month upto 12 years. Observed data can be directly read from the file of benchmark case for history matching. The history matching was performed for a period of 8 years and the observed field data was assimilated at every twelve months interval, starting from Jun `96 to Jun `04. The measurement covariance matrix (R values in ε_k^d matrix) was selected as 10 m³, 0.01 and 10 °C for OR, SOR and Temperature, respectively. The model covariance matrix was selected as 1.0E⁻⁴ for all grid blocks (Q values in ε^m matrix).

6.4 Single Multilateral Well SAGD Model Results

The results presented here are obtained by applying constrained EnKF based history matching technique to single multilateral well SAGD model.

6.4.1 Model Parameters Update

After applying constrained EnKF to perform history matching of single MLW-SAGD model, updated mean permeability is presented in Figure 6.15. The initial ensemble mean permeability field in this model is uniform, whereas updated mean permeability field has been well recovered and the variance decreases significantly. Compared with the reference field, the updated result at the end of analysis scheme has the similar structure.

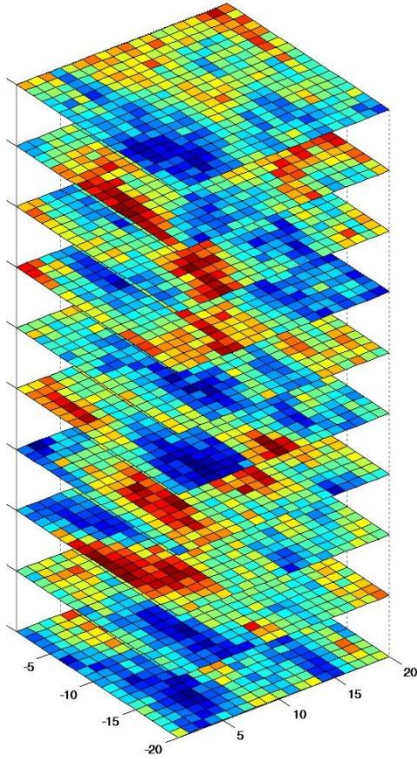


Figure 6.15: Updated Mean Permeability Field of Single MLW-SAGD Model

6.4.2 Dynamic Parameters Match

With the updated permeability fields, all the realizations were reran from the beginning and performed predictions upto the end of simulation. Figure 6.16 shows oil production rate, Figure 6.17 shows the Steam-oil-Ratio, both graphs illustrate that the predictions before history matching are too away from reference field data, it is because the initial ensemble generated with available geological information is not representing the actual reservoir state. But EnKF based history matching method once again proved that it assimilate data regard less how much it is contaminated and update model parameters that can regenerate simulated predictions which are close to field measurements. Figure 6.18 and Figure 6.19 present the graphs of temperature observations at two different locations. Temperature observations contain huge uncertainty before history matching predictions, successfully matched with field observations after history match.

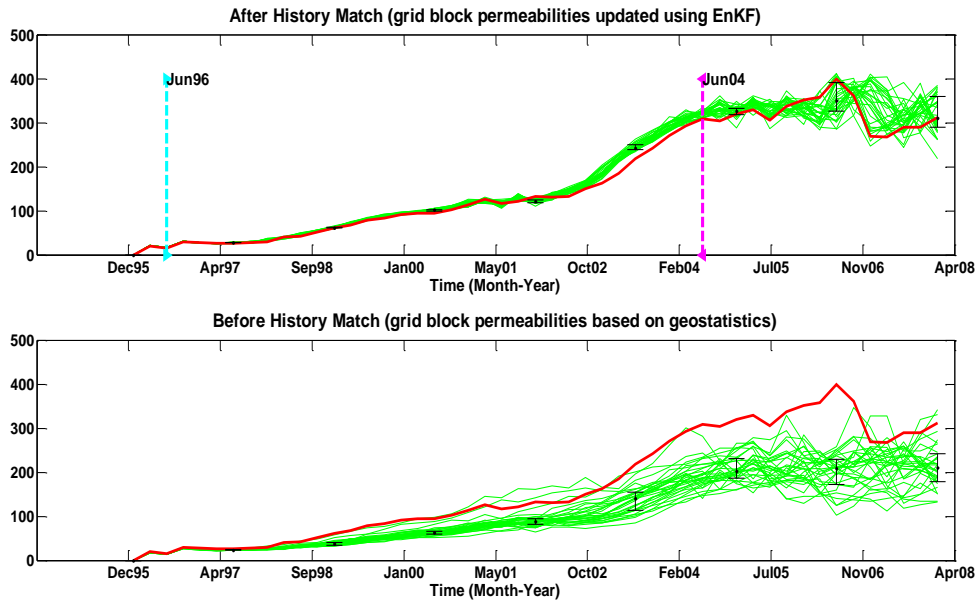


Figure 6.16: Field Oil Production Rate, m³/d, Single MLW-SAGD Model

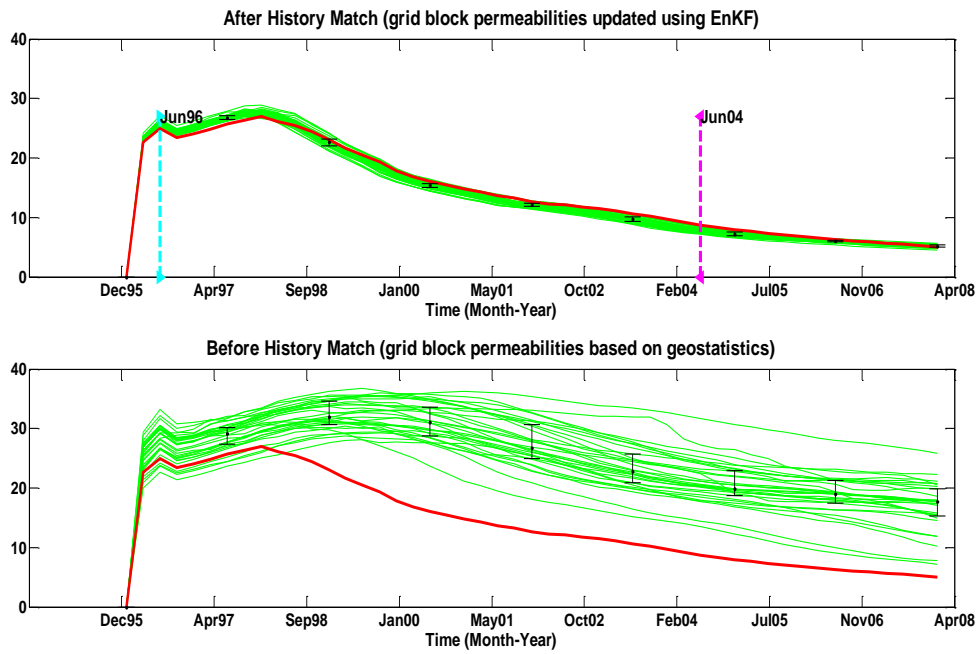


Figure 6.17: Cumulative Steam Oil Ratio (SOR), Single MLW-SAGD Model

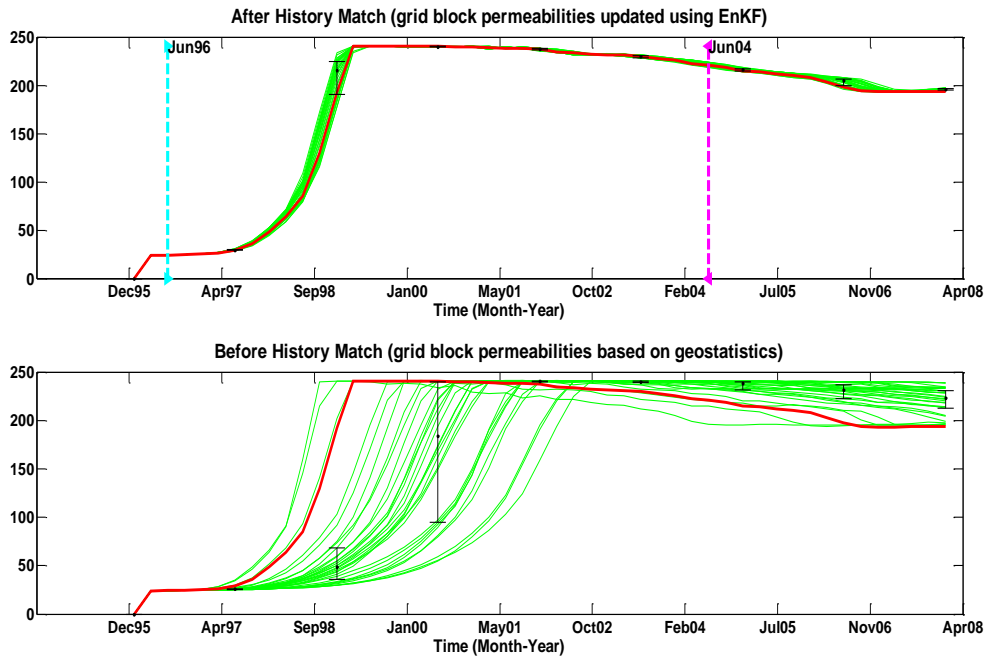


Figure 6.18: Reservoir Temperature at grid location 3, 10, 7, Single MLW-SAGD Model

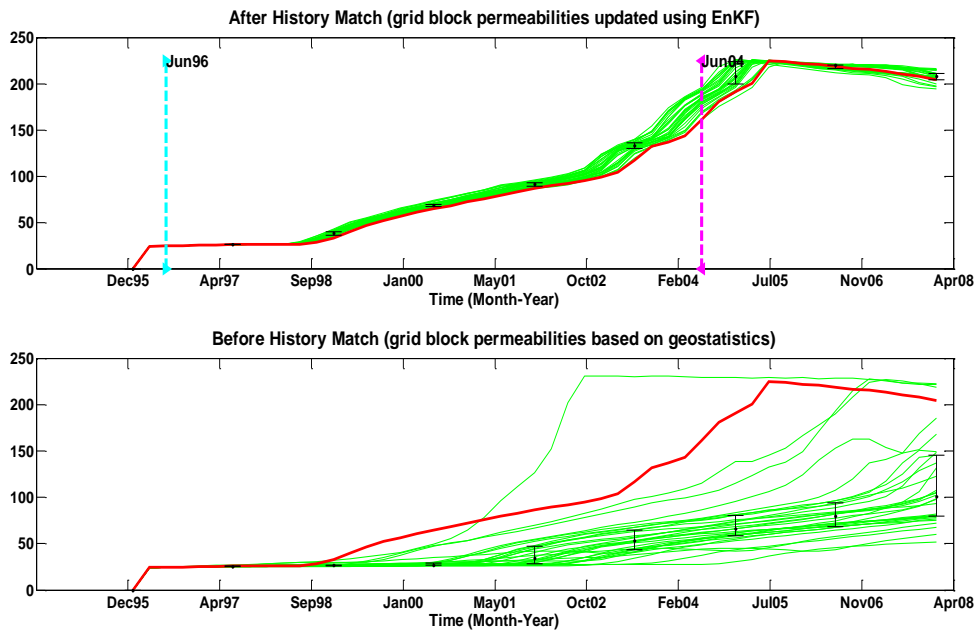


Figure 6.19: Reservoir Temperature at grid location 19, 10, 6, Single MLW-SAGD Model

6.4.3 Ranking of Realizations

In this case, we have same number of realizations (i.e. 30) as generated for previous cases. All the realizations were updated through CEnKF based history match method and at the end realizations were ranked according to their predictability and match with field measurements. Figure 6.20 depicts the weighted mean square error, in which best realization contains approximately 1000 mean square error and least matched realization contains approximately 1900 mean square error. Figure 6.21 depicts the weighted R^2 , which shows that all the realizations are matching with reference case more than 95%.

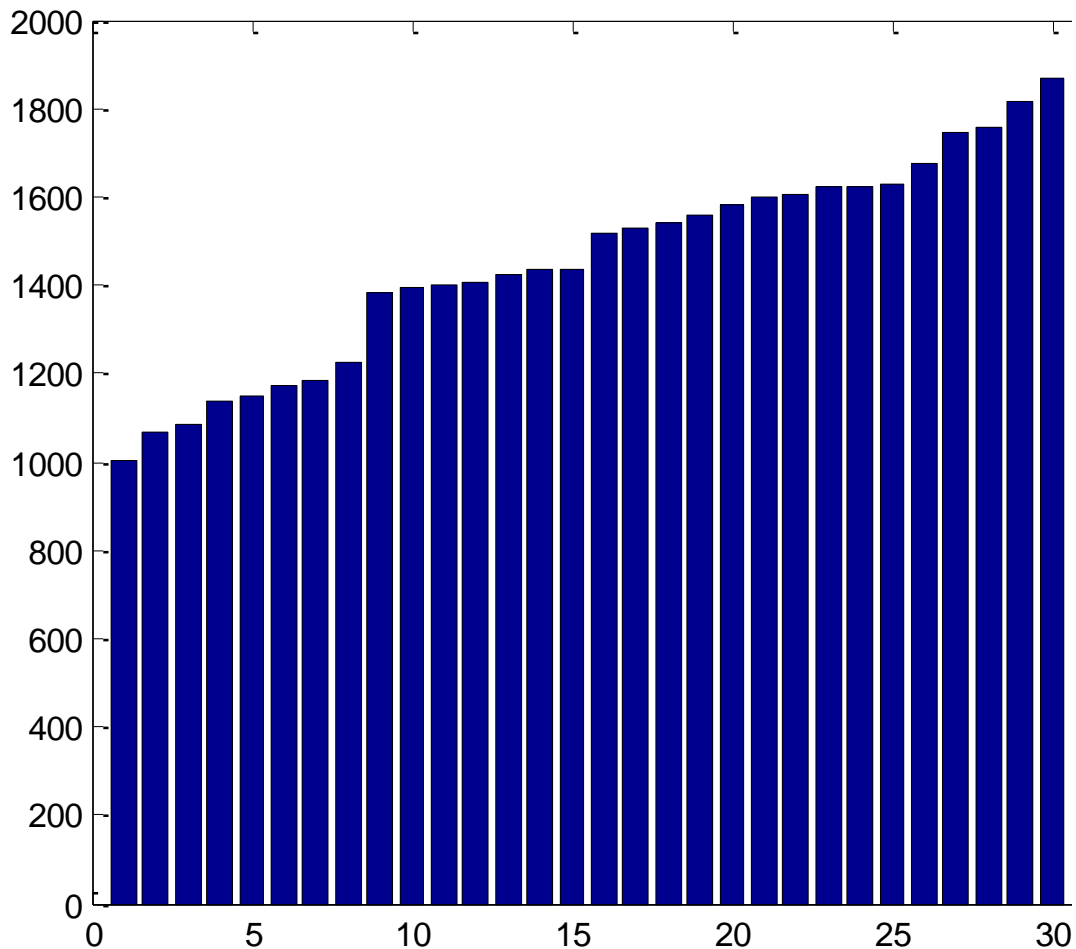


Figure 6.20: Weighted Mean Square Error (WMSE), Single MLW-SAGD Model

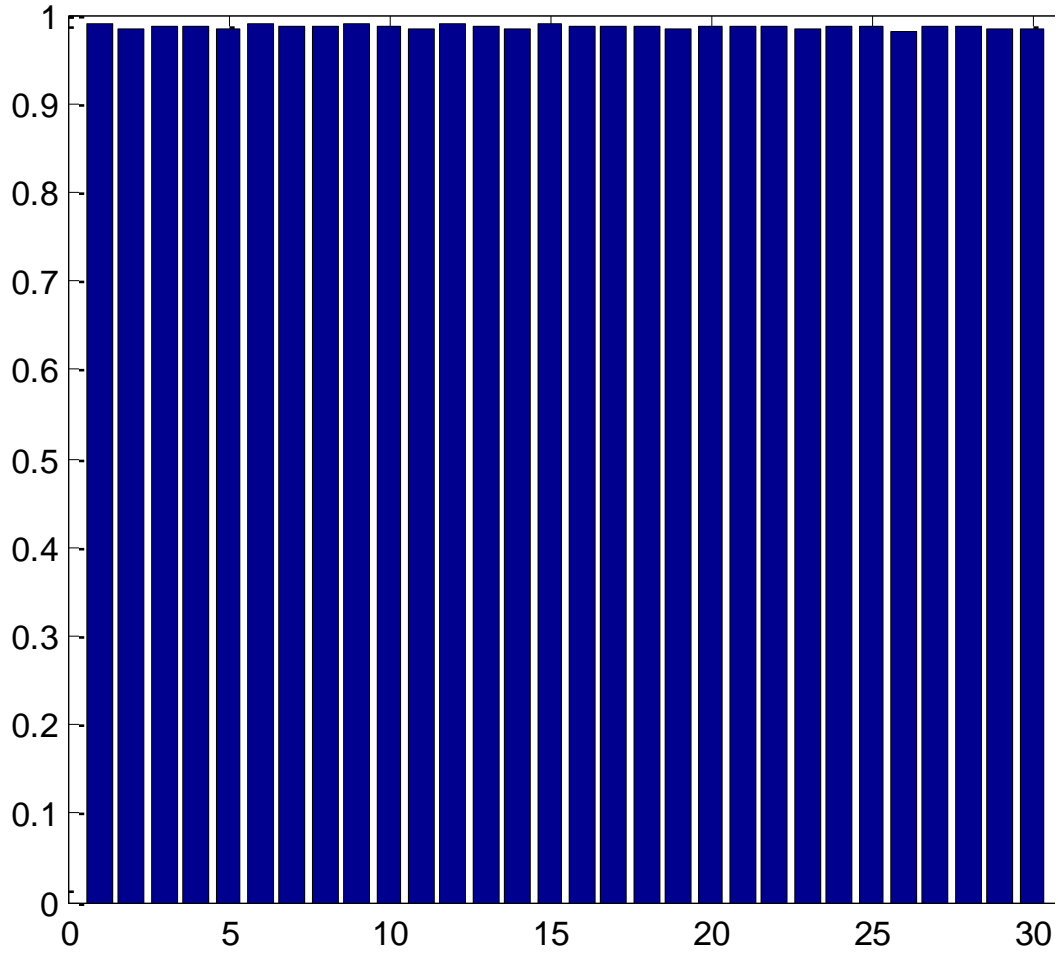


Figure 6.21: Weighted R Square (WR2), Single MLW-SAGD Model

Chapter 7

Discussion and Conclusions

7.1 Discussion

We have explained a technique based on the ensemble Kalman filter (EnKF) for continuous model updating with respect to the combination of production data and temperature observations. It is first time that we have used temperature observations in history matching to update reservoir permeability. The EnKF technique has been implemented to five synthetic unconventional oil reservoir models, where SAGD process was applied as in-situ recovery method. The SAGD models used in this study can be categorised in three types;

1. SAGD model with two parallel horizontal wells, one injector and one producer. Two models were studied, first with one well pair SAGD and second with two well pairs as to represent a field case
2. SAGD model with single horizontal well (tubing acts as injector and annulus as producer); two cases were studied, in the first case, data were assimilated with temperature observations and second without temperature observations
3. SAGD model with multilateral well technology; two models were studied, first model with twin well SAGD technique and second model with single well SAGD technique

The improvement of model parameters such as grid permeability values by assimilating field observed data and simulation predictions such as oil production rate; cumulative steam oil ratio and temperature observations will be beneficial for unconventional oil field developments. The EnKF takes-in data sequentially whenever they become available and its framework is compatible with real time reservoir monitoring with data from permanent down hole sensors and gauges. As

a Monte Carlo type of method, the correlation between model variables and data can be estimated from the ensemble models directly. By doing this, the EnKF avoids the complex calculation of the adjoint system for the forward problem.

It has been found that by using constrained ensemble Kalman filter (CEnKF) in a field implementation, a better history matched model can be achieved with improved permeability estimates. Using the updated permeability fields obtained at the last time step and rerunning the models from beginning provide better match to the dynamic parameters. Updating the model state with field observations gives the starting point for computing predictions. Ensemble of reservoir models consistent with the up-to-date production data is always available for predictions of future performance with the assessment of uncertainty. Therefore; the methodology of EnKF illustrates an ideal framework for reservoir monitoring and future prediction.

In this thesis, results from five SAGD models have been considered to evaluate the performance of constrained EnKF. Sequential Gaussian Simulation (SGSim) was used to generate the initial ensemble to estimate the model parameters conditioned on the core data. Since the field observed data is acquired at well locations, the measurements are sparse and contaminated. Therefore; it is necessary to incorporate some noise to measurements to overcome outliers. The size and complexity of the reservoir models bring constraint on number of ensemble realizations for EnKF based history match process. It is common to use from 30 to 400 ensemble members in the applications nowadays, however; for 3D thermal reservoir model, the process becomes still time consuming. Therefore; we have selected minimum number of ensemble members to initialize the EnKF process and that is 30 realizations for all models.

Some conclusions can be made from the results of SAGD models. From the updated permeability fields (Figures 4.5, 4.16, 5.5, 5.13, 6.5, 6.15) it can be concluded that the constrained EnKF improves the model state considerably after updating the model parameters through data assimilation process. It means that the number of realizations generated to calculate covariance matrix is optimum,

because this covariance matrix computes the Kalman gain which tune the state vector.

For predicting future performance of the SAGD reservoir models, oil production rate graphs (Figures 4.6, 4.17, 5.7, 5.15, 6.6, 6.16) show that after assimilation, the simulation predictions are matching with field history quite well from beginning except multi pair SAGD model oil production rate graph, which shows initially a high peak but quickly all predictions are centered around measurement data. Cumulative SOR graphs (Figures 4.7, 4.18, 5.8, 5.16, 6.7, 6.17) are good examples of data matching of model predictions with field measurements. Temperature observations graphs (Figures 4.8, 4.9, 4.19, 4.20, 5.9, 5.10, 5.17, 5.18, 6.8, 6.9, 6.18, 6.19) illustrate that they contain maximum information about reservoir heterogeneity, since before history matching, predictions contain huge uncertainty and after assimilation process, uncertainty reduces significantly. Also, the comparative study in chapter 5 shows the importance of temperature observations where two cases were history matched with and without temperature observations.

Considering the ranking of realizations after history matching, two methods were applied to calculate the performance of each realization basis on matching with field measurements and reference case permeability field. Figures (4.10, 4.21, 5.11, 5.20, 6.10, and 6.20) depict the weighted mean square error graphs where first realization is best and last realization is least matched with field measurements. Figures (4.11, 4.22, 5.12, 5.21, 6.11, and 6.21) depict the weighted root square graphs which show how much each realization is close to reference case.

7.2 Conclusions

We have implemented a constrained Ensemble Kalman Filter for characterization, production management and history matching of SAGD reservoirs. Three SAGD techniques i.e., twin well SAGD, single well SAGD, and multilateral well SAGD and two examples from each technique have been presented. The real-time

temperature measurements were used for continuous updating of the thermal reservoir simulation model parameters (grid permeability values) along with injection/production observations. This led to better prediction of geological heterogeneity and reservoir's response to well adjustments. This work implicates its usefulness in making best possible decisions about future well settings. Accurate information about the location, movement and rise rate of the steam chamber can be derived from updated ensemble model for heterogeneous SAGD reservoirs in temperature constrained EnKF framework. History matched ensembles provide an efficient and accurate measure for ranking the geological realization of SAGD reservoirs.

Nomenclature

Symbols

X, Y, Z	=	Random Variables
\Pr	=	Probability
σ	=	Standard deviation
σ^2	=	Variance
COV	=	Covariance
ρ	=	Correlation Coefficient
γ	=	Variogram
h	=	Lag distance
y	=	State Vector
A	=	Matrix describing the system dynamics
C	=	Covariance Matrix
K_e	=	Kalman Gain
m	=	Model Parameters
u	=	State Variables
d_{obs}	=	Field measurements
d	=	Perturbed observation data
H	=	Observation Operator
C_ε	=	Covariance matrix representing the model noise
C_y	=	Covariance matrix of the state vector of the system;

- C_D = Covariance matrix of the measurement error
 C_{yd} = Cross covariance matrix between model state variables and simulated data
 C_{dd} = Covariance matrix of simulated data
 Ψ = Ensemble of Initial State Vectors
 N_e = Number of Ensembles
 F = Function Representing Reservoir Simulator
 I = Identity Matrix
 ε = Noise

Superscript

- $1,2,3\dots$ = Ensemble Number
 N_e = Number of Ensembles
 p = Predicted
 j = Ensemble member
 a = Analyzed
 T = Transpose

Subscript

- k = Time Step
 obs = Observed

Bibliography

Aanosen, S.I., Naevdal, G., and Reynolds, A.C. (2009). The Ensemble Kalman Filter in Reservoir Engineering – a Review; SPE Journal, 14(3), 393–412. September.

Albahlani, A. M., and Babadagli, T. (2008). A critical review of the status of SAGD: Where are we and what is next?; Paper SPE 113283, presented at the SPE Western Regional and Pacific Section AAPG Joint Meeting, Bakersfield, CA. 31 March–2 April.

Agbalaka, C., and Oliver D. S. (2008). Application of the EnKF and localization to automatic history matching of facies distribution and production data; Mathematical Geosciences, 40(4).

Anderson, J. L., and Anderson, S. L. (1999). A Monte Carlo implementation of the nonlinear filtering problem to produce ensemble assimilations and forecasts; Mon. Weather Rev., 127, 2741 – 2758.

Ates, H., Bahar, A., El-Abd, S., Charfeddine, M., Kelkar, M., and Datta-Gupta, A. (2005). Ranking and Upscaling of Geostatistical Reservoir Models by use of Streamline Simulation: A Field Case Study; SPE Reservoir Evaluation and Engineering, 8(1), 22-32. February.

Bagci, S. (2004). The effect of fractures on the steam-assisted gravity drainage process; Energy & Fuels 18(6), 1656–1664.

Birrell G. E., and Putnam, P. E. (2000). A study of the influence of Reservoir Architecture on SAGD steam chamber development at the UTF, Northeaster AB, Canada, Using a Graphical Analysis of Temperature Profiles; Paper CIPC-2000-104, Calgary, Canada. June.

Bianco, A., Cominelli, A., Dovera, L., Naevdal, G., and Valles, B. (2007). History Matching and Production Forecast Uncertainty by Means of the Ensemble

Kalman Filter: A Real Field Application; Paper SPE 107161, presented at EUROPEC/EAGE Conference and Exhibition, London, U.K. June.

Baker, R., Fong, C., and Li, T. (2008). Practical Considerations of Reservoir Heterogeneities on SAGD Projects; paper SPE/PS/CHOA 117525 was presented at the 2008 SPE International Thermal Operations and Heavy Oil Symposium, Calgary AB, Canada. October.

Brown, R. G. and Hwang, P. Y. C. (1992). *Introduction to Random Signals and Applied Kalman Filtering*; Second Edition, John Wiley & Sons, Inc.

Burgers, G., Leeuwen, P.J.V., and Evensen G. (1998). Analysis scheme in the ensemble Kalman filter; *Monthly Weather Review*, 126(6), 1719-1724.

Butler, R.M., McNab, G.S. and Lo, H.Y. (1981) Theoretical Studies on the Gravity Drainage of Heavy Oil During In-Situ Steam Heating; *The Canadian Journal of Chemical Engineering*, 59(4), 455-460, August.

Butler, R.M. and Stephens, D.J. (1981). The Gravity Drainage of Steam-Heated oil to Parallel Horizontal Wells; *Journal of Canadian Petroleum Technology*, 20(2), 90-96 April - June.

Burton, R. C., Chin, L. Y., Davis, E. R., Enderlin, M., Fuh, G., Hodge, R., Ramos, G. G., VanDeVerg, P., Werner, M., Mathews, W. L. and Petersen, S. (2005). North slope heavy-oil sand-control strategy: Detailed case study of sand production predictions and field measurements for Alaskan heavy-oil multilateral field; Paper SPE 97279, presented at the SPE Annual Technical Conference and Exhibition, Dallas, TX. 9–12 October.

Caers, J. (2003). History matching under Training-Image-Based Geostatistical Model Constraints; *SPE Journal*, 8(3), 218-226.

Chitrlekha, S.B., Trivedi, J.J., and Shah, S.L. (2010). Application of the Ensemble Kalman Filter for Characterization and History Matching of Unconventional Oil Reservoirs; paper CSUG/SPE 137480 was presented at the

Canadian Unconventional Resources & International Petroleum Conference held in Calgary, Alberta, Canada, October.

Chen, Q., Gerritsen, M.G., and Kovysek, A.R. (2008). Effect of Reservoir Heterogeneities on the Steam-Assisted Gravity-Drainage Process; SPE Reservoir Evaluation & Engineering, 11(5), 921–932, October.

Chen, Y., and Zhang, D. (2006). Data assimilation for transient flow in geologic formations via ensemble Kalman filter; Adv Water Resources, 29(8), 1107–22.

Chow, L. and Butler, R. M. (1996). Numerical simulation of the steam-assisted gravity drainage process (SAGD); Journal of Canadian Petroleum Technology 35(6), 55–62.

Computer Modelling Group STARS Version 2009.10 User's Guide (2009). Computer Modelling Group, Calgary, Alberta, Canada.

Das, S. (2005). Improving the performance of SAGD; Paper SPE 97921 presented at the SPE/PS-CIM/CHOA International Thermal Operations and Heavy Oil Symposium, Calgary, Alberta, Canada. 1–3 November.

Deutsch, C.V. and Journel, A.G. (1998). GSLIB: Geostatistical Software Library and User's Guide; Oxford University Press, New York

Deutsch, C. V. And Srinivasan, S. (1996). Improved Reservoir Management through Ranking Reservoir Models; Society of Petroleum Engineers (SPE), Paper 35411, SPE/DOE Improved Oil Recovery Symposium, Tulsa, Oklahoma, 21-24 April.

Doan, L. T., Baird, H., Doan, Q. T. and Farouq, A. S. M. (1999). An investigation of the steam-assisted gravity-drainage process in the presence of a water lag; Paper SPE 56545 presented at the SPE Annual Technical Conference and Exhibition, Houston, TX. 3–6 October.

Dougherty, E. L. (1972). Application of optimization methods to oilfield problems: Proved, probable, possible; Paper SPE-3978, Prepared for the 47th annual fall meeting of SPE/ AIME, San Antonio, Texas, USA.

Dovera, L., and Rossa, D. E. (2007). Ensemble Kalman filter for Gaussian mixture models; Petroleum Geostatistics, Cascais, Portugal.

Edmunds, N.R., Haston, J.A., and Best, D.A. (1988). Analysis and Implementation of the Steam Assisted Gravity Drainage Process at the AOSTRA UTF; paper no 125 Fourth UNITAR/UNDP Conference on Heavy Crude and Tar Sands held in Edmonton, Alberta, Canada, August.

Edmunds, N. R., Kovalsky, J. A., Gittins, S. D. and Pennacchioli, E. D. (1994). Review of Phase A steam-assisted gravity-drainage test; SPE Reservoir Engineering 9(2), 119–124.

Edmunds, N. R. (1998). Investigation of SAGD steam trap control in two and three dimensions; Paper SPE 50413 presented at the SPE International Conference on Horizontal Well Technology, Calgary, Alberta, Canada. 1–4 November.

Evensen, G. (1994). Sequential data assimilation with a nonlinear Quasi-Geostrophic model using Monte Carlo methods to forecast error statistics; Journal of Geophysical Research, 95(C5), 10143–10162.

Evensen, G. (2003). The Ensemble Kalman Filter: theoretical formulation and practical implementation; Ocean Dynamics, 53, 343 – 367.

Evensen, G. (2004). Sampling Strategies and Square Root Analysis Schemes for the EnKF; Ocean Dynamics 54, 539–560.

Evensen, G. (2007). Data Assimilation: The Ensemble Kalman Filter; Springer Berlin.

Evensen, G., Hove, J., Meisingset, H.C., Reiso, E., Seim, K. S., and Espelid, O. (2007). Using the EnKF for Assisted History Matching of a North Sea Reservoir

Model; Paper SPE 106184, presented at SPE Reservoir Simulation Symposium, Texas, TX.

Evensen, G. (2009). The ensemble Kalman filter for combined state and parameter estimation; IEEE Control Systems Magazine, 29(3), 82-104.

Fenik, D.R., Nouri, A., and Deutsch, C.V. (2009). Criteria for Ranking Realizations in the Investigation of SAGD Reservoir Performance; paper PETSOC2009-191 was presented at Canadian International Petroleum Conference (CIPC), Calgary AB, Canada, June.

Farouq, A.S.M. and Redford, D.A. (1977). Physical Modeling of In Situ Recovery Methods for Oil Sands; Canada – Venezuela Oil Sands Symposium Edmonton AB Canada, CIM Special, 17, 319 - 326.

Farouq, A. S. M. (1997). Is there life after SAGD?; Journal of Canadian Petroleum Technology 36(6), 20–23.

Farouq A. S. M. and Thomas, S. (1996). The Promise and Problems of Enhanced Oil Recovery Methods; Journal of Canadian Petroleum Technology, 35(7), 47-56. September.

Gao, G., Zafari, M., and Reynolds, A. C. (2006). Quantifying Uncertainty for the PUNQ-S3 Problem in a Bayesian Setting with RML and EnKF; SPE Journal, December, 11(4), 506–515. November.

Gelb, A. (1974). *Applied Optimal Estimation*, MIT Press, Cambridge, MA.

Gittins, S.D., Edmunds, N.R. and Mukherjee, N.J. (1992). Numerical Simulation of the Steam Assisted Gravity Drainage Process at the Underground Test Facility; IEA Collaborative Project on Enhanced Oil recovery workshop and symposium, The Banff Springs Hotel and conference center, Banff AB, Canada, September.

Gilman, J.R., Meng, H., Uland, M.J., Dzurman, P.J., and Cosic, S. (2002). Statistical Ranking of Stochastic Geomodels Using Streamline Simulation: A Field Application; Society of Petroleum Engineers (SPE), Paper 77374, SPE

Annual Technical Conference and Exhibition, San Antonio, Texas, 29 September -2 October.

Gotamwala, D.R., and Gates, I.D. (2008). Flow and Energy Dynamics at the Edges of Steam Assisted Gravity Drainage Chambers; Paper PETSOC2008-113, presented at Canadian International Petroleum Conference (CIPC), Calgary AB, Canada, 17 - 19 June.

Govier, G.W. (1965). The Athabasca Oil Sands; Paper SPE 1079, presented at AIME Annual Meeting in Chicago, Illinois, February.

Grewal, M. S., and Andrews, A. P. (1993). *Kalman Filtering Theory and Practice*; Upper Saddle River, NJ USA, Prentice Hall.

Gu, Y., and Oliver, D. S. (2005). History Match of the PUNQ-S3 Reservoir Model Using the Ensemble Kalman Filter; SPE Journal, 217–224. June,

Gul, A., Nejadi, S., Shah, S., and Trivedi, J. J. (2011). Make Use of Dynamic Data - A Constraint Based EnKF for SAGD Reservoir Characterization and Production Management; Presented at 2011 World Heavy Oil Congress [WHOC11], Edmonton, Canada. 14-17 March.

Haugen, V., Natvik, L.J., Evensen, G., Berg, A., Flornes, K. and Naevdal, G. (2008). History Matching Using the Ensemble Kalman Filter on a North Sea Field Case; SPE Journal, 13(4), 382 – 391.

Hamill, T. M., and Snyder, C. (2000). A hybrid ensemble Kalman filter/ 3dvariational analysis scheme; Mon. Weather Rev., 128, 2905 – 2919.

Hamil, T., and Whitaker, J. (2001). Distance-dependent filtering of background error covariance estimates in an ensemble Kalman filter; Monthly weather Review, 129.

Houtekamer, P. L., and Mitchell, H. L. (2001). A sequential ensemble Kalman filter for atmospheric data assimilation; Mon. Weather Rev., 129, 123– 137

Ito, Y., and Suzuki, S. (1999). Numerical simulation of the SAGD process in the Hangingstone oil sands reservoir; *Journal of Canadian Petroleum Technology* 38(9), 27–35.

Jansen, J. D., Douma S. D., Brouwer D. R., Van-den-Holf, P. M. J., Bosgra. O. H. and Heemink, A. W. (2009). Closed-loop reservoir management; Paper SPE-119098, presented at SPE reservoir simulation symposium, Texas, USA, February 2-4.

Jacobs, O. L. R. (1993). *Introduction to Control Theory*, 2nd Edition. Oxford University Press.

Jazwinski, A. H. (1970). *Stochastic processes and filtering theory*; Academic Press New York.

Jimenez, J. (2008). The field performance of SAGD projects in Canada; Paper IPTC-12860, presented at the International Petroleum Technology Conference, Kuala Lumpur, Malaysia. 3–5 December.

Kalman, R.E. (1960). A New Approach to Linear Filtering and Prediction Problems; *Transactions of the ASME - Journal of Basic Engineering*, 82(Series D), 35 – 45.

Lewis, R. (1986). *Optimal Estimation with an Introduction to Stochastic Control Theory*; John Wiley & Sons, Inc.

Ljung, L. (1999). *Comparing model structures in System Identification: Theory for the User*; Prentice Hall PTR, New Jersey, USA.

Li, Z., Yin, J., Zhu, D., and Datta-Gupta, A. (2010). Using downhole temperature measurements to assist reservoir characterization and optimization; Paper SPE-131370, presented at the CPS/SPE International Oil & Gas Conference and Exhibition, Beijing, China, 8-10 June.

Lorentzen, R. J., Fjelde, K. K., Froyen, J., Lage, A. C. V. M., Naevdal, G., and Vefring, E. H. (2001). Underbalanced and low-head drilling operations: Real time

interpretation of measured data and operational support; In SPE Annual Technical Conference and Exhibition, New Orleans, Louisiana. Society of Petroleum Engineers Inc.

Maybeck, P. S. (1979). *Stochastic Models, Estimation, and Control*, Volume 1, Academic Press, Inc.

McCormack, M., Fitzgibbon J., and Horbachewski, N. (1997). Review of single well SAGD field operating experience; *Canadian Petroleum Society*, **97**, 1–15.

McLennan, J.A. and Deutsch, C.V. (2006). Best Practice Reservoir Characterization for the Alberta Oil sands; presented in 7th Canadian International Petroleum Conference, Calgary, AB, Canada.

Mukherjee, N.J., Gittins, S.D., Edmunds, N.R. and Kisman, K.E. (1995). A comparison of field versus forecast performance for Phase B of the UTF SAGD project in the Athabasca oil sands; 6th UNITAR Conference on Heavy Crude and Tar Sands, Vol. 1.

Nævdal, G., Mannseth, T. and Vefring, E.H. (2002). Near-well reservoir monitoring through ensemble kalman filter; Paper SPE-75235, Proceeding of SPE/DOE Improved Oil recovery Symposium, Tulsa, Oklahoma, USA.

Nævdal, G., Johnsen, L.M., Aanonsen, S.I. and Vefring, E.H. (2005). Reservoir Monitoring and Continuous Model Updating Using Ensemble Kalman Filter; *SPE Journal*, 10(1), 66 – 74.

Nejadi, S., Leung, J.Y.W., and Trivedi, J.J. (2011). Improving Characterization and History Matching Using Entropy Weighted Ensemble Kalman Filter for Non-Gaussian Distributions; Paper SPE-144578, presented at SPE Western Regional Meeting, Anchorage, Alaska, USA, 7 - 11 March.

Oliver, D.S., Reynolds, A.C. and Liu, N. (2008). *Inverse Theory for Petroleum Reservoir Characterization and History Matching*; Cambridge University Press, New York.

- Oliver, D. S. and Chen, Y. (2011). Recent progress on reservoir history matching: a review; *Computational Geosciences*, 15, 185-221.
- Phale, H. A., and Oliver, D. S. (2009). Data assimilation using the constrained ensemble Kalman filter; Paper SPE-125101, presented at SPE annual technical conference and exhibition, New Orleans, LA USA. 4-7 October.
- Redford, D.A. (1985). In Situ Recovery from the Alberta Oil Sands – Past Experience and Future Potential; *Journal of Canadian Petroleum Technology*, 24(3), 52 – 62, May - June.
- Redford, D. A. and Luhning, R. W. (1999). In Situ Recovery from the Alberta Oil Sands – Past Experience and Future Potential Part II; *Journal of Canadian Petroleum Technology*, 38(13), 1 - 13, Special Edition.
- Remy, N., Boucher, A., and Wu, J. (2009). *Applied Geostatistics with SGeMS: A User's Guide*; Cambridge University Press.
- Saad, N., Maroonge, V., and Kalkomery, C. (1996). Ranking Geostatistical Models Using Tracer Production Data; Paper SPE-35494, presented at European 3-D Reservoir Modelling Conference, Stavanger, Norway, 16-17 April.
- Seiler, A., Evensen, G., Skjervheim, J. A., Hove, J., and Vabo, J. G. (2009). Advanced reservoir management workflow using an EnKF based assisted history matching method; Paper SPE-118906, presented in SPE Reservoir Simulation Symposium, The Woodlands, Texas, USA, 2–4 February.
- Singhal, A.K., Das, S., Goldman, J. and Turta, T. (2000). A mechanistic study of single-well steam assisted gravity drainage; Paper SPE-59333, presented at SPE/DOE Improved Oil Recovery Symp, pp. 3–5, Tulsa, OK, USA, April.
- Singhal, A. K. and Card, C. C. (1988). Monitoring of Steam Stimulation in the McMurray Formation, Athabasca Deposit, Alberta; *Journal of Canadian Petroleum Technology*, 40(4), 483-490, April.

Siu, A., Kun, Y. U., Nghiem, L., and Redford, D. A. (1990). Numerical Modelling of a Thermal Horizontal Well; CIM/SPE Paper # 90 - 122 CIM and SPE Meeting Calgary, June.

Snyder, C., and Zhang, F. (2003). Assimilation of simulated Doppler Radar observations with an ensemble Kalman filter, *Mon. Weather Rev.*, 131, 1663–1677.

Sorenson, H. W. (1970). Least-Squares estimation: from Gauss to Kalman; *IEEE Spectrum*, 7, 63-68, July.

Stengel, R.F. (1994). *Optimal control and Estimation*; Mineola, New York: Dover Publication

Tan, T. B., Butterworth, E., and Yang, P. (2002). Application of a thermal simulator with fully coupled discretized wellbore simulation to SAGD; *Journal of Canadian Petroleum Technology* 41(1), 25–30.

Thacker, W. C. (2007). Data assimilation with Inequality Constraints; *Ocean Modelling*, 16(3-4), 264-276.

Vanegas, P. J. W., Duetsch, C. V., and Cunha, L. B. (2009). Transference of Reservoir Uncertainty in Multi SAGD Well Pairs; Paper SPE-124153, presented at the 2009 SPE Annual Technical Conference and Exhibition, New Orleans, Louisiana, USA, October.

Vincent, K. D., MacKinnon, C. J., and Palmgren, C. T. S. (2004). Developing SAGD Operating Strategy using a Coupled Wellbore Thermal Reservoir Simulator; Paper SPE-86970, presented at the 2004 SPE Thermal Operations and Heavy Oil Symposium and Western Regional Meeting, Bakersfield, California, USA, 16 – 18 March.

Wang, D., Chen, Y., and Cai, X. (2009). State and parameter estimation of hydrologic models using the constrained ensemble Kalman filter; *Water resources research*, 45, W11416.

Wen, X. H., and Chen, W. H. (2006). Real-Time Reservoir Model Updating Using Ensemble Kalman Filter With Confirming Option; SPE Journal, 11(4), 431 – 442, December.

Yang, G., and Butler, R. M. (1992). Effects of reservoir heterogeneities on heavy oil recovery by Steam Assisted Gravity Drainage; Journal of Canadian Petroleum Technology 31(8), 37–43.

Zhang, F., and Reynolds, A. C. (2002). Optimization Algorithms for Automatic History Matching of Production Data; paper presented at the 8th European Conference on the Mathematics of Oil Recovery, Freiberg, Germany, 3-6 September.